Engineered Science
DOI: https://dx.doi.org/10.30919/es1346

From Concept to Creation: Micro/Nanobot Technology from Fabrication to Biomedical Applications

Hafsa Bahaar,[1] B. Siva Kumar,[1,*] S. Giridhar Reddy,[1] Zhanhu Guo,[2] Aricson Pereira[3] and Terence Xiaoteng Liu[2,*]

Abstract

An ultimate frontier in nanomedicine has been the creation of micro and nanoscale devices capable of combating diseases within the human body. Micro/nanobots (MNRBs) engineered to perform specific programmed tasks are leading advancements in next-generation micromachinery. These MNRBs possess remarkable potential due to their ability to be chemically customized, allowing them to autonomously carry out tasks with enhanced precision and functionality while maintaining mobility. Their capability to navigate hard-to-reach areas of the human body using either self-contained or external power sources positions them as valuable tools for a wide array of medical and healthcare uses. A key factor in the success of MNRBs in biomedical applications, particularly for in vivo use, is the seamless integration of surface modifications, remote control systems, and imaging techniques. Most current reviews on nanorobotics selectively focus on specific fabrication or actuation methods, potentially missing broader research. There is a lack of comprehensive overviews of MNRBs. This paper aims to deliver a comprehensive review of medical MNRBs, detailing aspects such as fabrication techniques, material selection, propulsion mechanisms, structural designs, and applications. It also addresses the fast-paced advancements in the field, emphasizing significant challenges and possible solutions to guide future research while offering a centralized source of information.

Keywords: Traditional fabrication techniques; Advanced fabrication methods; Composition of micro/nanobots; Actuation mechanisms; Clinical applications.
Received: 10 October 2024; Revised: 14 November 2024; Accepted: 07 December 2024.
Article type: Review article.

1. Introduction

The concept of using tiny robots within the human body for diagnosing and treating diseases has been of interest for years, as vividly illustrated in the film *Fantastic Voyage*. Advances in nanoscience and technology have enabled the development of microbots, smaller than 1 mm, and nanobots, under 1 µm, to access hard-to-reach areas like cerebral vessels and bile ducts. These robots are designed for biomedical uses and can be remotely controlled to perform specific tasks. As surgery becomes more non-invasive, miniaturized robots or "mini-doctors" offer precise medical intervention. With developments in the clinical field, microbots are evolving to meet medical needs, while nano and micro motors, along with nanobots, possess significant potential for intricate tasks and on-chip uses because of their versatility and compatibility with biological systems.[1-3]

Micro/nanobots (MNRBs) have been widely employed for various mechanical and medical applications. Mechanical applications like biomechanics and nanomachines are progressing through both bottom-up and top-down methods. Notable advancements include nanotube tweezers for nanoscale manipulations and measurements, as well as carbon nanotube bearings with potential uses in high-frequency resonators and nano/micro engineered and molecular systems (NEMS) actuators.[4] Functional nanomaterials have crossed the gap between robotics and medicine as a result of significant developments in nanoscience and technology. Nanoscale robotic surgeons may be able to access remote, inaccessible portions of the body to perform a wide range of medical procedures, including minimally invasive surgeries, target therapies, and cellular manipulations. These

[1] *Department of Physical Sciences, Amrita School of Engineering, Bengaluru, Amrita Vishwa Vidyapeetham, 560035, India*
[2] *Department of Mechanical and Construction Engineering, Faculty of Engineering and Environment, Northumbria University, Newcastle upon Tyne, NE1 8ST, UK*
[3] *Engineered Multifunctional composites (EMC) nanotech LLC, Knoxville, TN, 37996, United States*
[*] *Email:* b_sivakumar@blr.amrita.edu (B. S. Kumar), Terence.liu@northumbria.ac.uk (T. X. Liu)

applications often require programmable energy inputs that are driven to perform a specified function on demand. Lately, there has been growing interest in the development and exploration of MNRBs constructed from a variety of materials.[5] Several research studies are being carried out to utilize MNRBs for purposes like sensing, imaging, drug vehicles, and surgery tools.[6-10] In this case, the system comprises two segments: a cargo segment and a motor segment. Its cargo segment includes advanced materials like carbon nanotubes, silica, graphene, polymeric nanoparticles, liposomes, and biohybrid systems, which are essential for carrying out the intended function. The motor segment helps it to propel or drive through the system.[11]

MNRBs are often divided into three categories based on their composition: biological, artificial, and biohybrid. Biological MNRBs are made from natural biological components, resulting in high biocompatibility, whereas artificial MNRBs are composed of various organic and inorganic components. Depending on the energy source, artificial MNRBs can be propelled by themselves or by an external field. Self-propelled MNRBs get their power from their surroundings, using propulsion techniques such as autonomous movement via electrical fields,[12,13] autonomous movement via temperature gradients,[14] autonomous movement via concentration gradients,[15] and microbubble-driven propulsion. Despite the appeal of autonomous propulsion, the usage of chemical fuels in these robots can be cytotoxic, restricting their utility in biomedical applications. Externally propelled MNRBs, which are driven by external fields such as ultrasonic waves,[16,17] magnetic,[18,19] light, and electric fields, do not require chemical fuels, making them more suitable for usage in biomedical settings.[20,21] Biohybrid MNRBs are small machines that combine biological and artificial components. They combine the benefits of biological organisms, such as autofluorescence and biocompatibility, with the multifunctional capabilities of artificial MNRBs, which result from the use of various materials.[22-25]

The successful development of MNRBs is increasingly dependent on advancements in fabrication methods. Critical factors affecting this fabrication process include the selected manufacturing techniques, the materials used in the composition of the MNRBs, their actuation and propulsion systems, and their overall geometric design. Studies have demonstrated that particle geometry has a major impact on intracellular uptake processes and kinetics. Particles with strong local curvatures are more easily swallowed than those with flat or concave surfaces. Cylindrical micelles stay in the bloodstream longer than spherical micelles because the hydrodynamic forces acting on elongated micelles oppose phagocytic forces. Furthermore, under capillary hydrodynamic circumstances, nonspherical particles are more likely to translate and adhere to vessel walls.[26] Building on this research, various shapes of MNRBs have since been developed by researchers, which include helical,[27,28] capsule type microbot,[29,30] rod shaped,[13,31] microneedles,[32,33] tubular,[34] conical hollow helices,[35,36] spherical,[37,38] and nanowires,[39, 40] *etc.*

The engines that provide propulsion remain functional and produce enough force to counteract surrounding resistance. This requires systems capable of continuously transforming various energy forms into motion. For instance, a non-uniform distribution of catalytic materials allows chemically driven MNRBs to navigate in targeted directions.[15] In a similar manner, materials with varying densities can create pressure gradients that facilitate the directed motion of ultrasound-driven robots. For this purpose, MNRBs are created using diverse organic materials, recognized for their biocompatibility and biodegradability, and inorganic materials, known for their superior properties. Recently, hybrid nanomaterials combining both types have emerged to enhance functionality. As a result, using diverse functional materials in robotics necessitates a variety of processing methods, such as using physical or chemical procedures to create structures with specified purposes.[41] This is a very complex research domain that deals with different methods and materials in sequence to meet the challenges of a useful, potent, and functional device. Therefore, it is important to understand and further improve the techniques in order to develop the fabrication and creation of MNRBs that can perform various applications in medicine, environmental management, and industry with high repeatability and efficiency.

Existing reviews on micro/nanorobotics often focus narrowly on studies that explicitly detail specific fabrication or actuation methods, which can introduce selection bias by potentially overlooking relevant research that does not emphasize these aspects. Currently, there are limited reviews offering a broad perspective on medical micro/nanobots. This paper offers an in-depth analysis of MNRBs in medicine, focusing on fabrication techniques, material choices, actuation and propulsion methods, structural design, and their uses. Acknowledging the swift progress in this area, the review seeks to present a current overview of MNRBs, monitor developments in this groundbreaking technology, and identify key challenges and advantages, thereby steering future research in this evolving field.

2. Fabrication of micro/nanobots

Fabrication techniques for MNRBs are crucial for their development, facilitating precise embedding of components and achieving desired dimensions and functionalities. MNRBs are created using various chemical and physical methods, classified as bottom-up and top-down. These methods have developed over time, starting from traditional techniques like physical vapor deposition and electrodeposition to more advanced methods such as self-assembly, self-curling, and 3D printing. Each approach presents unique benefits and drawbacks, affecting the selection of techniques according to the specific design requirements of the MNRBs. The principles and applications of these methods are provided in the sections below, and a summary of their pros and cons is

included in Tables 1, 2, and 3.

2.1 Traditional fabrication techniques

Traditional techniques, such as physical vapor deposition and electrodeposition, were developed years ago to create thin films for coating and other macroscale applications. However, with technological advancements and the availability of new materials, these methods have been adapted for the fabrication of robots at the nano/micro scale, showing significant potential for clinical applications.

2.1.1 Physical vapour deposition (PVD)

PVD is an advanced method for creating intricate MNRB structures, such as "yin-yang" spherical and helical forms. The processes involve physical operations in a vacuum to vaporize solid or liquid materials into gaseous atoms or molecules, which then condense into thin layers on a substrate.[42] PVD can also be employed to make nanomotors by scaling down the templates. The two common techniques of PVD in this process are sputtering (Fig. 1A-a) and electron beam evaporation (Fig. 1A-b).[43,44] The formation of nanomotors through the PVD process initiates the formation of a self-assembled monolayer of nanoparticles. The procedure entails dropping a droplet of nanoparticle suspension onto a smooth and clean substrate, typically a glass slide refined by using a plasma cleaner. The particles are dissolved in a hydrophilic solvent, such as ethanol, in concentrations that would avoid overload. This process ensures a uniform monolayer by maintaining the correct temperature and stable airflow conditions, thereby preventing the accumulation or evaporation of suspension particles. Catalytic or inert materials are then deposited to create hemispherical caps on the nanoparticles, forming Janus nanoparticles with distinct regions exhibiting anisotropic composition or surface characteristics.[45] Finally, the nanoparticles are removed from the substrate using sonication. The dimensions of the MNRBs are controlled by adjusting the template particle size. PVD offers a resolution of less than 5 nm.[42,46-48]

Various examples highlight the diverse applications of PVD in creating functional MNRBs. Firstly, Janus mesoporous silica nanomotors (JMSNMs) were synthesized by applying a 2 nm platinum (Pt) layer on monolayers of MSNPs using electron-beam evaporation at zero degrees. This results in nanoparticles with distinct dual faces and accessible mesopores for cargo loading. Fig. 1B illustrates the dark platinum (Pt) coatings on the surface of JMSNM. The catalytic activity of the Pt layer facilitated self-propulsion via H_2O_2 decomposition, driving the JMSNMs through self-diffusiophoresis.[49] Additionally, Xuan *et al*. detailed the creation of MSNMs using a vacuum sputtering technique to apply a 10 nm gold layer (refer to Fig. 1C), enabling high-speed movement through a localized photothermal effect induced by Near Infrared (NIR) laser irradiation on the metal half-shell.[50] Another study demonstrated the fuel-free motion of Macrophage cell membrane-cloaked JMSNM in biological environments under NIR light.[51] Accordingly, Fig. 1D shows that Baraban *et al*. covered a silica substrate with metal layers of Co/Pt (Pd) N by sputter coating, generating cathodic spherical microrobots that were able to realize mobility and magnetic field-triggered drug release.[52] These examples illustrate the versatility of PVD in enabling the direct synthesis of MNRBs with specialized structures, rendering them ideal for a range of clinical applications and technological advancements, despite its requirement for an expensive and meticulously maintained vacuum environment.[41]

2.1.2 Electrodeposition

Electrochemical techniques provide an excellent platform for fabricating micro/nanobots due to their straightforward experimental protocols and the availability of low-cost equipment and chemicals, making them easy to scale up. Two types of strategies have been developed using the electrochemical technique: template-based methods and template-less methods. Fig. 2A-a illustrates the template-based method, and Fig. 2A-b shows the template-less method. Template-based methods utilize structured substrates to define the size and shape characteristics of the robots precisely, hence taking control of their dimensions with extreme care. On the contrary, template-less methods enjoy greater design freedom due to the absence of predefined molds. Common to these processes is electrodeposition, which is an electrochemical process for the deposition of metals or alloys from solution or molten salts. The simplest form of electrodeposition includes the following three components: an electrochemical bath that contains metallic ions and additives, electrodes, such as cathodes and anodes, and systems that provide constant or variable potential or current controlling the applied magnitude. Deposition can occur at the cathode through electron gain (cathodic deposition), such as the electrodeposition of metals and alloys, or at the anode through electron loss (anodic deposition), which includes the electrodeposition of metal oxides.[53] Oxidation takes place at the anode. Much more applied is the cathodic deposition because many metal ions are positively charged, whereas anodic depositions are less common due to generally low adhesion and the absence of stoichiometry.[42,54-57]

The initial nanomotors created via electrodeposition using a porous membrane template, as shown in Fig. 2B, were bimetallic nanowires with gold at the anodic end and platinum. These rod-like particles, with a diameter of 370 nm and platinum and gold segments, each measuring 1 μm in length, exhibit autonomous movement in aqueous H_2O_2 solutions by catalyzing the production of O_2 at the platinum end.[58] Zhang *et al*. fabricated nickel nanowires (Fig. 2C) through electrodeposition in nanoporous templates with the ability to propel in water under uniform rotating magnetic fields.[59] A micro/nanobot using glucose from human body fluid as fuel and made of platinum anode and carbon nanotube cathode was fabricated by template electrochemical deposition and

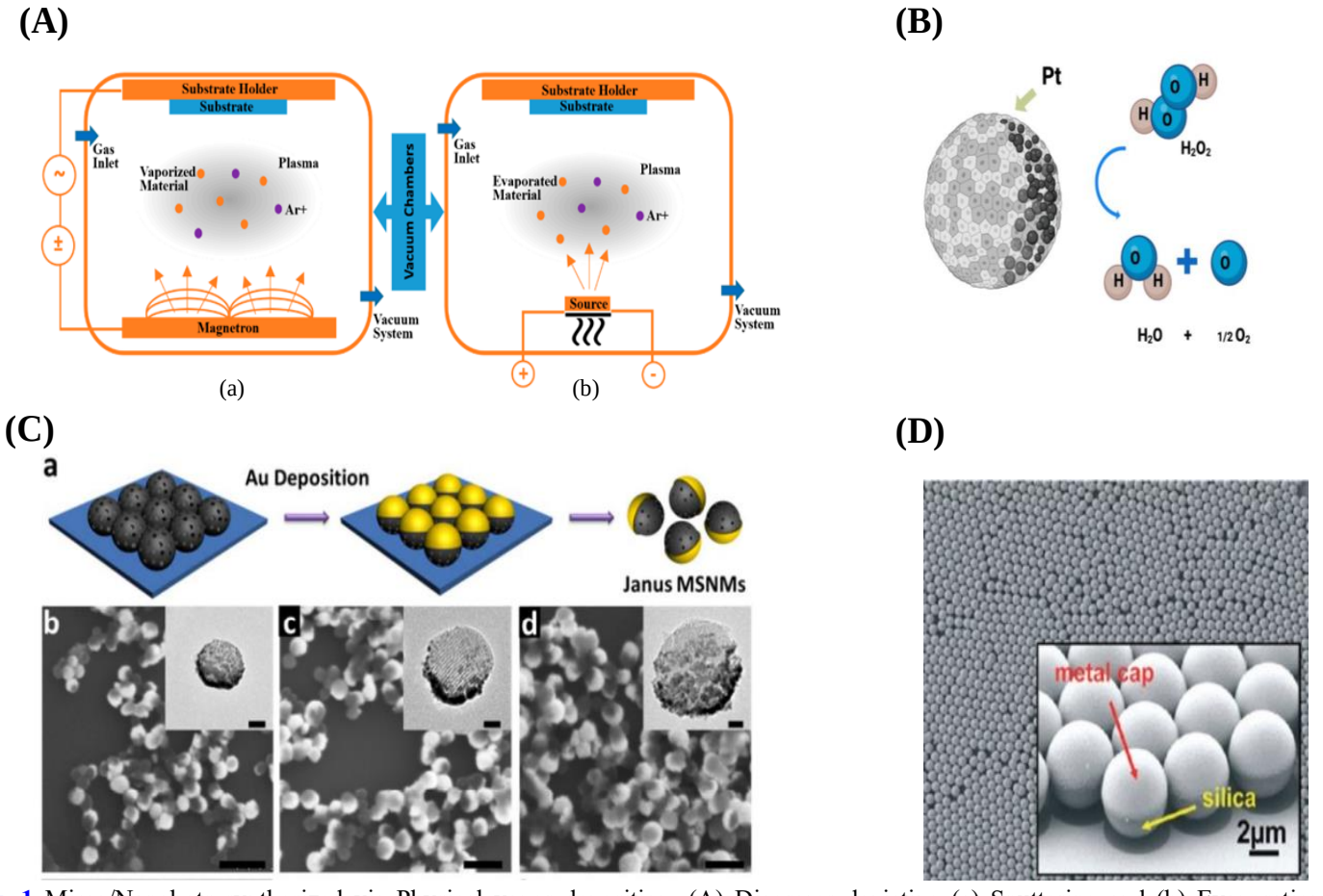

Fig. 1 Micro/Nanobots synthesized via Physical vapor deposition. (A) Diagrams depicting (a) Sputtering and (b) Evaporation processes utilizing Argon gas. Reproduced with the permission from [43], Copyright 2018, MDPI (B) JMSNM schematic illustrating catalytic self-propulsion reactions. Reproduced with the permission from [49], Copyright 2015, American Chemical Society. (C) (a) JMSNM fabrication technique, and (b-d) SEM images of JMSNMs in 50 nm, 80 nm, and 120 nm sizes. Reproduced with the permission from [50], Copyright 2016 American Chemical Society. (D) SEM image of self-assembled 5 μm spherical particles, highlighting a metal-coated Janus particle array with a catalytic platinum layer and a magnetic $(Co/Pt)_5$ multilayer stack. Reproduced with the permission from [52], Copyright 2012 American Chemical Society.

chemical vapor deposition in the work of Wang *et al.*[60] Zheng *et al.* created a modular anisotropic electrodeposition technique to construct an environmentally responsive modular microrobot (MMR) that measures between 500 μm and 3 mm after contraction. Such an MMR would then change shape into different forms depending on the attached materials at different portions and due to the electric field pattern modulation. The shape-morphing process will depend on different thickness, electrodeposition time, and current density conditions. A lower current density results in reduced cross-linking and increased swelling after the hydrogel shrinks, whereas a greater current density gradient improves the self-shaping ability of the hydrogel microstructures formed. Therefore, due to the shape of the microelectrode, the direction of the electrical field, and current density distribution, it is possible to preprogram different kinds of 3D shape morphing into relatively simple microstructures.[61]

Electrodeposition has been well embraced because it is relatively inexpensive, highly efficient, and highly accurate; hence, it has wide applications for the manufacture of MNRBs using diverse materials and at varying scales. However, the designs and configurations of the MNRBs are highly restricted due to limited control over morphology.[41]

2.2 Advanced fabrication techniques

As fabrication techniques advance, it is crucial to explore innovative approaches that improve our ability to construct complex structures using molecular and nanoscale components in a systematic way. The following sections will discuss the emerging opportunities, benefits, and challenges associated with integrating self-curling/crimping, self-assembly, and 3D printing in the development of MNRBs.

2.2.1 Self-crimping and self-assembly

Self-crimping, a top-down approach, and self-assembly, a bottom-up approach, are promising techniques for fabricating MNRBs with exceptional levels of organization, complexity, and functionality. The self-crimping technique is based on variations in properties like strain and stress distribution between material layers, which are introduced during

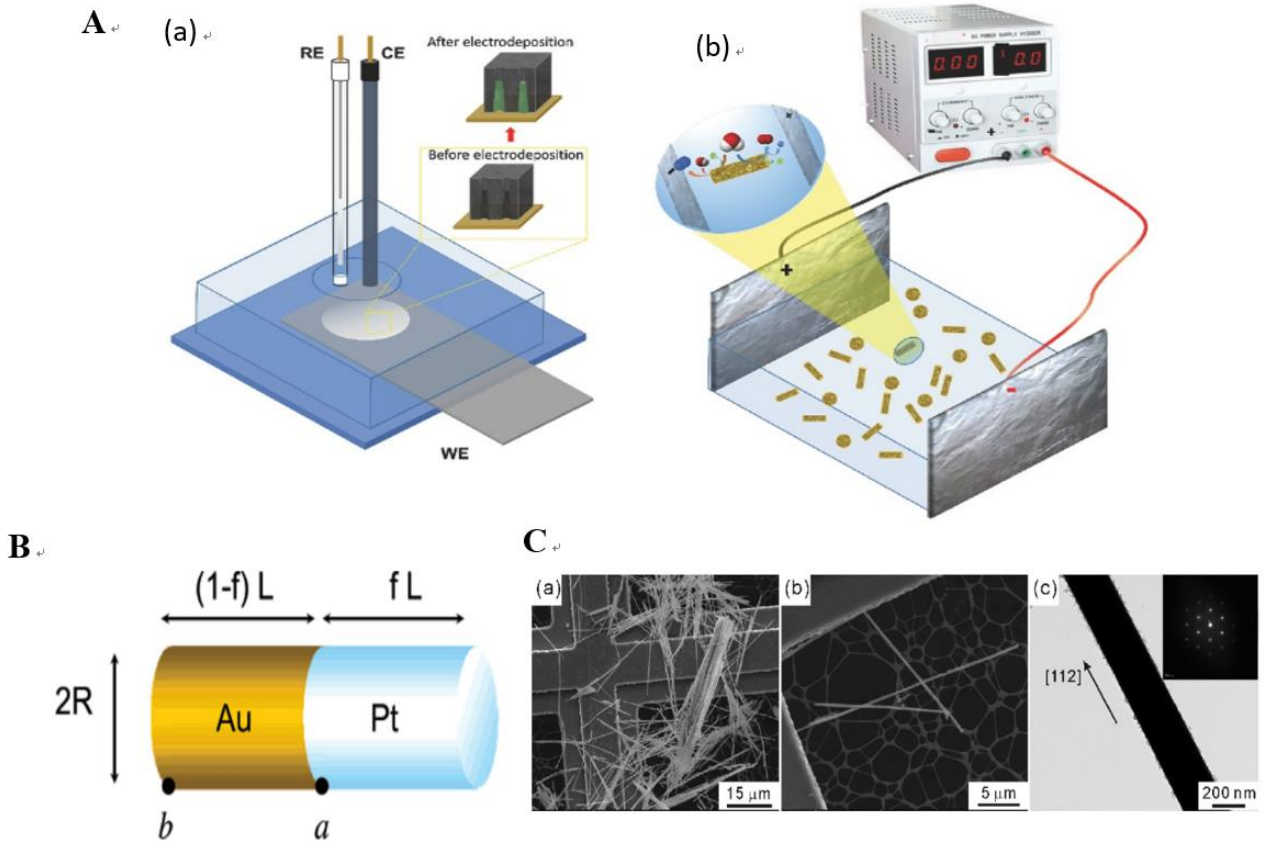

Fig. 2 Electrodeposition. (A) Diagram illustrating (a) template-based and (b) template-free electrochemical fabrication techniques for MNRBs. Reproduced with the permission from [54] Copyright 2017 WILEY VCH Verlag GmbH & Co. KGaA, Weinheim. (B) Diagram of a Pt/Au nanorod. Reproduced with the permission from [58], Copyright 2004 American Chemical Society). (C) SEM and TEM images of free-standing Ni nanowires: (a) on TEM grids, (b) single nanowires at 200 nm diameter, and (c) nanowire at 260 nm diameter. Reproduced with the permission from [59] Copyright 2010 American Chemical Society.

Table 1. Overview of various traditional techniques for MNRB fabrication.

Method	Principle	Resolution	Structure of MNRBs	Material composition	Advantages	Disadvantages	Ref
Physical vapor deposition (PVD)	Vaporizes solid or liquid materials in a vacuum and condenses them into thin layers on a substrate	< 5 nm	Spherical and helical configuration	Metals and metal alloys	Fabricating intricate designs of MNRBs	High equipment and maintenance of vacuum conditions are required, as well as the complexity of the process.	[41,46,48,62]
Electrical deposition	Applies electric potential to reduce metallic ions at the cathode, allowing deposition and structure formation		Tubular and rod-like configuration	Metals and metallic ions	High precision and efficiency, low cost	Highly restricted designs and configurations of MNRBs	[41,54,57]

deposition. Regardless of the material or the source of strain, the process involves removing a sacrificial layer to release internal tension within the thin film. This tension then causes the 2D film to fold into 3D spiral or tubular structures, as depicted in Fig. 3A.[41,63,64] Schmidt *et al*. proposed two methods. The first utilizes localized tension that bends the film as it detaches from the surface, creating a tube; the second relies on differences in lattice constants between two layers,

where the resulting stress spontaneously forms a tubular structure.[65]

Self-assembly in nanofabrication is an important process as it allows miniaturized elements to form desired structures. This is a reversible process in which disordered systems spontaneously arrange themselves in ordered patterns, stabilized by non-covalent interactions, including hydrogen bonds, van der Waals forces, hydrophobic interactions, and ionic bonds. Inorganic self-assembled nanostructures can take the form of various configurations such as films, spherical forms, tubes, *etc*. It is a spontaneous process whereby the molecules or nanophase entities get organized into stable, structured forms that balance the interfacial energy between their core composition and the surrounding solvent.[66] The building blocks go beyond atoms and molecules to the different nanostructures of variable composition. Certain distinctive characteristics of self-assembled monolayers render them advantageous for the construction of MNRBs, the creation of 3D structures, and in the incorporation of wanted components through encapsulation. The method offers a resolution of less than 5 nm.[48] One of the prominent techniques for developing multilayer structures is the layer-by-layer (LBL) self-assembly technique, which involves oppositely charged material layers deposited one over the other. The process utilizes a large range of materials, including organic and inorganic substances to colloids and macromolecules. LBL technique can be applied to different solvent accessible surfaces using various templates.[62,67-70]

Nanotechnology, drawing inspiration from biological systems, uses molecular components that self-assemble through a bottom-up approach to form organized structures. These structures have applications in drug delivery and other clinical applications. This process is adaptable, allowing for the inclusion and controlled release of drugs within the nanostructures as they are being created. It merely means that such ordered aggregates or networks arise spontaneously due to electrostatic, chemical, and other surface property interactions from a disordered system without any external guidance.

Flagella are structures that enable bacteria to move. Inspired by the movement of bacteria by using this organelle, Zhang *et al*. developed artificial bacterial flagella (ABF) that can be controlled in movement. These helical devices mimic the low-Re-number swimming technique used by bacteria and offer a new swimming mode that is particularly useful for targeted drug delivery to specific disease sites. As depicted in Fig. 3B, an ABF consists of a helical tail, which in size and shape is close to an exact replica of a natural flagellum, in combination with a ferromagnetic metal head. ABFs were created using a self-curling method. The process begins by growing a temporary layer of AlGaAs and a bilayer of InGaAs/GaAs on a GaAs (001) wafer through molecular beam epitaxy (MBE). A 15 nm layer of chromium is then deposited using e-beam evaporation. This trilayer of InGaAs/GaAs/Cr is patterned into a ribbon structure for the helical tail via reactive ion etching (RIE). The ferromagnetic head is created by evaporating thin films of Cr/Ni/Au, followed by a lift-off technique. Finally, the AlGaAs layer is removed with a 2% hydrofluoric acid (HF) solution, allowing the structure to be released and the 2D films to self-assemble into ABF.[71] Celi *et al*. have proposed an artificial elastomer-based sperm-like nanobot, as shown in Fig. 3C, fabricated by a straightforward self-assembly process with Fe_3O_4 nanobeads and flexible polymer flagella. This innovative nanobot can move on its own using a bidirectional flagellum in rotating magnetic fields. It was created through a template-assisted electrochemical method that deposited Au/PPy nanowires with tails modified with streptavidin, which are attached to biotin-coated magnetic nanobeads, resulting in sperm-like nanobots. When activated in thick glycerin, this self-assembled nanobot efficiently moves both forward and backward.[72] Magdanz *et al*. created magnetic bioinspired microbots called iron oxide nanostructured sperms (IRONSperms) by electrostatically combining non-motile sperm cells with magnetic nanoparticles (see Fig. 3E). These soft magnetic microswimmers imitate the movement of active sperm cells. Incorporating the biological component into the microrobots not only shapes them but also offers advantages for efficiently delivering chemotherapy drugs to specific targets.[73]

Alongside biologically-based and biomimetic MNRBs, other MNRBs have been developed using different materials and designs. For example, Peng *et al*. described the self-assembly of hematite-based micro-robots with various morphologies, which include walnut-like structures and microchains, as shown in Fig. 3D. These autonomous, light-driven hematite/Pt microrobots have been created in various cubic and walnut-like shapes using a hydrothermal method, followed by the addition of Pt layers to form Janus structures. The cubic hematite/Pt microrobots, due to their unique crystal orientation and magnetic properties, self-assemble into organized microchains, in contrast to the random clustering seen in walnut-like microrobots.[74]

Although the self-crimping technique is useful, it is primarily limited to creating simple 2D structures, making the large-scale production of complex MNRBs challenging and tedious. In contrast, the self-assembly technique offers benefits such as material compatibility, cost-effectiveness, and ease of use. However, it also has drawbacks, including being time-consuming, inefficient, and restricting the variety of shapes and structures available for MNRBs.[41]

2.2.2 3D Fabrication of Micro/nanobots

3D printing is among the most sophisticated technologies for manufacturing, where 3D structures are created by layer-by-layer deposition of materials, guided by predefined 3D models using Computer-aided design (CAD) and Computer-aided manufacturing (CAM). CAD/CAM software assists in designing, analyzing, reviewing, and documenting design models.[75] This method has revolutionized the production of advanced materials since its introduction in 1986 as

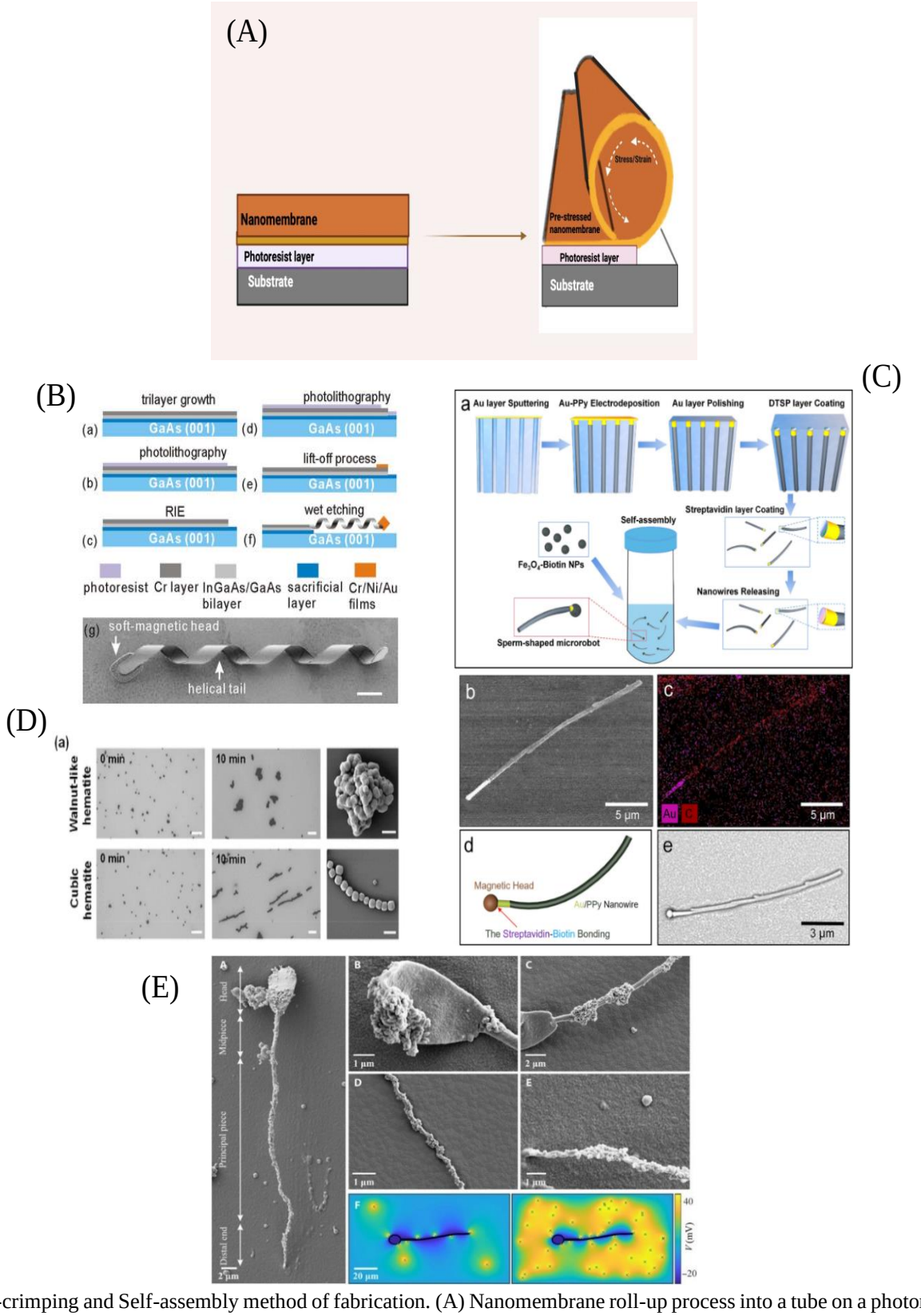

Fig. 3 Self-crimping and Self-assembly method of fabrication. (A) Nanomembrane roll-up process into a tube on a photoresist surface. (B) (a-f) Steps for fabricating an ABF with an InGaAs/GaAs/Cr helical tail, (g) FESEM image of a free-standing ABF. Reproduced with the permission from [71] Copyright 2009 American Institute of Physics. (C) a) Self-assembly of sperm-like nanorobots with Au/PPy nanowire, b-c) SEM images, and EDS analysis. Reproduced with the permission from [72] Copyright 2021, Celi *et al*,). (D) a) Walnut-shaped and cubic microrobots self-assemble in pure water. Reproduced with the permission from [74] Copyright 2022 American Chemical Society. (E) Cryo-SEM image of a sperm cell coated in 100-nm iron oxide nanoparticles, detailing the head, midpiece, and attachment distribution influenced by charge balance. Reproduced with the permission from [73] Copyright 2020 The American Association for the Advancement of Science.

Table 2. Features of the self-crimping and self-assembly fabrication method for MNRBs.

Method	Principle	Resolution	Structure of MNRBs	Material composition	Advantages	Disadvantages	Ref
Self-crimping	Uses strain differences to create stress, causing sacrificial layer erosion and tension release		Spiral and tubular configuration	Metals, semiconducting materials, and polymers	Effective and user-friendly	Highly restricted designs and configurations of MNRBs	[41]
Self-assembly	Uses layers of oppositely charged materials to form multilayer structures through weak interactions	< 5 nm	Tubular, walnut-shaped, nanowire, spherical	Metals, polymers, and biological entities	Inexpensive, Easy to operate, Compatible with diverse materials	Lengthy process, lacks efficiency, highly restricted designs and configurations of MNRBs	[41, 48, 72-74]

stereolithography for science and engineering. 3D printing technologies hold great potential for producing high-resolution MNRBs with intricate structures, using a variety of ink materials through different fabrication processes. The inks can be organic, inorganic, and cell-laden living materials, thus making it convenient to directly 3D print customizable and complex components. Also, with the combination of CAD/CAM, 3D printing is used to create even more intricate megastructures. Beyond these unique advantages, which it has in comparison with traditional methods of fabrication, 3D printing allows for an enabled, customized, precise 3D production with high reproducibility and automation using diverse materials with multiple dimensions to create an object that contains specific properties and functions. Design errors commonly encountered in traditional fabrication methods can be identified and rectified early in product development by easily creating and adjusting 3D models on a computer, thus avoiding expensive and complex corrections. 3D printing is extensively utilized across a variety of sectors, including the automobile industry, chemicals, food, pharmaceuticals, healthcare, and robotics, due to its numerous advantages.[76] The combination of the advantages of mobile robotics and 3D printing is significantly enhancing the development of MNRBs in the field of artificial micromachines for clinical applications. Today, 3D-printed microfluidics have attracted significant interest due to advantages like rapid production, cost efficiency, and precise design capabilities, which extend to complex geometries in device manufacturing.[77]

As per ASTM standard F2792-12a, 3D printing technology is categorized into seven types: (i) material extrusion, (ii) inkjet printing, (iii) binder jetting-3D powder printing, (iv) sheet lamination-laminated object manufacturing, (v) vat photopolymerization-Stereolithography (SLA), Two photon polymerization (TPP), Digital light processing (DLP) and Continuous liquid interface production (CLIP), (vi) powder bed fusion-selective laser sintering; and (vii) direct energy deposition.[76] Among these techniques, material extrusion, inkjet printing, vat photopolymerization, and powder bed fusion are widely utilized for creating MNRBs. The choice of a particular method is influenced by the materials used and the specific applications. Further details on these techniques and their uses are provided in the following sections.

2.2.2.1 Material extrusion-based 3D printing (ME3DP)

Material extrusion-based 3D printing (ME3DP) is currently the most common 3D printing platform, mostly using fused deposition modelling technology (FDM). Similar to other 3D printing techniques, the parts produced through ME3DP very often show anisotropy of their physical properties; in other words, the material's mechanical properties are influenced by the orientation of the build process.[78]

This widely recognized process entails the controlled dispensing of material through a nozzle or orifice, as illustrated in Fig. 4A. This technology can be divided into three primary printing methods: hot melt extrusion, filament extrusion, and syringe extrusion. Each method involves a phase change as the material exits the nozzle, either cooling or evaporating to settle on the substrate. In hot melt extrusion, semi-molten material is forced through a nozzle, where the polymer is melted, mixed, and extruded using heated screws. It is widely applied in printing gels and pastes at different temperatures to make solid dispersions containing active pharmaceutical ingredients (APIs). In filament extrusion, a solid polymer filament is driven through rollers into a heated chamber, where it melts into a semi-liquid form before being directed out through a nozzle. It cools and solidifies on the substrate, allowing subsequent layers to be built on top of it. In case of syringe extrusion, semi-molten materials like gels and pastes are forced via a nozzle using a plunger. After forcing, they are then dried.[79-81]

Depending on the characteristics of the materials utilized, extrusion-based printing can further be divided into two primary types: fused deposition modeling (FDM) and direct ink writing (DIW).[82] FDM is a widely utilized method, particularly for printing thermoplastic materials such as Polylactic acid (PLA) and Polycaprolactone (PCL). It relies on the heating of the polymer to such a temperature that it melts and becomes soft, followed by extrusion through a structured

mechanism that restricts its movement. Thus, allowing the material to cool and set into the intended form on a platform. In the process of extrusion, a heated liquefier melts the filament and pushes it through to the nozzle. A stepper motor moves the liquefier and print head assembly across the platform in the XY plane to deposit the melted filament. After each layer is laid down, either the platform lowers or the print head raises along the Z-axis by the height of one layer. This layering continues until the entire 3D structure is complete.[83-86] In contrast, DIW technology uses a computer-controlled nozzle that moves in 3D along the X, Y, and Z axes, extruding material under pressure to construct geometric shapes layer by layer. The ink used in DIW must have specific rheological properties, including viscosity, shear stress, compressive stress, and elastic modulus. It is crucial to maintain control over all these parameters.[87]

Light extrusion 3DP allows for the straightforward fabrication of soft microrobots at resolutions down to 150 µm. By using the appropriate ink, which can be photopolymerised, a 3D structure can be printed and permanently stabilized with light curing either during printing or in a post-processing step. The most flexible method for material choice and multi-material capabilities is DIW. These features have made DIW a promising technology in 3D printing, particularly for materials capable of deformation and of great use in biomedicine.[82] For instance, Chen *et al.*[88] developed the biodegradable magnetic hydrogel robot (BMHR) using bio-safe materials through a simple extrusion method, followed by drug functionalization. Fig. 4B shows the creation and analysis of the biodegradable microrobot, known as BMHR. This robot, shaped like a peanut, is primarily composed of biodegradable gelatin and biocompatible Fe_3O_4 nanoparticles. Its size and composition can be easily adjusted through a simple extrusion technique, which also allows for the incorporation of various drug-loaded microparticles. In contrast to current miniature robots, the BMHR provides multiple modes of movement, high biocompatibility, and considerable potential for drug delivery, demonstrating promising therapeutic effects in treating colon cancer.[88] Material extrusion is a cost-effective, fast, and straightforward technique that achieves a resolution of 5 to 200 µm. However, it has some limitations, including low precision, slower production rates, potential for drug degradation, weak structural integrity, restrictions to thermoplastics, rough surface finishes, and high temperatures that may not be suitable for cells.

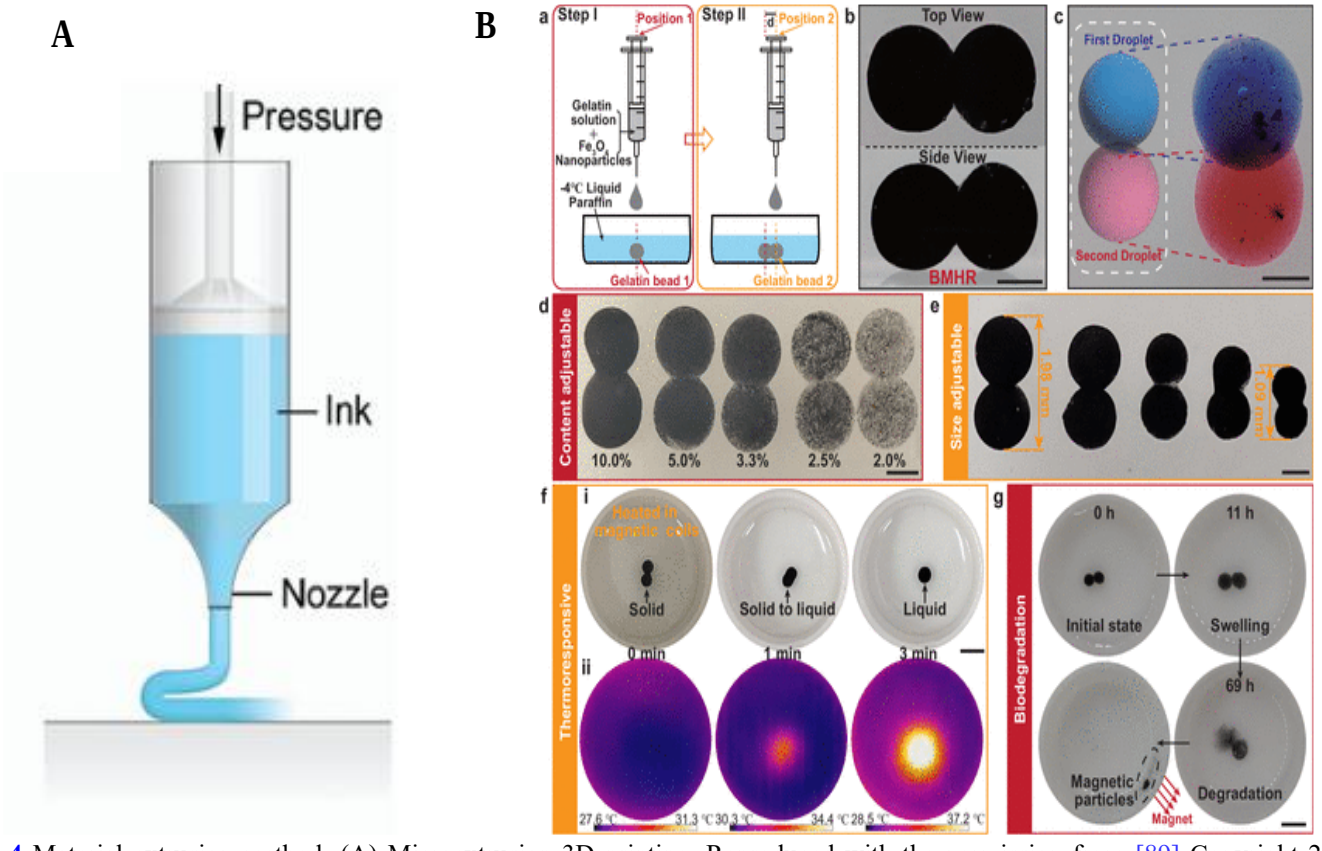

Fig. 4 Material extrusion method: (A) Microextrusion 3D printing. Reproduced with the permission from [89] Copyright 2020 American Chemical Society. (B) Production and analysis of BMHR (a) Illustration of the BMHR production process, (b) BMHR photograph, scale bar 500 µm, (c) Structure of BMHR without Fe_3O_4 nanoparticles, scale bar 500 µm, and (d) BMHR image showcasing various contents, scale bar 500 µm, (e) BMHR demonstrating size adjustability, scale bar 500 µm, (f) Gel-sol transition images showing thermoresponsive ness, scale bar 2 mm, and (g) Biodegradation sequence of BMHR, scale bar 2 mm. (Reproduced with the permission from [88], Copyright 2023 American Chemical Society.

2.2.2.2 Inkjet-based 3D printing (I3DP)

Inkjet-based 3D Printing (I3DP) is a contactless method whereby digital information from a computer is transformed into a physical form on substrates using ink droplets. The inkjet technique was an initial material-efficient technique for depositing materials, particularly liquid inks composed of a solute that is dissolved or distributed within a solvent. This method involves ejecting a precise volume of ink released from a reservoir through a nozzle, which is triggered by a rapid contraction of the chamber due to piezoelectric effects. When an external voltage is applied, piezoelectric action causes contraction in the liquid-filled chamber, which produces a shockwave, forcing the ejection of one liquid droplet from the nozzle. The inkjet droplet falls due to gravity and air resistance until it lands on the substrate, spreading out from its motion and aided by surface tension. It eventually dries as the solvent evaporates. Inkjet printing technologies are mainly divided into two categories: continuous inkjet (CI) and drop-on-demand (DOD) systems. As shown in Fig. 5A, CI systems continuously deliver ink through a nozzle, where it breaks into tiny droplets due to Rayleigh instability. Such droplets can be electrically charged and deflected by an electrostatic or magnetic field. Uncharged droplets are then caught by a catcher. In contrast, DOD systems create droplets on demand. The needed number of individual droplets is ejected by the printhead through thermal or piezo-electric mechanisms. The printhead is positioned mechanically to achieve accuracy in droplet placement. Inkjet 3D printing is gaining importance as one of the main techniques for polymeric material deposition in a customized fashion. The viscosity, which depends on the molar mass of the applied polymer, was recently shown to critically affect the spreading behavior and final shape of the printed drop.[90,91] Inkjet printing is effective in transferring digital data not only onto materials like paper and transparencies but also for creating 3D multilayer structures and functional arrays that include nucleic acids and proteins, such as enzymes. This technology has already shown its ability to fabricate energy-driven micromachines, including bio-friendly micro-rockets and stirrers.[92-95]

Gregory *et al*. developed silk-based microrockets powered by enzymes, utilizing inkjet printing, as shown in Fig. 5B. These microrockets exhibited autonomous movement in various fluid environments, including complex ones like human serum. The use of digital inkjet printing enables precise control over the distribution of catalysts, allowing for different trajectory behaviors. These microrockets, made from silk scaffolds containing enzymes, offer excellent biocompatibility and resistance to biofouling.[96] Bernasconi *et al*. showed that integrating inkjet-assisted lithography (IAL) with electroforming provides a scalable and cost-effective way to create disk-shaped ferromagnetic micromotors, as illustrated in Fig. 5C. They produced and characterized Ni and CoNiP devices, which could be actuated in swarms of hundreds, demonstrating controllable movement with multiple degrees of freedom. Coated with polypyrrole, the micromotors were also used for drug delivery, successfully loading and releasing Rhodamine B.[97] Descombes *et al*. showcased DOD inkjet printing of polymer composites with Fe_3O_4 nanoparticles to form spherical cap structures on flat and patterned glass substrates. Confining these structures on pedestals increased their aspect ratio by more than three times. Thicknesses of up to 88.8 μm were achieved with thermal curing to bypass UV limitations. In the next step, the structures were exposed to a magnetic field before curing, aligning the Fe_3O_4 nanoparticles into dense magnetic patterns.[98] The droplet-based inkjet printing method provides limited control over the shape of printed structures, with a resolution ranging from 5 to 200 μm. Although it offers fast printing, the interlayer adhesion is often weak.

2.2.2.3 Vat photopolymerization

A process that selectively solidifies a liquid photopolymer in a vat through light-induced polymerization is Vat photopolymerization. Photopolymers like photo-cross-linkable hydrogels and photoresists are crucial ink materials in these methods. In light-cured 3D printing, photoresists are key and come in two types: positive, where unexposed areas remain, and negative, where exposed areas are retained. This process is mainly categorized into the following types: Stereolithography (SLA), direct laser writing (DLW), digital light processing (DLP), and continuous liquid interface production (CLIP).

2.2.2.3.1 Stereolithography (SLA)

Stereolithography (SLA) is the most extensively researched vat polymerization method in the medical and pharmaceutical sectors and was the first 3D printing process developed. It works by using a liquid resin that, when exposed to high-energy light (often UV), undergoes polymerization and is activated by a photoinitiator to harden the material. The SLA setup is depicted in Fig. 6. The setup comprises a container filled with photocurable liquid resins, a UV laser source to initiate photopolymerization and liquid resin cross-linking, a system to provide horizontal movement to the laser beam, and a system providing vertical movement to the fabrication platform.[76,99,100] SLA printing involves two primary approaches: the top-down and bottom-up methods. In the top-down approach, the UV light source is positioned above the resin tank, with the build platform descending incrementally as each layer is solidified. The platform is initially submerged to some depth that corresponds to the thickness of the layer, and UV light solidifies the resin at some points. As layers form, the platform lowers incrementally. In the bottom-up method, the UV light is located at the lower part of the resin tank with a transparent window above, and the platform moves upward as layers form. After printing, the typical process involves washing the product with isopropanol to remove any excess resin, followed by UV light curing to harden the structure and finalize the polymerization. This step becomes very important in eliminating free radicals, which could have

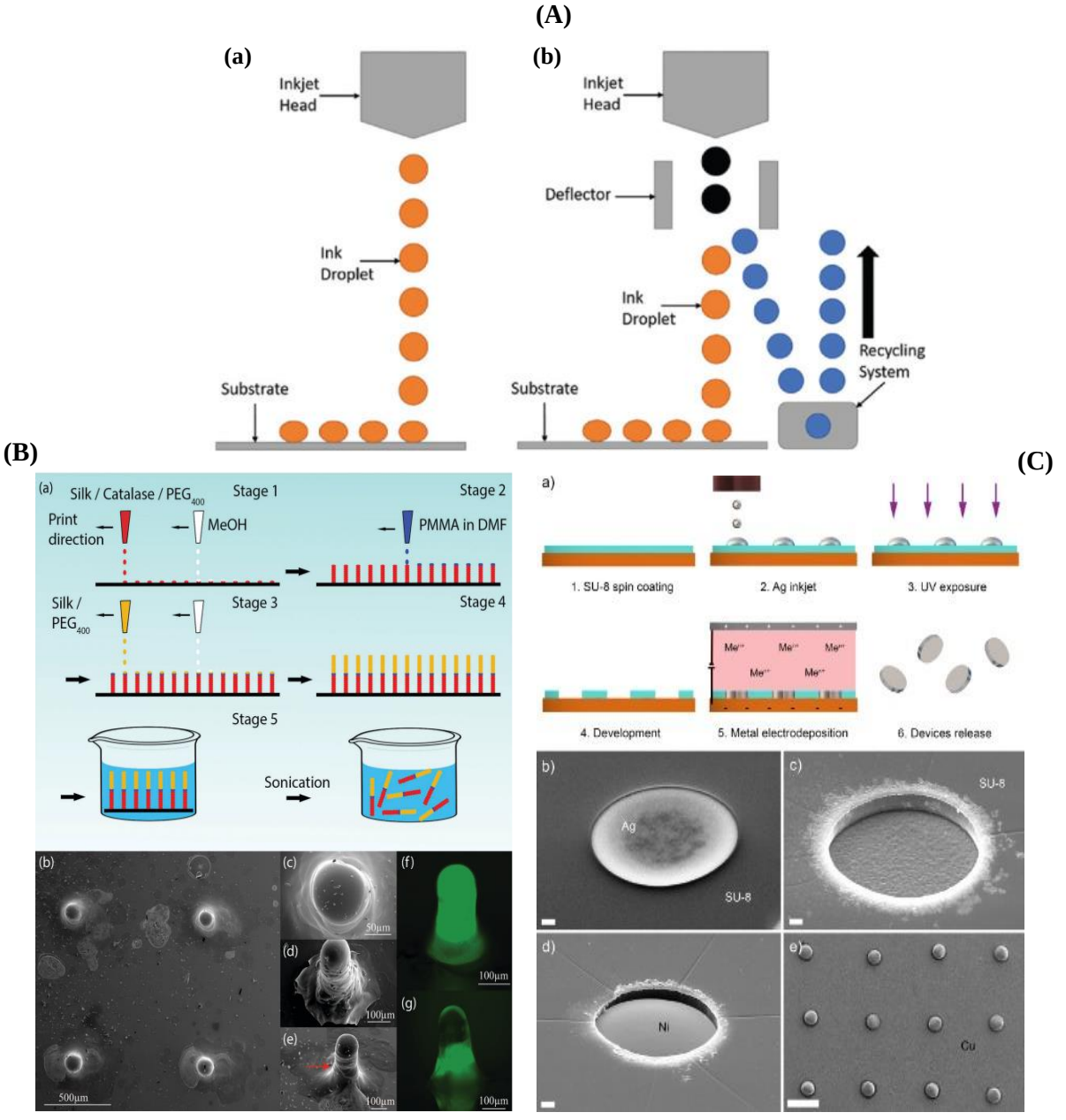

Fig. 5 Inkjet 3D printing. (A) (a) Drop on demand and (b) Continuous inkjet printing. Reproduced with the permission from [99] Copyright 2022, Mancilla-De-la-Cruz *et al*.) (B) (a) Diagram of the RIJ process for catalytic microrocket fabrication, (b) Overview of the RIJ array for silk-based rockets, (c-e) Close-up views of active silk-based and Janus microrockets. Fluorescence microscopy images: (f) single-ink symmetric microrocket and (g) Janus microrocket. Reproduced with the permission from [96], Copyright 2016 Gregory *et al*. Published by WILEY-VCH Verlag GmbH & Co. KGaA, Weinheim. (C) (a) Key steps in IAL production on a copper substrate, (b) SEM image of silver droplets printed on an SU-8-layer, (c) SEM image showing polymer cavities post-SU-8 development, (d) SEM of nickel-filled cavity used as a mask, and (e) SEM image of nickel devices on copper after removing SU-8 layer. Reproduced with the permission from [97], Copyright 2024 Bernasconi *et al*. Published by Elsevier. Ltd.

potential genotoxicity. Although most free radicals are removed, biocompatible resins remain necessary for use in human applications, be it tablets or implants.[101]

SLA allows precise control over internal structure and porosity, offering versatility in the composition, design, and geometry of biomaterial implants. This capability supports its use in areas like cell growth, tissue engineering, and therapeutic treatments.[102] Numerous examples of scaffold fabrication using SLA for clinical applications have been presented in the literature. To improve nerve regeneration, Li *et al*. fabricated a biodegradable composite for the controlled release of bioactive factors. They employed a co-axial electrospraying technique to create poly lactic-co-glycolic acid nanoparticles that encapsulated bovine serum albumin (BSA) and nerve growth factors. For the first time, these core-shell nanoparticles were integrated into SLA-printed nerve scaffolds to provide nano-topology and deliver bioactive molecules sustainably, promoting enhanced nerve

regeneration.[103] Other examples include Lee *et al*.'s creation of cartilage scaffolds with controlled porosity using 3D SLA,[104] Guillaume *et al*.'s biodegradable composite scaffolds with osteopromotive properties,[102] and Zhou *et al*.'s biphasic scaffold using nano-hydroxyapatite and transforming growth factor (TGF)-beta1 nanoparticles.[105] SLA has also been applied to functionalized dental prosthetics, including Totu *et al*.'s antibacterial nanocomposite prosthesis made from polymethyl methacrylate (PMMA) and TiO_2 nanoparticles.[106,107] Besides its use in tissue engineering, SLA has also been utilized to create drug delivery systems. Sharma *et al*. developed a delivery system that was able to withstand the chemically and mechanically aggressive environment across the gastric area and release drugs in the small intestine for enhanced absorption.[108] Ochoa *et al*. created an innovative print-and-shrink fabrication technique that included the combination of 3D SLA and Hydrogel casting for creating complexly shaped polymeric microneedles.[109] For transdermal delivery of a chemotherapeutic drug, dacarbazine, drug-loaded microneedle arrays were fabricated by Lu *et al*. by employing multi-material micro stereolithography.[110]

Micro stereolithography offers key benefits in biomedical manufacturing, such as 10 µm resolution, high precision, compact machinery, and fine surface finishes for micron-scale structures. However, current printers have resolution limits that affect the downscaling of objects, limiting MNRB production. The method also has drawbacks like high costs, required post-processing, and limited biocompatible materials. Despite these challenges, it holds promise for nano- and micro-structure fabrication. Although less accurate than DLW, SLA can produce microscale molds that are useful for microrobot fabrication when combined with other techniques.[111-113]

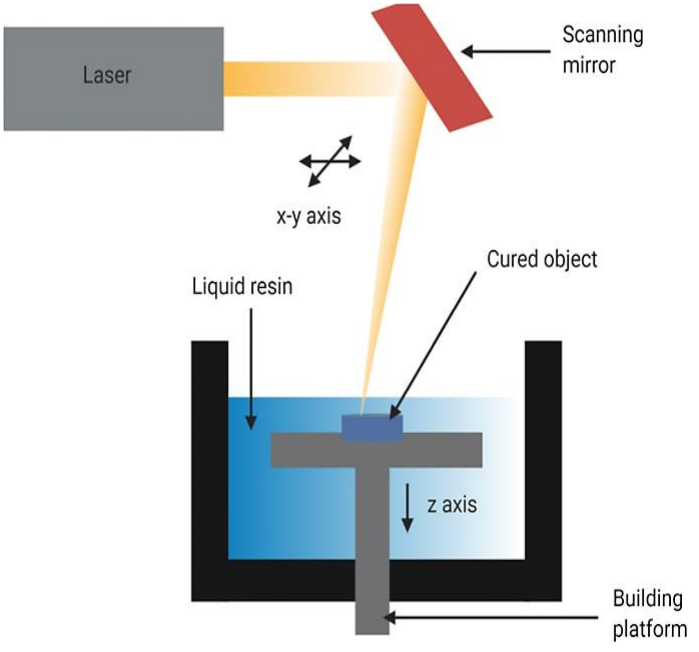

Fig. 6 Stereolithography. (A) Schematic diagram of the stereolithography setup. Reproduced with the permission from [114] Copyright 2021, Vaz *et al*.)

2.2.2.3.2 Direct laser writing (DLW)

Another cutting-edge technology that allows for the development of intricate structures with a resolution of up to 100 nm is Direct laser writing (DLW), which uses multi-photon polymerization (MPP). One of the basic principles of its work is the nonlinear absorption of photons by photopolymers via the tightly focused ultra-fast laser beam inside transparent material and two-photon absorption, locally polymerizing it. Following a preprogrammed path from a CAD/CAM model, a detailed micromodel of the design can be fabricated.[115-120] The DLW system consists of three main components (see Fig. 7A): (i) a laser source, (ii) a beam delivery system, and (iii) a substrate or target mounting system. In this process, a focused femtosecond pulsed laser generates high local intensity at the focal point within a photosensitive liquid that contains a mix of monomeric matrix molecules and a photoinitiator. When exposed to light, positive photoresists become more soluble and can be washed away with a developer, leaving behind the unexposed areas. Conversely, regions exposed to negative photoresists undergo polymerization, making them less soluble and allowing them to remain intact while the unexposed parts are washed away.[76] This high local intensity gives rise to the simultaneous absorption of two photons, leading to photochemical cross-linking. Since this cross-linking process is localized, arbitrary continuous 3D structures could be created by moving the laser focus through the liquid material. DLW techniques are typically divided into three main types: Laser direct-write subtraction method involves removing material through ablation, laser direct-write modification approach modifies the material to achieve a specific effect, and in this process of laser direct-write addition, the laser is used to add material.[121]

Recently, two-photon polymerization (TPP) has been in the limelight for printing 3D shapes at the micro level, which is quite significant in the case of medical, electrical, and sensing devices.[122] TPP enables the fabrication of a vast array of medical devices, such as microneedles,[123] prosthetic devices,[124] and supports for tissue engineering.[125-128] By combining the TPP microfabrication with Polydimethylsiloxane (PDMS) micro-molding, Gittard *et al*. developed polymer-based microneedles designed for the delivery of insulin and other protein-based medications via transdermal route. This method primarily enabled an accurate replication of microscale features with a coherence length, although there is still substantial scope for the replication of even smaller features, such as tips of the microneedles. The compressive strength of eShell 200 microneedle arrays was sufficient for uses related to the transdermal delivery of drugs. The initial microneedle array was produced using TPP with SR 259 polymer, incorporating 2 wt % of Irgacure 369 photoinitiator on a glass cover slip.[123]

Several examples of MNRBs created using DLW in the biomedical field involve controlled and targeted delivery of cargo molecules. Various systems have been loaded with these molecules for both diagnostic and therapeutic purposes.[129-135]

Ceylan *et al*.[129] described a method for creating biodegradable microrobotic swimmers with a double helical design made from hydrogels. These microswimmers are activated by sensing the matrix metalloproteinase-2 (MMP-2) enzyme and are powered by magnetic forces. They are made by 3D printing nanocomposite materials that combine iron oxide nanoparticles with gelatin methacryloyl (GelMA). Gelatin serves as the matrix and is biodegradable with specific sites for MMP-2 cleavage. Once digested by the enzyme, these swimmers release magnetic contrast agents tagged with anti-ErbB-2 antibodies, targeting ErbB2 overexpressing SKBR3 cancer cells. This advancement brings us closer to developing mobile microrobots that can navigate and respond to their environment while performing specific diagnostic and therapeutic functions. Lee *et al*. fabricated a microrobot designed to address the challenges of current cancer treatment methods through magnetically controlled drug delivery systems. As shown in Fig. 7B, this microrobot has a helical structure that enhances its movement in high-viscosity fluids and is constructed from GelMA and polyethylene glycol diacrylate (PEGDA) materials. It is designed to encapsulate doxorubicin (DOX) for secondary release while having gemcitabine attached to its surface for initial release. Furthermore, magnetic nanoparticles (MNPs) are bonded to the surface to enable actuation via the external magnetic field.[136] In a separate study, Li *et al*. described a microbot drug delivery system, illustrated in Fig. 7C, aimed at controlled release. This microrobot features a 3D ellipsoidal structure that compartmentalizes two different drugs, acetylsalicylic acid (ASA) and DOX, allowing them to retain their individual properties while providing a combined therapeutic effect. It includes a magnetically driven framework with two biodegradable drug-carrying components: the head and the body. The external magnetic field regulates the biocompatible Fe_3O_4 nanoparticles embedded in the microrobot's structure, directing it to the target site for drug release. The drug-carrying components, made of GelMA, are designed to encapsulate ASA and DOX for protease-triggered release in targeted cancer therapy.[137]

DLW provides an ultra-high resolution of about 100 nm. Even though it requires very expensive equipment, DLW has wide applications for printing 3D microbots. The shape of printed microstructures can be easily altered by adjusting the laser beam focus trajectory. As a result, DLW is well-suited for the precise fabrication of microrobots used in clinical applications. However, DLW operates at a reduced manufacturing speed in comparison to other 3D printing methods and is restricted to producing microstructures with a maximum height of less than 1 mm, which could limit its future applications.[76]

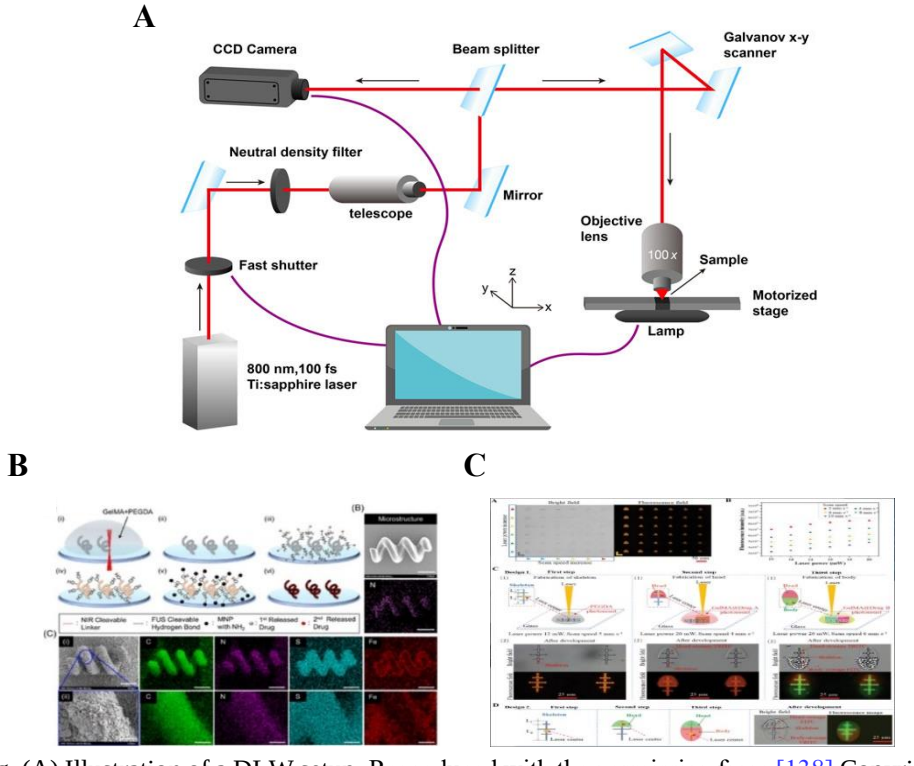

Fig. 7 Direct laser writing**.** (A) Illustration of a DLW setup. Reproduced with the permission from [138] Copyright 2024, Fu and Yu). (B) a) Overview of the fabrication process, b) SEM and EDS images of microrobots with a scale bar of 5 μm, and c) SEM and EDS images of the proposed microstructures with scale bars of 5 μm and 1 μm, respectively. Reproduced with the permission from [136] Copyright 2023, American Chemical Society. (C) (a) GelMA microstructures produced under different conditions, (b) a dot plot depicting the relationship between fluorescence intensity and laser power for these structures, and (c-d) fabrication steps alongside microscopy images showing "Design 1" and "Design 2" microrobot structures. Reproduced with the permission from [137] Copyright 2023, 2023 Wiley VCH GmbH).

2.2.2.3.3 Digital light processing (DLP)

Digital light processing (DLP) operates similarly to SLA by employing light to selectively crosslink photo resins layer by layer, creating self-supporting 3D structures. Unlike SLA, with DLP, each layer is exposed at one time due to the selectively masked light source. This process is less influenced by oxygen inhibition, as the polymerized layer consistently remains at the bottom of the vat and is not directly exposed to air.[76] The light sources for photosensitive materials are processed by optical micro-electromechanical technology-based chipsets in the DLP system. Fig. 8A illustrates the various components of a DLP setup. A fundamental component of the system is the digital micromirror device (DMD), which contains an array of micron-scale mirrors that can be manipulated to direct light onto photosensitive resin. These arrays can include nearly one to over two million mirrors, with pixel spacing measuring just a few microns. The resolution achieved in DLP-based 3D printing is determined by the projection plane managed by the DMD and lens, typically reaching micron-level resolution. The DMD chip generates dynamic bitmap images that are projected onto the photosensitive resin using UV light. An optical system with a projection lens ensures that the resin in the vat conforms to the mask pattern of each layer. This UV light triggers photopolymerization, solidifying the liquid polymer. Once photopolymerization is complete, the build platform, driven by a motorized stage, moves each layer in the Z-axis direction.[138]

DLP technology enables the rapid production of precise polymer models that can reach sizes of several centimeters in just a matter of minutes. Furthermore, it has greater flexibility when affecting variations in a large number of manufacturing parameters, which include printing time, light intensity, and light wavelength, among others, than other technologies of 3D printing.[139] Hence, areas where DLP is applied in printing include medical devices and models,[140] biodegradable and non-biodegradable implants,[141,142] functionalized devices,[143] and tissue engineering.[144,145] DLP-based 3D printing technology is utilized in developing drug delivery systems that provide tailored dosages, sizes, and shapes, as well as various release mechanisms. Tao *et al*. created microgels functionalized with nanoparticles aimed at addressing topical bacterial infections. These microgels were crafted with specific geometries using the DLP technique. Prior to the printing process, Polydiacetylene nanoparticles were blended into the gelatin-methacryloyl mixture to target and neutralize pore-forming toxins (PFTs). This integration allows the PFTs to penetrate the microgels, where they are subsequently captured and neutralized by the PDA nanoparticles. Following local injection into a mouse model, these microgels aided in the recovery of tissues affected by bacterial infections.[146] A photo-cross-linkable polymer matrix based on methacrylated O-acetyl-galactoglucomannan and nanocomposite lignin nanoparticles loaded with silver nanoparticles as the antimicrobial agent was used to formulate a bio-based antimicrobial resin for DLP printing by Tao *et al*.[147]

The DLP method has been utilized to fabricate structures for various biomedical applications, but limited work has been reported regarding nanostructured robotic systems fabricated via this technique for clinical applications.[148] Nevertheless, research is ongoing to assess the effectiveness and applicability of this method. For instance, Chen *et al*. developed 3D swimming artificial microfish utilizing the microscale continuous optical printing (mCOP) technique, a form of DLP 3D printing, using PEGDA hydrogels and various functional nanoparticles. Fig. 8B provides a schematic representation of this method. The nanoparticles included platinum for chemical propulsion, Fe_3O_4 for magnetic navigation, and polydiacetylene for toxin neutralization. These multifunctional 3D-printed microfish showcase the potential of bioinspired microrobots for biosensing and detoxification via wireless actuation.[149] DLP provides a resolution range of 25 to 100 μm. Rapid printing speed, combined with other advantages such as outstanding resolution and accuracy, cost efficiency, and the need for a smaller initial vat volume, makes DLP-based 3D printing one of the candidates for medical applications. However, it also has some drawbacks, particularly in terms of limited mechanical properties.

2.2.2.3.4 Continuous liquid interface production (CLIP)

CLIP is a state-of-the-art technology derived from digital light processing that has lately been gaining interest in both academia and industry because of its ability to fabricate models with high resolutions and complex geometries in a very short time. CLIP uses an oxygen-permeable build window (Fig. 9A) positioned beneath the UV projection plane at the base of the vat to establish a 'dead zone'-a thin layer of uncured resin where photopolymerization is inhibited between the build window and the solidified surface. The fundamental concept of this design is to eliminate the need for an intermediate photo resin recoating process between layers. The incomplete curing and tackiness of surfaces observed with most formulations is usually a result of oxygen inhibition in the course of photopolymerization in air. The oxygen can either quench the photoexcited photoinitiator or form peroxides with free radicals formed from the photoinitiator. Avoiding these inhibition pathways allows efficient initiation and propagation of polymer chains. CLIP allows for the formation of large overhangs without the need for supports, minimizing the staircase effect and achieving isotropic mechanical properties. As an emerging 3D printing technique, CLIP enables smooth structure fabrication at speeds up to 25–100 times faster than conventional methods, producing seamless, layer-free 3D objects with a 75 μm resolution. Johnson *et al*. employed CLIP to quickly prototype microneedles, as shown in Fig. 9B, allowing for a variety of sizes, shapes, and compositions, thereby demonstrating modular design flexibility. They created microneedle arrays using the biocompatible polymer trimethylolpropane

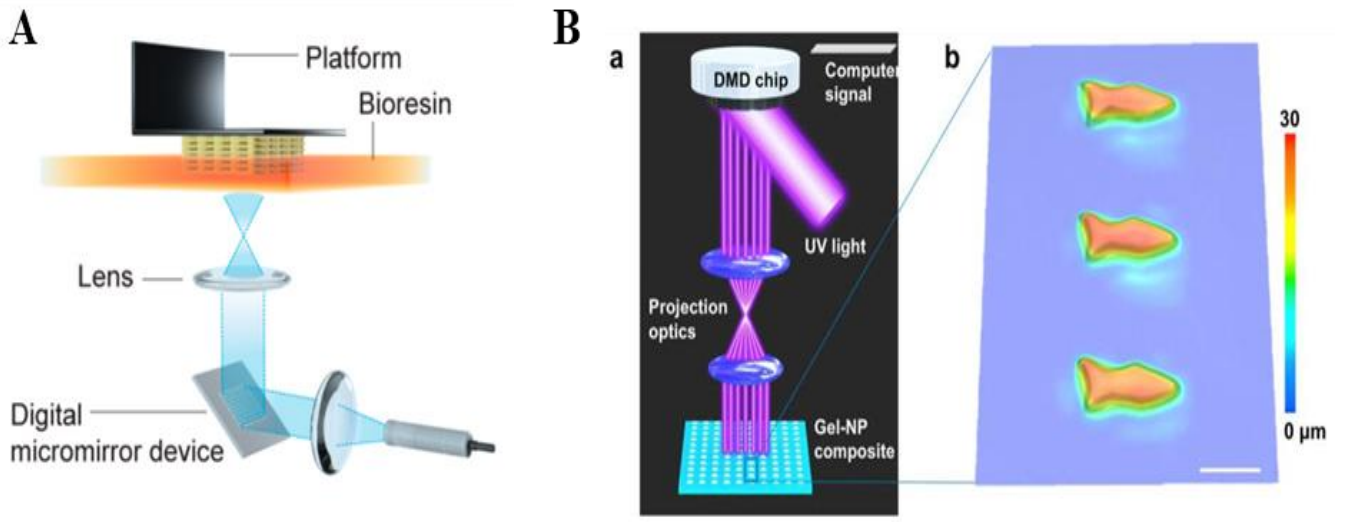

Fig. 8 Digital light processing (A) Illustration of the DLP fabrication method. Reproduced with the permission from [150], Copyright 2020 American Chemical Society (B) a) Schematic of mCOP method: UV light passes through DMD mirrors to project a pattern onto a photosensitive solution, forming the microfish layer by layer, (b) 3D microscopy image of a printed microfish array, 100 μm scale bar. Reproduced with the permission from [149], Copyright 2015 WILEY-VCH Verlag GmbH & Co. KGaA, Weinheim).

triacrylate, demonstrating that adjustments to size and shape could be made simply by modifying the CAD. The CLIP-based microneedles were able to penetrate murine skin, effectively delivering rhodamine and potentially facilitating faster clinical applications of microneedle technology.[151]

Even though CLIP has not yet been utilized for MNRB fabrication, its potential to form complex micro-scale formations describes huge potential for future MNRB fabrication.[76,99,151-153] This method presents benefits like a fast production rate and improved accuracy, but it also has some drawbacks, including the need for low-viscosity resins, possible toxicity issues, and high costs.

2.2.2.4 Powder bed fusion (PBF)

In the powder bed fusion (PBF) process, thermal energy selectively fuses targeted areas of a powder bed. After each layer is completed, the bed lowers by a specified thickness, a fresh powder layer is applied and smoothed by a roller, and the new layer is fused with the previous one. Selective laser sintering (SLS) is a well-known technique within the PBF category.

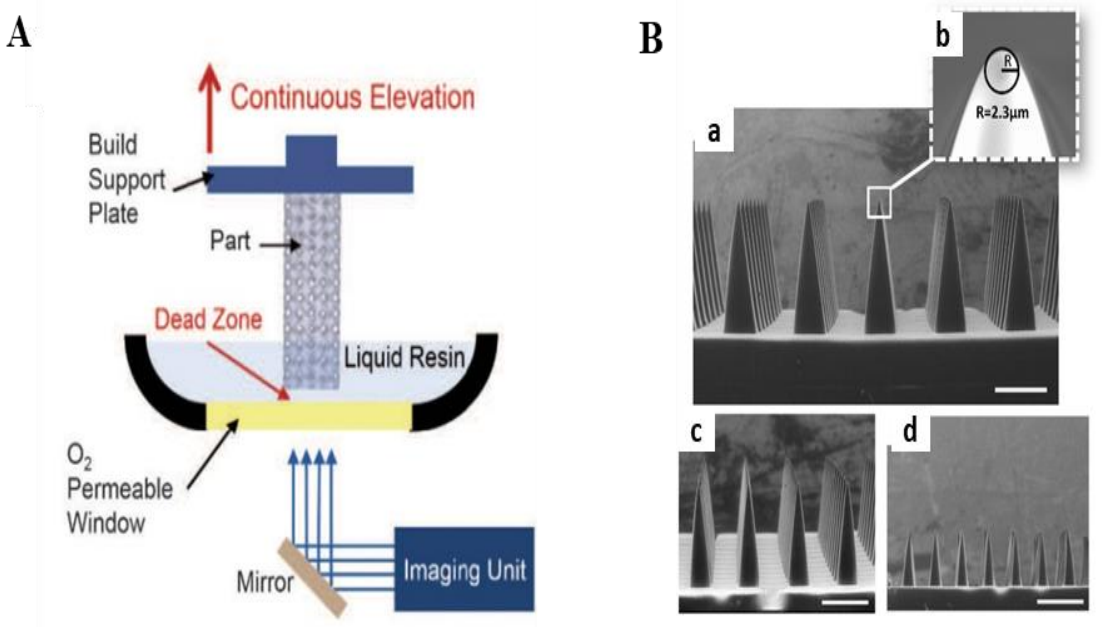

Fig. 9 CLIP (A) Schematic of CLIP printer. (Reproduced with permission from reference [154] Copyright 2015 American Association for the Advancement of Science). (B) TMPTA microneedles are available in heights of a, c, d) 1000 μm, 700 μm, and 400 μm, all with an aspect ratio (AR) of 3. b) An image shows a microneedle tip with a radius of about 2.3 μm. (Reproduced with permission from reference [151] Copyright 2016, Johnson *et al.*).

2.2.2.4.1 Selective laser sintering (SLS)

As a PBF additive manufacturing technique, SLS uses a high-powered laser to sinter or melt powder resin, metal, or polymer, fusing particles into a solid structure. The SLS process fuses the powder particles, which are heated by the laser, to form solid 3D objects. Fig. 10A illustrates the SLS setup, which includes a spreading platform, a powder bed, and a laser system. The powder is spread uniformly onto the platform. The laser, following a pre-designed pattern, will then scan, fusing particles below the melting temperature. The main steps that SLS has to go through are the following: (i) deposition of powder, (ii) solidification of the powder, and (iii) bringing the build platform down by one layer's thickness. For each new layer, it lowers the powder bed, and the process continues with the subsequent layers until the object reaches its final completion. By repetition of this cycle, the final 3D object will be produced. The product is then cooled and removed from the loose powder. The final product is attained through shaking and sieving off the excess powder. In the processing chamber, high temperatures are kept just below the powder's softening point to minimize processing time, which also reduces thermal stress and distortion. Unsintered powder particles act as support material, allowing for the creation of intricate structures with a resolution of 45 µm.[76,154-157]

SLS is a very attractive rapid prototyping technique for tissue-engineered scaffolds, as it permits control over the pore structure, pore size, and customized design of the scaffold.[158,159] Shuai *et al*. described the creation of composite porous scaffolds made from Poly(lactide-co-glycolide) (PLGA) and nano-hydroxyapatite (nano-HAP) that feature a precisely engineered pore structure and significant exposure to bioactive ceramics at the scaffold's surface, achieved through selective laser sintering.[160] Similarly, Duan *et al*. developed 3D nanocomposite scaffolds using calcium phosphate/poly(hydroxybutyrate-co-hydroxyvalerate) and carbonated hydroxyapatite/poly (l-lactic acid) nanocomposite microspheres through selective laser sintering. These scaffolds displayed a well-regulated material microstructure characterized by a fully interconnected porous network and high porosity.[161] SLS can also be utilized for the fabrication of 3D rationally designed devices for drug or biomolecule delivery and carriers. Maher *et al*. described the engineering of novel 3D-printed titanium implants (Fig. 10B) for drug-releasing purposes, with dual micro- and nano topography, to enhance the osseointegration and drug-delivery properties of the implants.[162]

Some of the influential factors in the quality of SLS-printed objects include the size of powder particles, refresh rate, spacing between scans, speed of scans, power of the laser, raster angle layer thickness, temperature of the part bed, and hatch pattern. The SLS method achieves a resolution of 100 µm. It provides benefits such as high resolution and precision, faster production times, elimination of post-curing processes, and low anisotropy. However, it also has several drawbacks, including inefficiency, high costs, significant waste of powder materials, limited availability of compatible active pharmaceutical ingredients (APIs) and excipients, and slower printing speeds. With most of the materials used in SLS being poorly biocompatible and biodegradable, its applications have been limited in biomedical nanobots and microrobots.

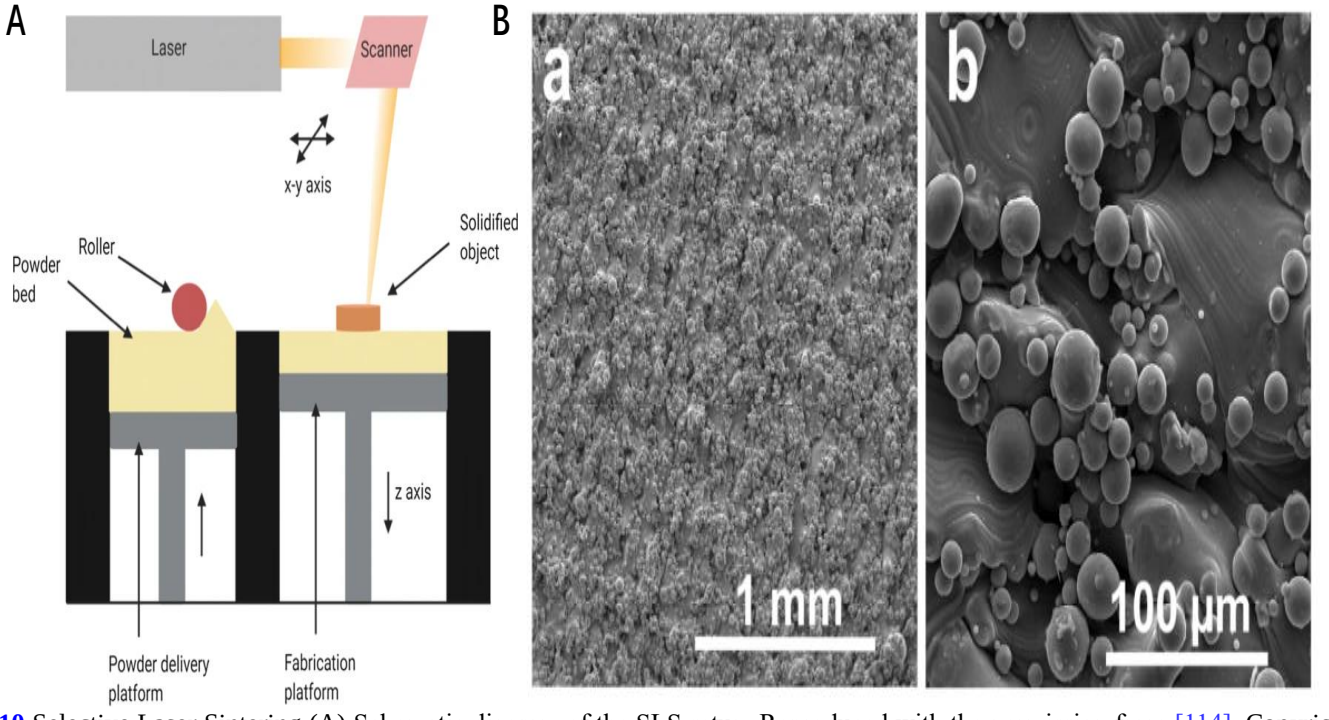

Fig. 10 Selective Laser Sintering (A) Schematic diagram of the SLS setup. Reproduced with the permission from [114], Copyright 2021, Vaz *et al*.) (B) SEM images showcasing the morphology of 3D-Ti implants at varying magnifications (a) low resolution and (b) high resolution. Reproduced with permission from [162], Copyright 2017 American Chemical Society.

Table 3. Summary of various 3D printing techniques.

Method	Principle	Resolution	Structure of MNRBs	Material composition	Advantages	Disadvantages	Ref
Material extrusion	Dispensing molten or semi-molten materials through a nozzle onto a surface, where they cool and harden in layers	50–200 μm	3D geometric structures	Thermoplastic polymers, hydrogels	Cost-efficient, fast, and simple	Low precision, slower output, risk of drug degradation, weak strength, limited to thermoplastics, rough surface, and high temperatures unsuitable for cells.	[78,79, 111-113]
IP	Ejecting ink droplets onto a substrate via piezoelectric action	50–200 μm	3D multilayer structures, microrockets, microstirrers, *etc*	Hydrogels, biological materials	Fast printing	Poor adhesion between layers	[90-92]
DLW	Uses laser to initiate photochemical cross linking of the photopolymer followed by photocuring	70-100 nm	Spherical, double helical, walnut shaped, microneedles, *etc*	Photopolymer biodegradable polymers, nanocomposites and metals	Enhanced spatial precision	Low printing speed	[76,111, 113, 123, 129, 136, 137]
SLA	Uses a digital mirroring device that uses a laser beam to trigger a photochemical reaction, converting a liquid monomer into a solid structure.	10 μm	Microneedles, scaffolds, *etc*	Photopolymer biodegradable polymers, nanocomposites, resins and metals	Excellent precision, fine spatial resolution, compact equipment and high-quality surface finishes.	Expensive, requiring rinsing and post-curing procedures, limited access to biocompatible photopolymerizable polymers.	[104, 105, 108-113]
DLP	Laser beam directed via a digital mirror device	25-100 μm	Sphere, gyroid, scaffolds, *etc*	Resins, hydrogel	Exceptional resolution and precision, rapid production, Cost-effective, requires a smaller initial vat volume	Restricted mechanical characteristics	[111-113, 146, 163]
CLIP	Projecting ultraviolet light through a membrane that allows oxygen to pass through	75 μm	Intricate geometries with fine details	Photopolymer resins	Rapid production rate and enhanced accuracy	Require low-viscosity resins, potential toxicity concerns, and high cost	[76, 111-113, 151-153]
SLS	Selective fusion/melting of powdered material with a laser	100 μm	Simple structures like the sphere	Metals, metal alloys, polymers	High resolution and accuracy, quicker production, and no need for post-curing, low anisotropy	Inefficient, costly, considerable waste of powder materials, restricted access to compatible API ingredients and excipients, and slow printing speed.	[111-113, 158, 159, 162]

The creation of MNRBs primarily relies on conventional methods such as PVD and electrodeposition, which are favored for their cost-effectiveness and efficiency in producing basic structures. In contrast, advanced 3D printing techniques, particularly direct ink writing (DIW) and direct laser writing (DLW) have emerged as the preferred options for MNRB production due to their enhanced precision, high resolution, and capability to fabricate intricate, customizable designs using a variety of materials. These 3D printing methods are increasingly valued for their flexibility and compatibility with CAD/CAM systems, facilitating the development of complex designs that are crucial for both biomedical and technological applications. Although electrodeposition is still popular for its straightforward approach and scalability, the advanced features and versatility of 3D printing have established it as the leading technique for creating sophisticated MNRBs tailored to specific functional needs.

3. Material selection and actuation strategies for micro/nanobots

The selection of materials is a critical factor in the design and fabrication of MNRBs intended for biomedical applications, as it directly affects their performance and potential for clinical integration. Identifying the right materials is essential to transition MNRB research from theoretical studies to practical medical applications. For biomedical use, MNRBs must possess key properties such as biocompatibility to avoid immune reactions or toxicity and biodegradability, ensuring they can be safely broken down and eliminated once their tasks are complete.[164] Achieving mechanical strength and mobility is also vital for their stability, though balancing these characteristics is a significant challenge.

In the development of MNRBs, both inorganic and organic materials are employed for their distinct advantages. Inorganic materials, including metals, metal oxides, ceramics, and glasses, are prized for their mechanical durability, thermal resistance, and magnetic properties, often associated with porous structures. On the other hand, organic materials derived from natural or synthetic polymers, lipids, and proteins offer exceptional biocompatibility, high biodegradability, and minimal toxicity, making them well-suited for medical purposes. Recently, hybrid nanomaterials, which combine both inorganic and organic components, have been created to address the growing need for materials with multiple functionalities that combine robustness with biocompatibility.[165]

These materials not only define the physical structure of MNRBs but also contribute to their functionalities including propulsion and actuation mechanisms. MNRBs can be powered using different actuation techniques, which are essential for movement and task execution, such as drug delivery, within biological environments. Propulsion methods are classified into self-propelled systems, which utilize chemical energy from sources like hydrogen peroxide or water, and external field-propelled systems, driven by magnetic, electric, or light fields. While self-propelled systems may be limited by specific environmental conditions, externally powered MNRBs offer greater flexibility for biomedical tasks. Additionally, bio-hybrid approaches-where biological components are integrated with MNRBs-further improve their efficiency and adaptability in complex environments.[1,166-168]

Consequently, the selection of materials and propulsion systems is crucial in influencing the overall effectiveness, functionality, and clinical applicability of MNRBs. The upcoming sections explore the various materials used in the fabrication of MNRBs, their reported applications in the literature, and the diverse actuation and propulsion mechanisms utilized.

3.1 Metals

Metals and metal oxides rank among the most frequently utilized inorganic materials for the production of MNRBs in clinical applications. At the nano/micro scale, they offer several benefits, such as high stability, straightforward preparation, customizable size, shape, and porosity, and ease of functionalization due to their surface charge.[169] These properties make them ideal for integrating into both hydrophobic and hydrophilic systems. Metals and metal oxides can serve either as the core material for MNRBs or be incorporated into a system to perform specific functions such as propulsion. Common metals used include platinum (Pt), copper (Cu), gold (Au), nickel (Ni), silver (Ag), magnesium (Mg), aluminum (Al), gallium (Ga), palladium (Pd) and titanium (Ti) while metal oxides often include silicon monoxide (SiO), titanium dioxide (TiO_2), calcium carbonate ($CaCO_3$), manganese oxide (MnO), iron oxides ($FeCO_3$), and zinc oxide (ZnO).[11]

Chemically powered MNRBs transform chemical energy into mechanical motion for self-propulsion. They often rely on redox reactions in their surroundings, creating an uneven distribution of products that propel the robots forward. Common propulsion methods include bubble propulsion,[170] self-diffusiophoresis,[15] self-electrophoresis,[58] and self-thermophoresis.[14] These robots typically consist of two elements: an active metal or catalyst combined with inert materials, resulting in asymmetric configurations like bimetallic nanowires, Janus nanoparticles, and tubular microjets.[167] The first chemically propelled MNRB was introduced by Mallouk *et al*., sparking significant interest in chemically powered MNRBs. For this purpose, they developed bimetallic rods composed of Au-Pt metals which are capable of self-propulsion by decomposing hydrogen peroxide.[58] Wilson *et al*. designed a supramolecular nanorobot by encapsulating platinum nanoparticles (PtNPs) in the cavity of artificial stomatocytes. The oxidation of H_2O_2 in the presence of catalyst PtNPs results in the production of oxygen and water, from which thrust is generated to propel the nanorobot in a particular direction.[171] However, due to the cytotoxicity of hydrogen peroxide, researchers have since

been exploring alternative fuel sources. Gao *et al*. have reported a water-powered bubble-propelled micromotor with no need for the usual hydrogen peroxide fuel. This novel Janus micromotor, which was fabricated via the physical vapor deposition method, works in water and is fabricated from an Al-Ga binary alloy microsphere prepared by its partial coating through microcontact mixing of aluminum microparticles with liquid gallium.[172] Wang *et al*. developed an MNRB that utilizes glucose from human body fluids as fuel. This robot was constructed with a platinum anode and a carbon nanotube cathode, using template electrochemical deposition and chemical vapor deposition techniques.[60] Gao *et al*. conducted the first in vivo experiment using zinc-based micromotors composed of an outer Poly(3,4-ethylenedioxythiophene) layer and an inner zinc layer powered by stomach acid for drug delivery in mice. The acidic conditions in the stomach provided sufficient fuel for propulsion, as hydrogen bubbles generated in the zinc layer propelled the micromotors in the presence of stomach acid (H^+), enhancing tissue penetration and drug retention.[173] In another study, Li *et al*. fabricated a microtube by coating a Pt layer onto the top of a prestrained bilayer of SiO / TiO_2 or Si / Cr laid on top of a sacrificial PMMA layer.[174] In a similar approach, Wu *et al*. developed a technique for creating microtube motors by utilizing membrane template-assisted layer-by-layer (LbL) deposition rather than electrodeposition. They alternately deposited two biodegradable materials with opposite charges, chitosan (CHI) and sodium alginate (ALG), onto a nanoporous membrane. Subsequently, platinum (Pt) nanoparticles were introduced into the membrane's pores. Additionally, Wu *et al*. fabricated a Janus capsule motor that was half-coated with Pt nanoparticles using a combination of template-assisted LbL assembly and microcontact printing. This involved assembling five bilayers of oppositely charged polystyrene sulfonate and poly (allylamine hydrochloride) onto the surface of silica template particles, followed by stamping Pt nanoparticle ink onto the substrate using a stamp.[175] Chemically propelled MNRBs have demonstrated self-propulsion in mildly acidic environments, both in vitro and in vivo. However, they are slow and lack precise positioning, necessitating further research for their clinical application.[168] Metals are also integrated into systems to enable propulsion through stimuli-responsive mechanisms. Xing *et al*. prepared a pH-responsive nanomotor with multimetal and multi-phoretic propulsion for biomedical applications. The nanomotor was fabricated by loading AuNPs-cys (L-cysteine-modified AuNPs) onto MSNs-NH_2 (Amino-functionalized Mesoporous Silica Nanoparticles) through a Cu^{2+} coordination bridge. Further, PtNPs deposited on the MSNs-NH_2-Cu^{2+}@AuNPs-cys monolayer through physical vapor deposition to form a Janus MSNPt@Au nanomotor (JMPA).[176]

MNRBs are magnetized by incorporating magnetic nanoparticles (MNPs), with soft paramagnetic materials like iron, which are preferred for biomedical use due to their biocompatibility and magnetic responsiveness.[164] Metals and metal oxides with magnetic properties are integrated within the MNRBs systems to allow actuation and propulsion via external magnetic fields. This enables precise 3D control, making MNRBs ideal for non-invasive medical applications and targeted drug delivery, with systems like Helmholtz coils and permanent magnets, thus providing real-time adjustments.[167,168] By the process of electron beam evaporation, Li *et al*. added a layer of magnetic Ni onto Pd nano springs to develop magnetically driven helical micromotors.[177] Dong *et al*. developed a core-shell microrobot made of Cobalt Ferrite and Bismuth Ferrite that operates in a phosphate-buffered saline (PBS) microfluidic channel using a rotating magnetic field (RMF) of 8 mT at a frequency of 4 Hz. Utilizing magnetogenesis principles, the core-shell structure experiences strain, leading to temporary surface changes when subjected to an external alternating RMF. This microrobot can perform targeted tasks, such as facilitating nerve cell differentiation, under RMF conditions.[178] Bergeles *et al*. created a cylindrical microrobot made of NdFeB, measuring 1 mm in length and 0.5 mm in diameter, capable of moving within a human eye model under the influence of a gradient magnetic field.[179] Tottori *et al*. fabricated a helical microrobot using SU-8 and IP-L. A thin bilayer of Ni with 150 nm and Ti with 20 nm was deposited on the surface of the microrobot using electron-beam evaporation. The Ti layer improves the biocompatibility of Ni while preserving the microrobot's magnetic properties.[180] Pane *et al*. have designed enzymatically biodegradable soft helical microswimmers using TPP. They created soft helical microswimmers from photo-cross-linkable GelMA. To enable magnetic actuation of the microswimmer, the GelMA microstructures were infused in a suspension of PVP-coated Fe_3O_4 nanoparticles, which adhered to the surface of the GelMA.[181]

Metals such as Au and metal oxides like TiO_2 are also used in the development of light-driven MNRBs. He *et al*. synthesized tubular polymer multilayer rockets using template-assisted layer-by-layer assembly wherein platinum nanoparticles are encapsulated and a gold shell is outside. The gold shell was then functionalized with tumor-targeting peptides and antifouling polymers. This can instantly induce the motion of microrobots upon NIR light due to self-thermophoresis. In addition, the photothermal effect achieved by NIR proved that the robots can target the tumor and thus have a possibility of treating the tumor as well.[182] Sen *et al*. introduced UV-powered TiO_2 micromotors and micropumps, sparking considerable interest among researchers in TiO_2-based micro/nanorobots.[183] Later, Ren *et al*. showed a TiO_2-Au Janus micromotor that can achieve speeds of up to 25 body lengths per second under very low-intensity UV light. The propulsion of these 1 μm diameter micromotors is through self-electrophoresis, which arises from the asymmetrical forces. Moreover, by depositing a paramagnetic Ni layer between the Au layer and the TiO_2, the same light-powered

Janus micromotor can also be controlled by a magnetic field.[184]

Despite growing research on metal-based systems for various applications, their effects on the human body are not fully understood. Nanoparticles are considered more toxic than bulk materials, with reported side effects like immunogenic reactions, nephrotoxicity, and neurotoxicity. Key concerns include high reactivity, extended circulation time, off-target accumulation, and unintended exposure. More studies are needed to assess the potential health risks of NPs fully before they can be safely applied to humans.[185]

3.2 Photopolymers

Photopolymers, especially photo-cross-linkable hydrogels, are particularly noteworthy as ink materials due to their ability to form complex 3D structures through the photopolymerization of monomers, oligomers, or macromers. In laser 3D printing with photopolymers, the key elements include photoinitiators alongside monomers, oligomers, or macromers, while additives such as stabilizers, light absorbers, and radical inhibitors are also used.[76]

3D photopolymerization uses liquid monomers or oligomers that solidify into thermosetting structures under specific light wavelengths. A photoinitiator with high absorption is needed to create reactive species like free radicals or cations, driving chain growth. Short UV wavelengths (below 400 nm) are commonly used, and photopolymerization proceeds via free radical or cationic mechanisms. Recently, NIR -induced photopolymerization has enabled the creation of 3D structures within photocured materials. Various photoinitiation systems have been developed, including UV light-responsive photoinitiators like Irgacure, Benzophenone, Lithium Phenyl-2,4,6-trimethylbenzoylphosphinate (LAP), and Monoacyl phosphane oxide (MAPO). Visible light-responsive photoinitiators include 3-Hydroxyflavone (3HF), Azahelicene 3 (AZ3), Ivocerin, Eosin Y, and Rose Bengal. Additionally, NIR-responsive photoinitiators, such as Pheophorbide A (PheoA) and Aluminum phthalocyanine (AlPc), have also been introduced.[82]

Photoresist, a widely used photosensitive material, plays a key role in light-cured 3D printing. It is classified into two types: negative and positive photoresists. In positive photoresists, the unexposed areas remain after development, while in negative photoresists, the exposed parts are retained. During development, specific regions dissolve, revealing the final image. Positive photoresists are generally used to create templates for fabricating microrobots, while negative photoresists are directly used in 3D printing for microrobot production by adjusting printing parameters.[186-188] SU-8 is widely utilized as a negative-tone photoresist in lithography for 3D microfabrication, particularly in the development of MNRBs. SU-8 is highly biocompatible, which makes it a popular material in biomedicine and life sciences. For 3D cell culture and targeted transportation, Choi *et al*. fabricated 3D porous magnetic microrobots by TPP technique with SU-8 and e-beam evaporation of magnetic Ni (150 nm) and biocompatible Ti (20 nm). Porous structures with nontoxic materials made the microrobots excellent for culturing human embryonic kidney 293 cells and could be controlled via a magnetic field for targeted cell transport. The use of 3D porous magnetic microrobots studied herein shows great promise for targeted cell delivery in biomedical applications.[189] By utilizing the directed nanoparticle self-organization method, the scientists fabricated single and double 3D soft magnetic twist-type microrobots using TPP printing of a superparamagnetic polymeric nanocomposite prepared with 11 nm Fe_3O_4 nanoparticles and SU-8 negative photoresist. Such types of microrobots manifested programmed magnetic anisotropy, allowing for their actuation with a weak rotating magnetic field and corkscrew propulsion without wobbling.[190] IP series, developed by Nanoscribe GmbH, represent state-of-the-art materials in high-resolution 3D microfabrication because of their precision and high resolution and are easy to handle. They have been used in the fabrication of functional micro-optics and biomedical devices, such as 3D scaffolds and micro-implants. Ready-to-use formulations within the series comprised IP-L, IP-S, IP-DIP, IP-G, IP-Q, and IP-Visio.[76] Wang *et al*. showcased the ability to selectively control individual swimmers in a swarm of geometrically and magnetically identical artificial bacterial flagella (ABFs) by modifying their surface chemistry. They created helical microswimmers through TPP of IP-L 780 photosensitive polymers. Magnetic actuation was achieved by first coating the microhelices with nickel and then applying a layer of gold.[191] Recently, Schmidt *et al*. published a study in which they achieved real-time dynamic optoacoustic tracking of individually moving micro-objects located deep within phantom tissues and ex vivo chicken breast tissues using multispectral optoacoustic tomography (MSOT). The micro-objects were created through TPP using IP-Dip negative photoresist and subsequently coated with chromium (10 nm), nickel (130 nm), and titanium (15 nm) via electron-beam PVD. By introducing the gold nanorods, the contrast of the MSOT signal further improved and could be distinctly differentiated from the surrounding tissues. In this work, the feasibility of using MSOT for imaging and tracking swimming microrobots deep inside the human body was demonstrated.[192] While the biocompatibility of IP-series polymer materials continues to improve, their excretion from the human body remains problematic. SU-8 photoresists provide the needed mechanical stability when complex MNRBs are fabricated, but have been studied for their potential to trigger inflammatory responses upon in vivo applications. Consequently, the microrobots leave residues of the material that can induce foreign body reactions in the body for a very long time, which can cause toxicity to the cells or tissues nearby, contribute to chronic inflammation, and delay recovery.[193]

3.3 Polymer hydrogels

Hydrogels are 3D networks of hydrophilic polymer chains that possess adjustable properties, making them highly promising for applications in both medical and environmental fields. They provide a biomimicry extracellular matrix with cell and drug delivery capability and are helpful in 3D bioprinting. Hydrogels can be modified by chemical, physical, or biological means, and their porous nature provides various applications. Water-soluble photoinitiators like LAP and Eosin Y are utilized in laser-based 3D microfabrication. Several hydrogel polymers, such as gelatin methacrylate (GelMA), hyaluronic acid (HA), polyethylene glycol (PEG), poly (lactic-co-glycolic acid) (PLGA), and alginate, can be used in the development of MNRBs. For cell culturing, which is usually required while developing biohybrid MNRBs, hydrogels made from degradable polymers like PEG and GelMA are favoured due to their excellent biocompatibility and support for high cell viability. Their cross-linked networks allow ion exchange, which promotes cell growth and differentiation, while the mechanical strength varies depending on the cross-linking method and irradiation time. In drug delivery systems, hydrogels such as alginates and GelMA are used as drug carriers, with drug release controlled by their adjustable porosity and swelling properties. These hydrogels also offer high encapsulation efficiency and reduced systemic toxicity. [76,193]

GelMA-based hydrogels have found a wide application in biomedicine since their properties are easily tunable and show several biological advantages. GelMA can undergo photopolymerization under UV light with the use of photoinitiators, resulting in the creation of covalently crosslinked hydrogels under mild conditions, such as room temperature and neutral pH, which enables good control of this process.[76] Terzopoulou *et al*. showed that a composite of a magnetic metal-organic framework (MOF) made from Fe, zeolitic-imidazole framework-8 (ZIF-8), and GelMA facilitated targeted drug delivery when an external magnetic field was applied. This composite showed improved biodegradability compared to their previous designs. GelMA degrades through proteolytic enzyme cleavage of amide bonds, while Fe@ZIF-8 represents a magnetic MOF composite responsive at acidic pHs-hence particularly suitable for tumor-targeted delivery since the extracellular pH of cancerous tissues is slightly acidic and lies between 5 and 6, while the pH of normal tissue is 7.4. This structure was fabricated by TPP.[194] Sitti *et al*., however, employed TPP 3D printing to fabricate double-helical microswimmers (20 μm long, 6 μm in diameter) using GelMA and superparamagnetic iron oxide nanoparticles (SPIONs). This hydrogel microswimmer can transport, deliver, and release therapeutic drugs when subjected to a rotating magnetic field. Additionally, it completely degrades into non-toxic byproducts within 118 hours due to MMP-2 and swells in reaction to elevated MMP-2 levels to improve drug release. Moreover, SPIONs labeled with anti-ErbB2 antibodies are released from the degraded microswimmers, enabling targeted labeling of SKBR3 breast cancer cells in vitro. These microswimmers, therefore, represent a promising approach toward integrating biodegradability, medical functions, environmental sensing, and magnetic control for complex tasks to be performed within the human body.[129] Hyaluronic acid (HA) is a water-soluble glycosaminoglycan and, for a long time, one of the most common components used in hydrogels for biomedical applications. Since HA naturally occurs in all tissues, it can be enzymatically degraded in the body by hyaluronidases. The presence of amide, carboxylate, and hydroxyl groups in its structure allows chemical modifications such as methacrylation to yield methacrylated HA. Applications of this photocrosslinkable system include drug delivery, tissue engineering scaffolds, and microdevices, while it is also suitable for 3D printing and bioprinting of hydrogel scaffolds.[76] PEG, a synthetic polyether polymer, has attracted considerable interest due to its excellent biocompatibility, making it widely used in biomedicine and pharmaceuticals. Its high hydrophilicity, water solubility, and resistance to protein adsorption establish PEG as the preferred choice for stealth polymers in drug delivery systems (DDS). Additionally, its ease of chemical modification has led to the synthesis of numerous PEG-based derivatives and copolymers for various biomedical applications. Photocrosslinkable hydrogels based on PEG acrylate have been designed for the 3D laser-printed microrobots.[76] Chen *et al*. created 3D swimming artificial microfish using the mCOP technique, a variant of DLP 3D printing, along with PEGDA hydrogels and various functional nanoparticles. These included platinum nanoparticles for chemical propulsion, Fe_3O_4 nanoparticles for magnetic navigation, and polydiacetylene nanoparticles for neutralizing toxins. The multifunctional 3D-printed microfish demonstrated the potential of bioinspired microrobots for applications in biosensing and detoxification through wireless actuation.[195] Huang *et al*. fabricated a PEGDA, Fe_3O_4, and N-isopropylacrylamide-based microrobot by adopting the self-assembly technique. The tail of the microrobot is made up of PEGDA, providing increased flexibility for the microrobot, while the head contains Fe_3O_4 particles that permit the movement of the microrobot.[196] PLGA, a biocompatible and biodegradable polymer, is synthesized by the ring-opening copolymerization of lactic and glycolic acids. Specific properties improve the performance of PLGA in several biomedical fields. In the last few years, PLGA has been one of the most common encapsulation matrices for organic and inorganic materials, including small molecule drugs, metal or magnetic nanoparticles, proteins, and vaccines.[76] Alginate is a naturally derived polysaccharide found in brown algae and has been recognized as biocompatible and nontoxic. This polysaccharide has been extensively applied in many recent studies to create various controlled drug-release delivery systems.[197-202] Combined with HA, it is used in composite hydrogel and develops the physical, mechanical, and biological properties of microrobot structures.[203] Additionally,

polymers like polycaprolactone and polylactic acid (PLA) are excellent choices for 3D printing due to their cost-effectiveness, flexibility, lightweight, and elasticity. These materials are widely applied in biomedical fields because they are available in both bioinert and biodegradable varieties, with many receiving FDA approval for biological uses. Extrusion-based printing is often used with polymers, particularly PLA, owing to its affordability, biocompatibility, easy processing, and suitable degradation rate.[204] Liu *et al*. created a PLA-based platform for drug screening and toxicity assessment, highlighting its ease of use, affordability, and effective integration with 3D cell culture and activity evaluation.[205]

3.4 Functional materials

Functional materials actively react to environmental changes or external stimuli in visible and measurable ways. Often referred to as "intelligent" or "responsive" materials, they possess abilities like self-adaptation, sensing, or memory retention. These special characteristics are driving their growing importance in various industries, especially in the development of microrobots.[206]

MNRBs require diverse propulsion methods to move independently through complex environments. Often, they utilize external forces like magnetic fields, ultrasound, or light for propulsion. To facilitate this movement, the commonly used fabrication techniques, including 3D printing, integrate functional or active materials, such as nanoparticles, into the microrobots' surfaces or internal structures.[76] Various propulsion techniques, such as magnetic, chemical, enzymatic, and biohybrid methods, have been covered in other sections. Besides these, additional propulsion methods include light-based, ultrasound, and electric-driven approaches, utilizing a range of functional materials. Chen *et al*. integrated Polydopamine nanoparticles (PDA NPs) into a PEGDA polymer matrix to 3D print a claw-like microrobot, enhancing propulsion efficiency with a DLP 3D printing system. When exposed to NIR light, the photothermal properties of PDA cause the breakdown of NH_4HCO_3, releasing biocompatible materials such as NH_3, CO_2, and H_2O. This process leads to bubble formation and bursts, which produce propulsive forces.[207]

Acoustic waves offer great potential for noncontact manipulation of micro- and nanoscale objects through acoustic radiation force and drag force. These forces, interacting in biofluids, allow precise control based on sound wave properties. With strong propulsion and biocompatibility, acoustic methods are gaining attention for guiding MNRBs in biomedical applications, providing an efficient, eco-friendly, and cost-effective solution.[167,168] Wang *et al.* fabricated a highly accurate and powerful micro ballistic apparatus capable of loading and launching nano bullets, including silica and fluorescent microspheres, using electrochemically fabricated micro cannons triggered by an acoustic signal. The local ultrasound pulse creates the rapid evaporation of perfluorocarbon emulsions near nano bullets, allowing them to be shot at ultrahigh velocities. This allows the controlled firing of nano bullets from a microstructure, but along with that, it renders easier access to the target areas and better tissue penetration for in vivo applications.[208] Electrical actuation enables precise, wireless, and fuel-free control of MNRBs using direct or alternating electric fields. To activate electrically, MNRBs need to be conductive, semi-conductive, or charged. This cost-effective, contactless method utilizes forces like electrophoresis, electro-osmotic flow, or electrorotation. While direct current (DC) fields move charged objects through Coulomb forces, alternating current (AC) fields offer more adaptable control through dielectrophoretic forces and electro-osmotic flow.[1,166-168] Conjugated polymers, including electroactive types like polypyrrole (PPy), polyaniline (PANI), and Poly(3,4-ethylenedioxythiophene) (PEDOT), are inherently conductive and show significant potential for creating soft microscale actuators, robots, and artificial muscles for various applications.[209] Wang *et al*. developed poly(pyrrole)-cadmium (PPy-Cd) and CdSe-Au-CdSe semiconductor nanowires that were driven by an external alternating current (AC) electric field, facilitating controlled movement through electro-osmotic flow. In contrast to conventional micromachines that rely solely on electro-osmotic flow, the electric field also induced asymmetric bubble formation through redox reactions on both sides of Janus particles. This bubble generation provided continuous propulsion to the micromotors, enabling both linear and rotational movement.[210] Fan *et al*. demonstrated that tumor necrosis factor-alpha (TNF-α) can be accurately transported to specific subcellular sites when attached to gold nanowires, utilizing electrophoretic and dielectrophoretic forces produced by an external electric field.[211]

3.5 Biohybrid materials

Bioinks are defined as fluid materials that contain cells and may also include material matrix components. These materials are used in 3D printers to create structures resembling biological tissues.[212] Bioinks differ significantly from cell-free material inks. For materials to be considered bioinks, they must maintain cytocompatibility during formulation, printing, and post-printing stages. Encapsulated cells can include mammalian cells like cardiac and skeletal muscle cells and stem cells, as well as microorganisms such as microalgae, fungi, and bacteria, and small tissue constructs or cell spheroids. The materials utilized can be hydrogels, hydrogel precursors, or decellularized matrices.[76] In terms of propulsion, biohybrid MNRBs utilize motile cells such as sperm, bacteria, or blood cells to drive the movement of the MNRBs. These robots overcome microscale challenges like high viscosity and Brownian motion with the flexible movement of flagella. Unlike conventional MNRBs, they are biocompatible, sustainable, and offer targeted movement, making them ideal for biomedical use. Biohybrid propulsion is divided into bacteria-based and eukaryotic cell-based microrobots.[1]

Different types of natural cells exhibit self-directed movement and perform specific functions within biological environments, including contractile and immune cells. Contractile cells, like cardiomyocytes and skeletal muscle cells, are adapted to produce movement through the interaction of the protein's actin and myosin,[213] generating directional tension during contractions. Immune cells, such as white blood cells, demonstrate chemotaxis, a process that allows them to detect the direction and intensity of an external chemical gradient and move toward the source of the stimulus.[214] By merging such natural cells with artificial materials to form biohybrid MNRBs, tasks impossible for purely artificial bots have been accomplished.[215,216] Williams *et al*. created synthetic swimmers modeled after the structure of sperm using an innovative fabrication method in which cardiomyocytes were selectively grown on Polydimethylsiloxane (PDMS) filaments. The resulting biohybrid device utilized flagellar propulsion, driven by the contraction of the cardiomyocytes, which generated a bending motion along the filament, propelling the system forward.[217] In research carried out by Shao *et al*., neutrophils, known for their intrinsic chemotactic abilities, were engineered into self-orienting hybrid micromotors based on the use of mesoporous silica nanoparticles (MSNs) that have significant drug-loading capacity. To provide for compatibility of the neutrophils with the drug-encapsulated MSNs, the nanoparticles were first coated using a camouflaging approach with bacterial membranes from *E. coli* before being used in the system. The biohybrid micromotors produced retained the chemotactic properties innate to natural neutrophils and allowed them to navigate efficiently through chemoattractant gradients established by *E. coli*.[218] Wu *et al*. introduced erythrocyte-membrane-coated gold nanobots. Red blood cells (RBC)-based nanobots are potentially able to move within the bloodstream when exposed to an ultrasound field. The design is aimed at neutralizing membrane-damaging toxins.[219] Bibette *et al*. designed MNRBs that feature red blood cells as the head and DNA-linked superparamagnetic spheres as a flexible tail, which has a diameter of 1 μm and a length of 24 μm. These robots are powered by an oscillating magnetic field, where the magnetic spheres in the tail respond to both the external magnetic field and adjacent spheres by generating magnetic moments. This interaction causes the flexible tail to oscillate in sync with the magnetic field, effectively driving the robot forward.[220]

Bacteria-powered MNRBs represent a class of biohybrid systems propelled by microorganisms. These structures utilize the force generated by motile cells to drive synthetic components attached to them. Because of their flagella and excellent sensing capabilities, some bacteria present ideal candidates for the design and development of MNRBs.[221] *E. coli*-based microbots were created by Park *et al*. by placing single bacteria on a polyelectrolyte multilayer, followed by assembly with magnetic nanoparticles. The size of the resulting microbots was approximately 1 μm and displayed viscoelastic properties. They moved seemingly erratically at an average speed of 2.25 μm/s. More importantly, the inherent magnetic or chemoattractant abilities of the microbots directed them toward target cells. Thus, these microbots were employed to deliver an anticancer drug, encapsulated in a polyelectrolyte multilayer, specifically to 4T1 breast cancer cells through magnetically guided delivery.[222] Song *et al*. used magnetotactic cells, which were noted for their extraordinary motility, to make a bacterium robot. Particularly, the MO-1 bacterium is classified as a polar magnetotactic bacterium and can move its magnetic field through the two powerful flagella. Both filaments of seven layers are enclosed within a special sheath that enables the bacterium to swim at speeds of up to 300 μm/s. The researchers created a reliable connection by binding the bacteria to polystyrene microbeads using an antigen-antibody interaction. Trials revealed the smooth movement of the bacteria through microfluidic channels under the control of a rotating magnetic field.[223] Similarly, other bacteria, such as Salmonella typhimurium and Magneto spirillum, have been employed for the fabrication of MNRBs.[224-226]

Viruses are microscopic organisms consisting of a protein shell that encloses nucleic acid. They are used as carriers for diagnostics and targeted drug delivery as they can transfer genetic material into host cells for the purpose of replication.[227] Tang *et al*. used adeno-associated virus serotype 2 to deliver KillerRed, a light-sensitive protein used for photodynamic treatment, via the expression of a customized gene. The ability of the virus to target the tumor was improved by chemical modification of the system with iron oxide nanoparticles, allowing it to be magnetically targeted. The viral system with iron oxides accumulated under magnetic guidance in well-defined sites in the tumor. After the injection into the mouse model, tumor growth was prevented by photodynamic therapy.[228] Alemzadeh *et al*. utilized the spent shells of the Johnson grass chlorotic stripe mosaic virus as virus-like particles (VLPs) for drug delivery, leveraging their reversible swelling in vitro. After cloning and transforming the VLPs, they tested their potential as nanocontainers for doxorubicin delivery. The findings indicated that the structure closely resembled the native virus, making it an excellent candidate for loading chemotherapeutic drugs. This research was groundbreaking in exploring the use of icosahedral viruses for creating nanocontainers in biomedical applications.[229] Recently, microalgal swimmers have been utilized as biomedical robotic actuators, mainly in in vitro environments. Zhang *et al*. developed a promising algae motor system based on natural microalgae, *Chlamydomonas reinhardtii,* swimming very fast and for a long time in intestinal fluid. For the purpose of appropriate delivery to the small intestine, functionalized algae motors covered with fluorescent dyes or cell membrane-coated nanoparticles were encapsulated within a pH-sensitive capsule. In vitro testing proved that these algae motors remained moving in the simulated intestinal fluid after 12 hours of

continuous operation.[230] Shchelik *et al*. designed a method for surface engineering microalgae to produce biohybrids with phototactic activity to target antibiotic effects in 3D space. The two antibiotics, vancomycin (VAN) and ciprofloxacin (CIP), each having different mechanisms of action, were covalently attached on the surface of *Chlamydomonas reinhardtii*. Such modification does not hinder the motility or phototactic behavior of the engineered biohybrid microalgae.[231] In another work, Yan *et al*. introduced a multifunctional, helical biohybrid magnetite MNRB designed for therapy guided by imaging. These helical MNRBs were produced using Spirulina microalgae, coated via a dip-coating method in magnetite (Fe_3O_4) suspensions. The natural fluorescence of the microalgae allowed for in vivo imaging and remote diagnostic sensing without requiring additional surface modifications. Furthermore, the MNRBs demonstrated the ability to degrade autonomously and exhibited selective cytotoxic effects on cancer cell lines.[232]

Biological MNRBs, including DNA origami robots, kinesin motors, and ATP synthase (ATPase), have garnered significant interest and are extensively utilized for several applications. For instance, Li *et al*. designed in vivo applications of DNA origami-based nanobots for the treatment of cancer. They fused an aptamer with DNA origami to create a tubular DNA nanorobot that could be engineered to carry thrombin and shield it from platelets and plasma fibrinogen. Upon the specific engagement of the aptamers at tumor-associated antigens, the DNA nanorobots were programmed to degrade, thus exposing thrombin and initiating localized coagulation at the tumor site. Such regional activation leads to necrosis and regression of the tumor.[233] Ma *et al*. conducted a study in which they developed an intelligent DNA nanorobot using a DNA framework to selectively degrade tumor-specific proteins in cancer cells. They attached an anti-HER2 aptamer (HApt) to a tetrahedral framework nucleic acid (tFNA), forming the DNA nanorobot (HApt-tFNA). This nanorobot specifically targeted HER2-positive breast cancer cells, inducing the lysosomal degradation of the HER2 membrane protein. In mouse models, injecting the DNA nanorobot showed that the tFNA improved the stability and prolonged the circulation time of HApt, enhancing the efficiency of HER2 degradation in lysosomes.[234] Enzyme-powered MNRBs offer significant potential in biomedical fields due to their strong activity and compatibility. Using natural fuels like glucose and urea, these robots move through enzyme-driven reactions. For instance, Ma *et al*. developed Janus nanomotors with silica nanoparticles and enzymes such as catalase, urease, and glucose oxidase, which propel via reactions with H_2O_2, urea, and d-glucose, making them suitable for drug delivery.[235] Similarly, cell-based MNRBs have been developed and propelled via an enzymatic approach. Recently, Tang *et al*. developed a cell-based MNRB by asymmetrically loading ureases onto platelet surfaces. This uneven distribution of ureases leads to the asymmetric decomposition of urea in biofluids, generating increased propulsion for the platelet-based nano-robots. Additionally, these robots maintain the natural properties of platelets, enabling them to target cancer cells and bacteria, thus offering a novel approach for delivering anticancer or antibiotic drugs.[236]

Material selection plays a critical role in the development of MNRBs for biomedical applications, highlighting the importance of properties like biocompatibility, biodegradability, and mechanical stability. Among the materials, polymers and hydrogels, particularly photo-cross-linkable hydrogels like GelMA, are emphasized for their tunability, biocompatibility, and capacity for drug delivery. Metals and metal oxides, such as platinum and titanium, are frequently used for their stability and ease of functionalization, while functional materials like magnetic nanoparticles and electroactive polymers enable various propulsion methods for MNRBs. Biohybrid materials, incorporating live cells with artificial components, offer unique functionalities, exemplified by systems that use cardiomyocytes for propulsion or immune cells for targeted movement. Overall, photopolymers and hydrogels emerge as the most suitable materials due to their adaptability in 3D printing and compatibility with biological systems, making them ideal for the effective fabrication of nanobots.

Similarly, actuation and propulsion technologies are also crucial for the effective control of micro/nanobots, allowing accurate movement tracking in biomedical settings. MNRB propulsion can be categorized into self-propelled systems that use chemical reactions and external field-driven systems powered by magnetic, electric, light, or acoustic forces. While chemical propulsion often relies on redox reactions, such as in zinc-based micromotors, its use can be hindered by issues of biocompatibility. Enzyme-based MNRs, on the other hand, are highly active and biocompatible, leveraging natural fuels for movement, which makes them attractive for drug delivery applications. External actuation methods, particularly magnetic and acoustic propulsion, enhance precision and adaptability in clinical use. Biohybrid propulsion, which incorporates living motile cells as power sources, shows great potential due to its compatibility with biological systems. Ultimately, external field methods, especially magnetic actuation, are most suitable for clinical applications because of their precise and non-invasive control, while enzyme-based and biohybrid approaches also offer promising alternatives for specific situations.

4. Structural design and size of micro/nanobots

Although the material properties are well known to influence interactions with biological environments, the effect of shape has been less explored due to previous manufacturing constraints. Recent advancements in micro- and nanofabrication now allow for the creation of complex shapes, enabling researchers to study how geometry impacts these interactions. For example, particles with high curvature are more easily absorbed by cells,[237] cylindrical micelles stay in the bloodstream longer,[238] and nonspherical particles adhere

more effectively to vessel walls, presenting opportunities for targeted organ delivery.[239] The structure and shape of micro/nanocarriers significantly influence controlled drug delivery. Research shows that particle shape plays a key role in targeting specific organs, with studies indicating that non-spherical designs enhance drug specificity. Additionally, shape affects surface area, influencing drug solubility and release kinetics. Rod-shaped nanoparticles, for example, interact more effectively with cell receptors, improving uptake and extending circulation time by reducing immune rejection. This suggests that altering nanoparticle shapes can improve the targeting of specific cells and tissues for drug delivery.[240] Over time, numerous techniques for fabricating microstructures have emerged, significantly aided by the advancement of additive manufacturing methods.[241] To achieve various functionalities in microrobots, it is essential to design a range of microstructures, from simple forms like spherical, helical, and tubular shapes to more complex designs that integrate multiple geometries. Jeon *et al*. developed a variety of micro-scaffold robots in cylindrical, hexahedral, spiral, and spherical configurations, as illustrated in Fig. 11A. These robots exhibited self-motion when subjected to magnetic fields for their specific applications. They were employed to transport colorectal carcinoma cells to tumor microtissues in a body-on-a-chip system and effectively navigated through mouse brain slices and blood vessels in a rat brain. Additionally, they transported mesenchymal stem cells into a mouse's intraperitoneal cavity, highlighting their potential for stem cell culture and precise delivery. They studied the movement of various structures in deionized water under rotating magnetic fields (RMF) and gradient magnetic fields (GMF). The results showed that spherical and helical microrobots exhibited rolling and corkscrew motions under RMF, achieving higher propulsion efficiencies compared to those driven by GMF. The helical microrobot demonstrated faster movement in 3D fluid environments compared to the spherical one under the same RMF conditions. Spherical microrobots were able to overcome adhesion forces to roll through curved channels. In contrast, cylindrical and hexahedral microrobots moved more slowly, even under stronger GMF.[242]

Spiral structures are foundational in designing various microrobots with diverse functionalities. Among these, Janus micro/nanorobots with spherical shapes are widely researched in biomedical applications due to their larger surface area, ease of synthesis, and more controlled movement. The increased surface area provides ample space for both functional group modifications and cargo loading.[242-244] Sridhar *et al.* created Janus hollow mesoporous TiO_2/Au microswimmers, illustrated in Fig. 11B. Powered by ultraviolet light, these microswimmers deliver the anticancer drug doxorubicin. They utilize light-induced self-electrophoresis for propulsion, which is generated by the asymmetric TiO_2−Au structure that creates an electric field due to uneven ion distribution. The hollow design enhances both the swimming speed and drug loading capacity.[245] Helical microstructures are frequently incorporated into microrobot designs because of their capacity to maneuver with controlled precision at sub-micrometer levels in low-Reynolds number environments using weak rotating magnetic fields (<10 mT). They hold significant potential for clinical applications, including minimally invasive surgery, cell manipulation, and targeted therapy; however, several obstacles must be addressed to ensure their successful medical use.[246] Mhanna *et al*. showed that helical actuators driven by a magnetic field (Fig. 11C) could successfully transport the hydrophilic model drug calcein to C2C12 mouse myoblasts in vitro. The microrobots were non-toxic, allowing the cells to adhere, migrate, and proliferate on their surfaces.[247] Tubular robots, with cone or cylinder shapes, propel like miniature jets or rockets and remain a widely researched design in micro/nanorobot development.[248] Wang *et al*. created a tubular nanoswimmer, depicted in Fig. 11D, that is functionalized with gold nanoshells and can perforate HeLa cell membranes through photomechanical action when exposed to NIR light. The tubular structure was fabricated using a template-assisted layer-by-layer (LbL) deposition method, allowing for enhanced control over parameters such as length and wall thickness compared to conventional techniques.[249] Ussia *et al*. presented light-powered, self-propelled tubular nanorobots (Fig. 11E) made of Black-TiO_2 with silver nanoparticles (Ag NPs) fabricated via physical deposition. These nanorobots were designed for bacterial biofilm degradation on commercially used titanium facial miniplate implants.[250]

Besides the most frequently used shapes, several other micro/nanorobot designs have been reported in the literature. The cargo transport and drug delivery at the microscale can be achieved by using microbowls.[251] For guided cargo transport, targeted drug delivery, pH sensing, and nanoimaging, microrockets.[252] have been developed. Microcannons are ballistic devices using micro/nanorobotics for cargo loading and firing.[208] Other examples are the microwheels for targeted transport.[253] Microdaggers are used in single-cell surgery as well as in delivery applications.[254] Microfish have been developed for cancer treatment applications.[255]

The size of MNRBs is essential for biomedical applications, influencing their mobility and ability to interact with biological barriers, including the blood-brain barrier and vascular endothelial barrier. Smaller nanorobots could be eliminated by the kidneys, whereas larger ones may be intercepted by immune cells or resident phagocytes in organs like the liver and spleen, potentially provoking an immune response. Additionally, size impacts motion control; smaller robots are more influenced by Brownian motion, leading to more disordered movement, making trajectory analysis necessary for accurate control. Thus, size must be considered during robot design to optimize their functionality and clearance.[256]

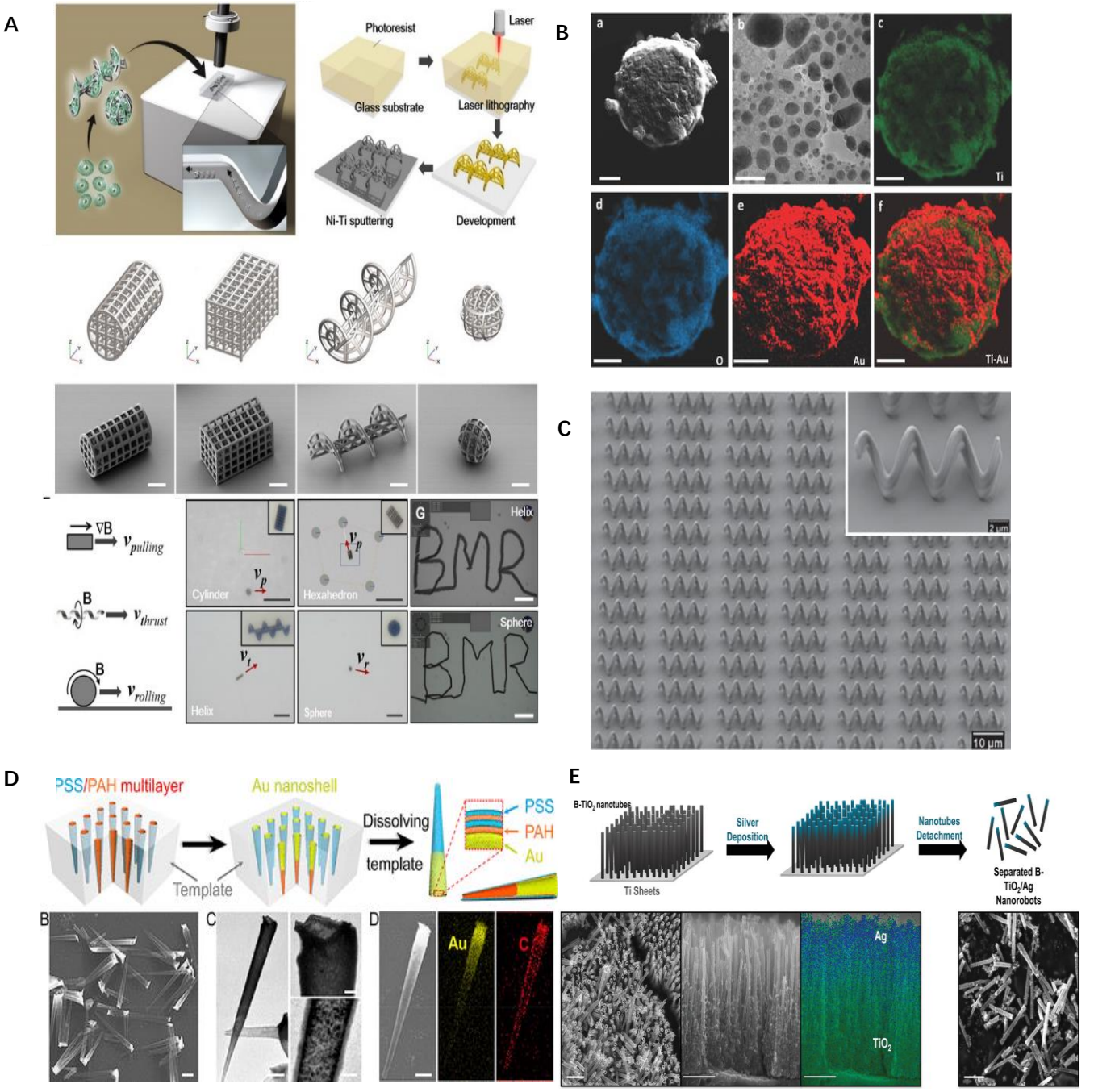

Fig. 11 Representative forms of Micro/nanobots. (A) Microrobot Manufacturing and Magnetic Regulation: A) Overview: (a) Schematic diagrams of microrobots, (b) Outline of the fabrication process, (c) CAD designs for cylindrical, hexahedral, helical, and spherical microrobots, (d) SEM images with 40 μm scale bars, (e) Illustration of propulsion mechanisms, (f) Cylindrical and hexahedral microrobots guided by magnetic field gradients, while helical and spherical ones use rotating magnetic fields, (g) BMR trajectories of helical and spherical microrobots. Reproduced with the permission from [242], Copyright 2019 The American Association for the Advancement of Science. (B) a-f) TEM image of a spherical hollow mesoporous TiO_2 microswimmer with a gold cap. Reproduced with the permission from [245] Copyright 2018, WILEY-VCH Verlag GmbH & Co). (C) SEM image showing a horizontal arrangement of artificial bacterial flagella (ABFs), with the inset displaying a helical swimmer at a higher magnification. Reproduced with the permission from [247] Copyright 2014 Wiley-VCH Verlag GmbH & Co) (D) Discusses the fabrication of AuNS-functionalized (PSS/PAH)10 tubular nanoswimmers, showing (a) the preparation process, (b) SEM image (2 μm scale bar), (c) TEM images with varying scales, and (d) EDX mapping for gold and carbon distribution (1 μm scale bar). Reproduced with the permission from [249] Copyright 2019 American Chemical Society. (E) Fabrication and characterization of B-TiO_2/Ag tubular nanorobots: Schematic of the fabrication process, with cross-sectional SEM-EDX images and top and cross-sectional SEM images displayed before and after detachment from Ti sheets. Scale bars are 2 μm. Reproduced with the permission from [250] Copyright 2022, Wiley VCH GmbH).

4.1 Biomedical applications

The integration of medicine with microrobotics and nanorobotics has swiftly evolved into a burgeoning interdisciplinary research area. These medical MNRBs, or Medbots, are designed to perform precise tasks within the complex human physiological environment. MNRBs enable access to hard-to-reach areas of the body and can carry out a range of medical procedures. Their potential applications in medicine are extensive, from disease prevention, diagnosis, and treatment to monitoring, regulating, and maintaining tissue homeostasis.[256,257]

4.2 Drug delivery

One of the main challenges of conventional drug delivery systems is reaching remote areas of the body. MNRBs, guided by external fields, offer a solution for targeted and intelligent drug delivery. These micro/nanorobots can carry various therapeutic cargos, including drugs, biologics, and cells.[76] MNRBs enable controlled release triggered by external stimuli, such as magnetic, acoustic, or infrared signals, allowing for more efficient dosing and reduced toxicity. They also respond passively to physiological conditions like temperature or pH at the target site. While promising, clinical applications are still being developed.[164]

Recently, Pané *et al*. combined TPP 3D printing with bottom-up synthesis to create a new class of biomedical microrobots called motile metal-organic frameworks or MOFbots. This began with the fabrication of 3D helical microstructures with a magnetic feature through TPP; on these structures, zinc-based MOF crystals, specifically zeolitic imidazole framework-8, were deposited. These crystals lend MOFbots biocompatibility and degradability, as well as pH sensitivity. The MOFbots moved along pre-programmed trajectories by control under a very weak rotational magnetic field. Additionally, they selectively targeted and delivered drugs to individual 3T3 cells and breast cancer cells MDA-MB231, as illustrated in Fig. 12A, using a complex microfluidic platform that facilitated the uptake of Rhodamine B as a model drug. This hybrid method combines the principles of 3D printing and surface modification to realize multifunctional microrobots and, as such, promises promising prospects for advanced drug delivery in cancer therapy.[130] Park *et al*. created a biodegradable microrobot that uses magnetic propulsion for targeted drug delivery and thermal therapy. Constructed from PEGDA and pentaerythritol triacrylate (PETA), it incorporates Fe_3O_4 nanoparticles and the anticancer drug 5-fluorouracil (5-FU). The microrobot is guided to its target site by a rotating magnetic field, where it releases 5-FU. Additionally, an alternating magnetic field raises the microrobot's temperature, improving its effectiveness in reducing cancer cell viability.[258] Likewise, various other nanobots have been created to improve the effectiveness of cancer treatment by delivering medications like Doxorubicin through the use of MNRBs.[259,260]

MNRBs can function as active drug delivery systems (DDS) for targeted treatment of bacterial infections, reducing the need for systemic antibiotic administration.[261] For instance, Bhuyan *et al*. prepared biocompatible micromotors from tea buds, called T-Budbots, that could be steered magnetically toward biofilm matrices for the precise fragmentation or removal of biofilms in a non-invasive "Kill-n-Clean" approach. Further, it has been reported that the porous T-Budbots can take up the ciprofloxacin antibiotic through electrostatic interactions in order to amplify their impact against antibacterial activity towards pathogenic bacterial communities, including *Pseudomonas aeruginosa* and *Staphylococcus aureus*. The antibiotic release can be controlled by pH, with acidic biofilm environments triggering release and higher pH levels limiting it. Fig. 12B demonstrates the antibiofilm activity of the Budbots, which was confirmed by the observed destruction of biofilms following treatment with the T-Budbots. This development of plant-based microrobots with magnetic therapeutic abilities for safe, non-invasive removal of biofilm infections is a notable advancement.[262]

As a step towards the assessment of the potential of micromotors in circulation, Schmidt *et al*. prepared a series of biohybrid Spermbots using photoresist IP-Dip by 3D printing with the TPP method. These Spermbots used rheotaxis, swimming against the blood flow and delivering heparin-loaded liposomes to target sites. In the present microrobotic design, the flagella of sperm provided an exceptionally good propulsion. For the 3D-printed microcapsules, magnetic navigation and therapeutic transport functions were achieved through the sequential coating of layers of Ti (2 nm) and Fe (15 nm), Ti (2 nm), and SiO_2 (10 nm) onto the 3D-printed microcapsules by e-beam evaporation. Coating the Fe layer at an angle of 75° enabled a lot of Spermbots to align into a train-like structure upon magnetization, thus enabling efficient drug transport into the targeted area. Such results, therefore, indicate that the possibility of applying Spermbots for use as microcarriers in anticoagulant delivery in cases of blood clots and other circulatory-related conditions might be possible.[263] Cell-based therapy holds great potential for treating neurodegenerative diseases that result in irreversible neuronal damage and cell death. Pané *et al*. recently developed multifunctional soft 3D helical microswimmers using TPP 3D printing. Made from GelMA hydrogels and infused with magnetoelectric multiferroic nanoparticles, these microswimmers enable targeted magnetic delivery of SH-SY5Y neuronal cells and wireless cellular electrostimulation. Designed to be enzymatically degradable, this approach could advance microrobotic systems for targeted therapies in central nervous system disorders.[178] Sanchez *et al*. demonstrated the transport and release of CAD cells (a catecholaminergic cell line from the central nervous system) using catalytic microbots. These microbots generated oxygen bubbles from the catalytic decomposition of peroxide fuel within microtubes (m-tubes) for propulsion. Their movement was guided by an external magnetic field, enabling precise cell release at

targeted locations through rapid rotation.[263]

4.3 Imaging and diagnosis

Medical MNRBs play a crucial role in clinical settings by enabling individual or collective monitoring. These small robots can effectively navigate the body to deliver cargo and perform microsurgical procedures in hard-to-reach areas, enhancing medical imaging capabilities. Advanced microrobots can be tracked in real time using current medical imaging technologies for precise navigation and positioning.[76]

Fluorescence-based imaging is beneficial because it utilizes safe, visible light and cost-effective materials. When integrated into MNRBs, this technique improves tracking and targeting and broadens applications in bioimaging and diagnostics.[264-268] Various fluorescent MNRBs have been developed using fluorescent materials or by incorporating labels during fabrication.[269-271] Yan *et al*. created Spirulina-based biohybrid helical magnetic microrobots through a simple dip-coating method in magnetite (Fe_3O_4) suspensions. As shown in Fig. 12C, they performed fluorescence-based in vivo imaging of the microrobots in the intraperitoneal cavity of nude mice, demonstrating strong red-light emission under green light due to microalgae autofluorescence, without needing additional fluorescent markers. This facilitated real-time tracking and sensitive detection in vivo, especially within subcutaneous tissue and the intraperitoneal cavity. The fluorescence intensity rose with increasing sample concentration but diminished over time, underscoring their potential for real-time tracking and image-guided therapy via magnetic control.[233] RI imaging techniques are also effective for visualizing MNRBs. Vilela *et al*. showed that PET-CT imaging can monitor 124 iodine-labeled bubble-propelled tubular micromotors, which were fabricated using template-directed electrodeposition and metal evaporation, with iodine-124 radiolabelling applied to their gold surface. This labelling allowed detection via PET, making it suitable for future in vivo studies. Imaging in linear phantoms revealed that the movement of these microrobots could be tracked using PET-CT, providing dynamic quantitative data on their spatial distribution, consistent with optical microscopy observations.[272] MRI is a valuable method for visualizing magnetic MNRBs in both in vitro and in vivo scenarios, providing high contrast and advantages over other imaging modalities. Go *et al*. described microrobots visualized via real-time X-ray and MRI, designed for magnetic guidance to tumor feeding vessels for transcatheter liver chemoembolization in vivo. The study also highlighted MRI's potential for monitoring these microrobots in postoperative imaging.[273] In addition to MRI, micro/nanobots can also employ photoacoustic imaging. Wrede *et al*. created microrobots the size of microcapillaries, made from nanoliposomes loaded with ICG and coated with multiple layers of gold. The gold improves the optoacoustic signal in the NIR spectrum, facilitating deeper tissue imaging. Real-time volumetric optoacoustic imaging of circulating microrobots, measuring 5 to 20 μm in diameter, was successfully shown in ex vivo models of porcine heart vessels and mouse brain blood vessels, even against a highly absorptive blood background (Fig. 12D). These microrobots can be effectively controlled and maneuvered magnetically within the blood vessels.[268,274]

4.4 Tissue engineering/regeneration

Cell-based regenerative medicine has gained significant attention lately. For successful cell transplantation, an adequate 3D structure is essential. MNRBs present a promising approach, facilitating the attachment, growth, and differentiation of cells while enabling their movement and functions to be remotely controlled using various energy sources.[264] Stem cell therapies have quickly become a highly effective method for regenerating damaged tissues and organs.[265] Yasa *et al*. created magnetically controlled double-helical micro transporters, measuring 76 μm long with a 20 μm inner diameter, using TPP 3D printing for remote operation. These transporters mimic the mesenchymal stem cell (MSC) environment by encoding mechanical and biological cues at the single-cell level, enhancing differentiation into osteogenic cells. In a rotating magnetic field, the MSC-loaded transporters followed defined paths in a confined microchannel while preserving the osteogenic potential of the MSCs. These microrobotic carriers hold great promise for precise and targeted cell delivery in therapeutic settings.[266] Tian *et al*. developed a magnetically driven microbot composed of magnetic microsphere scaffold (MMS) beads that encapsulate mesenchymal stem cells (MSC). This microbot features seven MMS beads—four with low and three with high concentrations of magnetic nanoparticles—resulting in a soft structure that bends under magnetic torque from an oscillating field for targeted navigation. The MMS beads, made from biocompatible and biodegradable alginate, dissolve in extracellular fluid, allowing sodium ions to replace calcium and break down the gel structure, thereby releasing MSCs expected to retain high viability and proliferation. as shown in Fig. 13E.[275]

There is an increasing demand for multifunctional microrobots with complex microscale designs that can be fabricated, controlled, and functionalized. Liu *et al*. developed chrysanthemum pollen biohybrid magnetic microrobots (CDBMRs) featuring intricate attributes like spiny protrusions, hollow cavities, and porous surfaces for cancer treatment and tissue repair. They optimized a fabrication process to maintain the natural structure of the pollen templates. Under the influence of a magnetic field, CDBMRs demonstrated a range of behaviors, both individually and collectively. These microrobots facilitated synergistic tumor therapy through magnetically regulated destruction and active drug delivery. Additionally, CDBMRs showed enhanced capabilities in cell delivery and tissue regeneration, confirmed by their improved osteogenic properties. This innovative approach leverages the inherent structure of pollen grains,

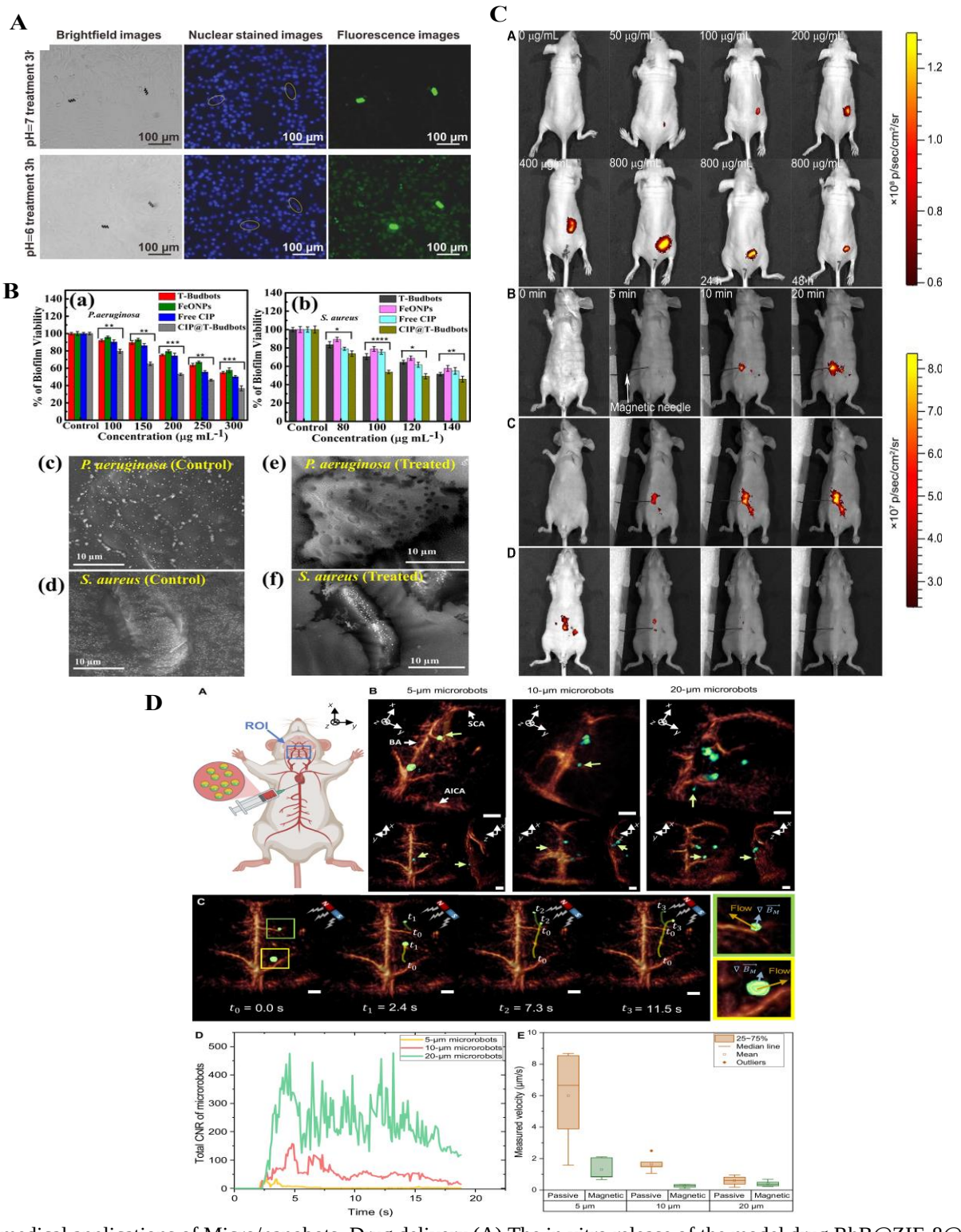

Fig. 12 Biomedical applications of Micro/nanobots. Drug delivery (A) The in vitro release of the model drug RhB@ZIF-8@ABF in PBS solutions at pH 7.4 and pH 6.0, targeting fixed MDA-MB231 breast cancer cells. Reproduced with the permission from [130], Copyright 2019 WILEY-VCH Verlag GmbH & Co. KGaA, Weinheim) (B) Antibiofilm effects of T-Budbots, FeONPs, free CIP, and CIP@T-Budbots against *P. aeruginosa* and *S. aureus*, with significant statistical differences indicated. FESEM images show biofilms for the control group and those treated with CIP@T-Budbots. Reproduced with the permission from [262], Copyright 2020 American Chemical Society). Imaging**:** (C) Fluorescence-based in vivo imaging of MSP at various residence times in the intraperitoneal cavity. Reproduced with the permission from [233], Copyright 2017 The American Association for the Advancement of Science.). (D) Non-invasive OAT imaging tracks microrobots in mouse brain vasculature with a schematic of their injection and monitoring. OAT images show Lipo-ICG-coated microrobots, with control via a magnet and a comparison of velocity between magnetic manipulation and passive flow. Reproduced with the permission from [268], Copyright 2022 The American Association for the Advancement of Science.

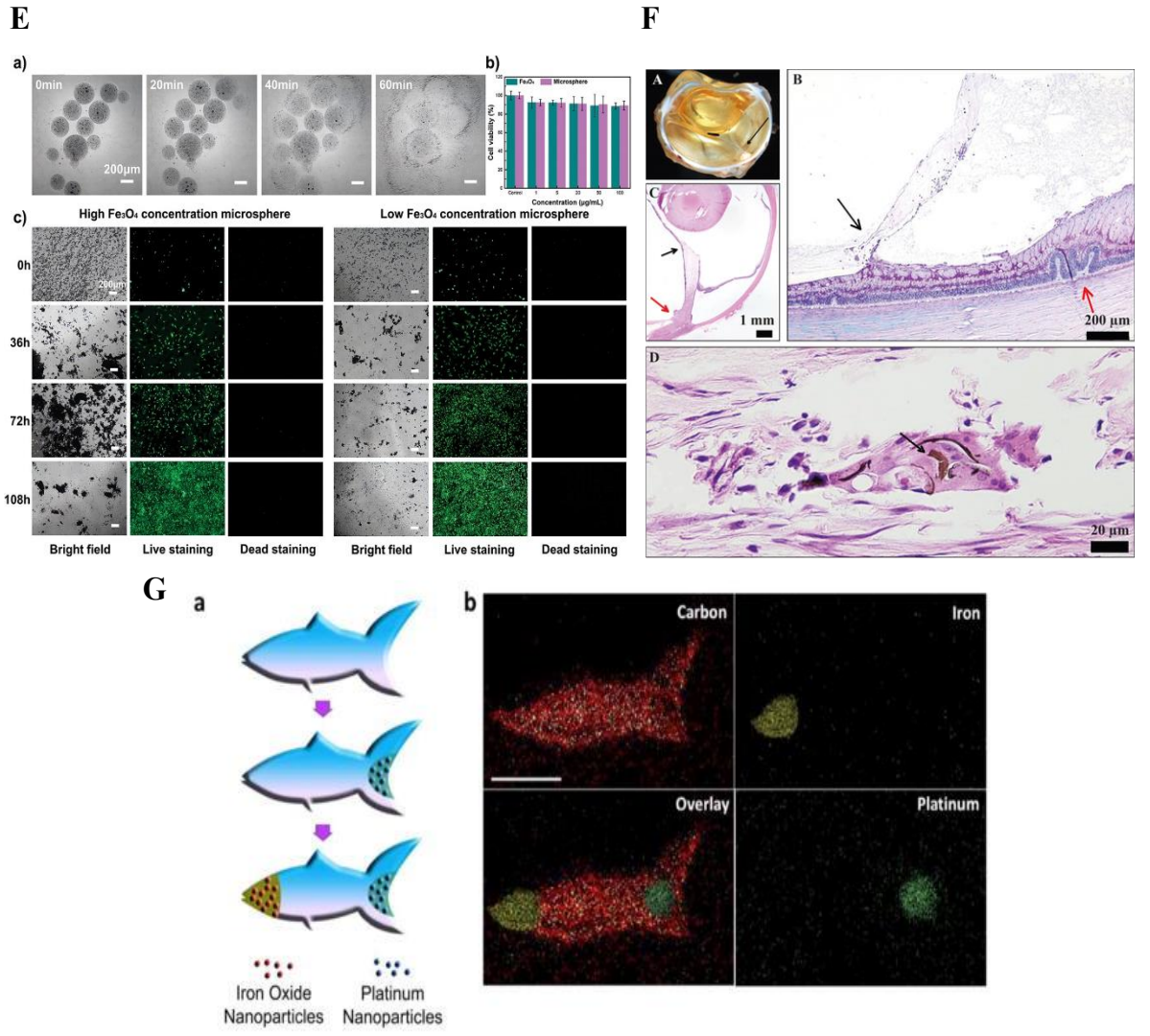

Fig. 13 Biomedical applications of Micro/nanobots. Tissue Engineering**:** (E) Delivery of mesenchymal stem cells (MSCs) from magnetic microspheres (MMS), with optical images showing MMS dissolution in PBS and viability assessed by MTS assay. Bright-field and live/dead staining images show viable MSCs. Scale bars: 200 μm. Reproduced with the permission from [275], Copyright 2023, Wiley-VCH GmbH. Microsurgery: (F) Macroscopic image shows a hemisected eye with a microrobot embedded in the vitreous. Indicators of complete retinal detachment and other features are noted. Reproduced with permission from [278], Copyright 2016 Wiley Periodicals, Inc. Biosensing**:** (G) Schematic of the functionalization process for a microfish designed for guided catalytic propulsion, with EDX images showing the distribution of iron oxide and platinum in the microfish body. Reproduced with permission from [149], Copyright 2015, WILEY-VCH Verlag GmbH & Co. KGaA, Weinheim.

presenting a promising alternative for effective tumor treatment and tissue regeneration.[268] In summary, these functional designs indicate that microrobots could be used for tissue engineering applications, though additional in vivo research is required.

4.5 Microsurgery

Micro/nanobots are essential in minimally invasive surgery, providing access to areas that traditional tools cannot reach. Their use in techniques like endoscopic or robot-assisted surgery reduces incision size and postoperative complications while speeding up recovery. Additionally, remote microscopy enhances precision and control, lowering physical trauma and infection risks. Overall, research suggests that these technologies significantly improve outcomes and reduce tissue damage in surgical procedures.[276]

Small robots can act as wireless biopsy tools, effectively extracting single cells or tissue samples from both healthy and diseased organs. Jin *et al*. developed a thermosensitive magnetic microrobot, measuring 70 μm in length and 15 μm at the tip, with a paraffin wax thermal response layer embedded with magnetic iron. This design allows the microrobot to navigate narrow tissues when an external magnetic field is applied, capturing cells as the temperature rises. Although the research has primarily been in static liquid environments, in vivo applications remain untested.[277] MNRBs have the potential to transform intravitreal injection therapy in ophthalmic medicine. Unlike traditional drug

delivery methods that depend on passive diffusion, which struggles to target specific areas behind the eyes, these microrobots offer improved precision. Research by Pokki *et al*. (Fig. 13F) on gold-plated cobalt/nickel microrobots coated with polypyrrole (PPy) demonstrated a significantly reduced inflammatory response in rabbits compared to the control group. Thus, MNRBs hold great promise for enhancing drug delivery in retinal procedures.[278]

4.6 Biosensors

MNRBs are promising as biosensors in advanced sensing systems. Kong *et al*. sought to enhance glucose detection in human serum using Mg/Pt Janus micromotors, eliminating the need for toxic fuels or surfactants. They utilized electrochemical sensing for its rapid speed, high sensitivity, selectivity, and cost-effectiveness in detecting biomolecules. By immobilizing glucose oxidase (GOx) on the electrode surface, they developed a method for selective blood glucose measurement. Their use of a second-generation glucose biosensor with a screen-printed electrode (SPE) allowed for miniaturization and minimized sample volume. Results indicated that the Mg/Pt Janus micromotors improved detection current, establishing a linear relationship between current signal and glucose concentration, thus supporting the creation of point-of-care diagnostic devices that leverage autonomous micromotors for swift analysis.[278] Li *et al*. created a live biosensor and microrobot that uses a red blood cell waveguide to monitor pH levels in the body. This waveguide is sensitive to environmental changes and the shape of red blood cells, which varies with blood pH, allowing it to detect pH fluctuations and related blood diseases within a range of 5.0 to 9.0.[279] At the same time, Chen *et al*. created 3D swimming microfish using microscale continuous optical printing (mCOP) with PEGDA hydrogels and various functional nanoparticles. These include platinum (Pt) for propulsion, iron oxide (Fe_3O_4) for magnetic control, and polydiacetylene for neutralizing toxins (Fig. 13G). The 3D-printed microfish demonstrate significant potential for biosensing and detoxification, featuring controlled movement.[149,280]

5. Conclusion and outlook

The scientific revolution has facilitated the convergence of information technology, biotechnology, medicine, and robotics. This integration has significantly advanced various fields, particularly medicine, where nanoscale and microscale robots are now being developed to assist in disease detection, targeted drug delivery, and treatment. This review explores recent developments in materials, fabrication methods, actuation techniques, and designs for micro/nanobots (MNRBs) intended for biomedical applications. In the past ten years, there has been considerable advancement in the biomedical sector with the creation of MNRBs serving multiple purposes. Compared to traditional medical treatments, MNRBs offer key benefits, such as greater load-bearing capacity and enhanced mobility, which enable them to deliver therapies more effectively to targeted areas. These robots are typically biocompatible and powered by external energy sources, allowing them to be directed precisely to the affected site. This results in fewer side effects, improved surgical outcomes, and faster patient recovery. The main conclusions from the survey of recent advancements in MNRB technology include certain aspects right from materials used to fabrication techniques. MNRBs designed for in vivo applications must meet rigorous material criteria, particularly concerning biocompatibility, biodegradability, and scalability. A major challenge lies in identifying new materials that meet these needs. The review explores these materials, focusing on their machinability, biodegradability, and compatibility with biological environments. Recent advances in non-degradable, degradable, biological, and functionalized materials have been used since they exhibit suitability for respective fabrication methods, properties, and characteristics from required applications. When designing MNRBs for medical purposes, factors such as cost, targeting precision, biocompatibility, and degradability must be carefully considered. The fabrication technique chosen greatly impacts the performance of MNRBs. While methods like SLA, SLS, FDM, PVD, and self-assembly are available, 3D printing excels in creating detailed designs. In contrast, two-photon polymerization (TPP) achieves superior resolution and complexity, but at the cost of higher expenses, material restrictions, and longer production times. The review highlights several common methods for controlling MNRBs, such as using external electric fields, magnetic fields, ultrasound, or light fields via wireless communication or self-propulsion. Magnetic actuation offers distinct advantages, including high power, precision, and fast response times, making it ideal for controlling MNRBs in biological systems. MNRBs propelled via magnetic field are effectively utilized for targeted drug delivery and in minimally invasive surgeries, functioning in biological environments characterized by low Reynolds numbers, where viscous forces prevail. Wireless communication is crucial for real-time interaction between surgeons and these microrobots during procedures. Research highlights the significant potential of MNRBs in this field, with their structure being key to performance. Common designs, such as helical, spherical, and tubular shapes, are used for drug delivery in weak magnetic fields, while multi-porous surfaces enhance their load-bearing capacity. Microneedles can penetrate cell membranes to deliver substances mechanically. Despite the variety of structures developed, a more systematic approach to design is needed to fulfill specific functional requirements, with future research aimed at creating innovative solutions tailored to medical applications.

Despite the considerable progress made in micro/nanobot technology, many existing systems are still in the preliminary phases of advancements and primarily remain prototypes. To effectively expand the use of MNRBs in therapeutic interventions within living organisms, substantial research

efforts and innovative breakthroughs are required. Key areas for research include: (a) the need for new preparation technologies that optimize and functionalize the structures of micro/nanorobots, enabling cost-effective, high-volume production of diverse designs; (b) ensuring that the materials used meet biomedical and environmental standards, enhancing biocompatibility and biodegradability while reducing toxicity in medical settings; (c) improving external control systems for more precise manipulation of micro/nanorobots, along with developing complementary driving methods; (d) utilizing collective behavior among swarms of micro/nanorobots to perform tasks in intricate biological settings that individual robots cannot, thereby enhancing operational efficiency; (e) utilizing biological imaging technologies to facilitate closed-loop feedback control and real-time observation of micro/nanobots in living organisms.

Despite the considerable obstacles that must be addressed before micro/nanobots can be extensively used in clinical practice, their potential influence on precision medicine is substantial. Successfully tackling these challenges could greatly enhance the progress of contemporary biomedicine and significantly elevate human health and quality of life.

Conflict of Interest

There is no conflict of interest.

Supporting Information

Not applicable.

References

[1] Z. Sun, Y. Hou, Micro/nanorobots as active delivery systems for biomedicine: from self-propulsion to controllable navigation, *Advanced Therapeutics*, 2022, **5**, 2100228, doi: 10.1002/adtp.202100228.

[2] G. Chen, F. Zhu, A. S. J. Gan, B. Mohan, K. K. Dey, K. Xu, G. Huang, J. Cui, A. A. Solovev, Y. Mei, Towards the next generation nanorobots, *Next Nanotechnology*, 2023, **2**, 100019, doi: 10.1016/j.nxnano.2023.100019.

[3] R. Wu, Y. Zhu, X. Cai, S. Wu, L. Xu, T. Yu, Recent process in microrobots: from propulsion to swarming for biomedical applications, *Micromachines,* 2022, **13**, 1473, doi: 10.3390/mi13091473.

[4] G. University, V. A. Rahul, A brief review on nanorobots, *International Journal of Mechanical Engineering*, 2017, **4**, 15-21, doi: 10.14445/23488360/ijme-v4i8p104.

[5] S. Mazumder, G. R. Biswas, S. B. Majee, Applications of nanorobots in medical techniques, *International Journal of Pharmaceutical Sciences And Research*, 2020, **11**, 3150, doi: 10.13040/IJPSR.0975-8232.11(7).3138-47

[6] Á. Molinero-Fernández, M. Moreno-Guzmán, L. Arruza, M. Á. López, A. Escarpa, Polymer-based micromotor fluorescence immunoassay for On-the-move sensitive procalcitonin determination in very low birth weight infants' plasma, *ACS Sensors*, 2020, **5**, 1336-1344, doi: 10.1021/acssensors.9b02515.

[7] V. Iacovacci, A. Blanc, H. Huang, L. Ricotti, R. Schibli, A. Menciassi, M. Behe, S. Pané, B. J. Nelson, High-resolution SPECT imaging of stimuli-responsive soft microrobots, *Small*, 2019, **15**, 1900709, doi: 10.1002/smll.201900709.

[8] B. E. de Ávila, P. Angsantikul, J. Li, M. Angel Lopez-Ramirez, D. E. Ramírez-Herrera, S. Thamphiwatana, C. Chen, J. Delezuk, R. Samakapiruk, V. Ramez, M. Obonyo, L. Zhang, J. Wang, Micromotor-enabled active drug delivery for in vivo treatment of stomach infection, *Nature Communications*, 2017, **8**, 272, doi: 10.1038/s41467-017-00309-w.

[9] M. Wan, Q. Wang, R. Wang, R. Wu, T. Li, D. Fang, Y. Huang, Y. Yu, L. Fang, X. Wang, Y. Zhang, Z. Miao, B. Zhao, F. Wang, C. Mao, Q. Jiang, X. Xu, D. Shi, Platelet-derived porous nanomotor for thrombus therapy, *Science Advances*, 2020, **6**, eaaz9014, doi: 10.1126/sciadv.aaz9014.

[10] G. Muthukumaran, U. Ramachandraiah, D. G. H. Samuel, Role of nanorobots and their medical applications, *Advanced Materials Research*, 2015, **1086**, 61-67, doi: 10.4028/www.scientific.net/amr.1086.61.

[11] S. Andhari, G. Khutale, R. Gupta, Y. Patil, J. Khandare, Chemical tunability of advanced materials used in the fabrication of micro/nanobots, *Journal of Materials Chemistry. B*, 2023, **11**, 5301-5320, doi: 10.1039/d2tb02743g.

[12] J. Guo, J. J. Gallegos, A. R. Tom, D. Fan, Electric-field-guided precision manipulation of catalytic nanomotors for cargo delivery and powering nanoelectromechanical devices, *ACS nano*, 2018, **12**, 1179-1187, doi: 10.1021/acsnano.7b06824.

[13] W. F. Paxton, K. C. Kistler, C. C. Olmeda, A. Sen, S. K. St Angelo, Y. Cao, T. E. Mallouk, P. E. Lammert, V. H. Crespi, Catalytic nanomotors: autonomous movement of striped nanorods, *Journal of the American Chemical Society*, 2004, **126**, 13424-13431, doi: 10.1021/ja047697z.

[14] J. Liu, L. Li, C. Cao, Z. Feng, Y. Liu, H. Ma, W. Luo, J. Guan, F. Mou, Swarming multifunctional heater-thermometer nanorobots for precise feedback hyperthermia delivery, *ACS Nano*, 2023, **17**, 16731-16742, doi: 10.1021/acsnano.3c03131.

[15] X. Zheng, M. Wu, F. Kong, H. Cui, Z. Silber-Li, Visualization and measurement of the self-propelled and rotational motion of the Janus microparticles, *Journal of Visualization*, 2015, **18**, 425-435, doi: 10.1007/s12650-015-0299-5.

[16] V. Garcia-Gradilla, S. Sattayasamitsathit, F. Soto, F. Kuralay, C. Yardımcı, D. Wiitala, M. Galarnyk, J. Wang, Ultrasound-propelled nanoporous gold wire for efficient drug loading and release, *Small*, 2014, **10**, 4154-4159, doi: 10.1002/smll.201401013.

[17] F. Soto, G. L. Wagner, V. Garcia-Gradilla, K. T. Gillespie, D. R. Lakshmipathy, E. Karshalev, C. Angell, Y. Chen, J. Wang, *Acoustically propelled nanoshells, Nanoscale*, 2016, **8**, 17788-17793, doi: 10.1039/c6nr06603h.

[18] W. Gao, S. Sattayasamitsathit, K. M. Manesh, D. Weihs, J. Wang, Magnetically powered flexible metal nanowire motors, *Journal of the American Chemical Society*, 2010, **132**, 14403-14405, doi: 10.1021/ja1072349.

[19] S. S. Andhari, R. D. Wavhale, K. D. Dhobale, B. V. Tawade,

G. P. Chate, Y. N. Patil, J. J. Khandare, S. S. Banerjee, Self-propelling targeted magneto-nanobots for deep tumor penetration and pH-responsive intracellular drug delivery, *Scientific Reports*, 2020, **10**, 4703, doi: 10.1038/s41598-020-61586-y.

[20] Q. Cui, T. H. Le, Y. J. Lin, Y.-B. Miao, I. T. Sung, W. B. Tsai, H. Y. Chan, Z. H. Lin, H. W. Sung, A self-powered battery-driven drug delivery device that can function as a micromotor and galvanically actuate localized payload release, *Nano Energy*, 2019, **66**, 104120, doi: 10.1016/j.nanoen.2019.104120.

[21] J. G. S. Moo, C. C. Mayorga-Martinez, H. Wang, B. Khezri, W. Z. Teo, M. Pumera, Nano/microrobots meet electrochemistry, *Advanced Functional Materials*, 2017, **27**, 1604759, doi: 10.1002/adfm.201604759.

[22] M. Li, J. Wu, D. Lin, J. Yang, N. Jiao, Y. Wang, L. Liu, A diatom-based biohybrid microrobot with a high drug-loading capacity and pH-sensitive drug release for target therapy, *Acta Biomaterialia*, 2022, **154**, 443-453, doi: 10.1016/j.actbio.2022.10.019.

[23] W. Xu, H. Qin, H. Tian, L. Liu, J. Gao, F. Peng, Y. Tu, Biohybrid micro/nanomotors for biomedical applications, *Applied Materials Today*, 2022, **27**, 101482, doi: 10.1016/j.apmt.2022.101482.

[24] S. Xie, T. Xia, S. Li, C. Mo, M. Chen, X. Li, Bacteria-propelled microrockets to promote the tumor accumulation and intracellular drug uptake, *Chemical Engineering Journal*, 2020, **392**, 123786, doi: 10.1016/j.cej.2019.123786.

[25] D. Gong, N. Celi, D. Zhang, J. Cai, Magnetic biohybrid microrobot multimers based on Chlorella cells for enhanced targeted drug delivery, *ACS Applied Materials & Interfaces*, 2022, **14**, 6320-6330, doi: 10.1021/acsami.1c16859.

[26] S. Fusco, H. W. Huang, K. E. Peyer, C. Peters, M. Häberli, A. Ulbers, A. Spyrogianni, E. Pellicer, J. Sort, S. E. Pratsinis, B. J. Nelson, M. S. Sakar, S. Pané, Shape-switching microrobots for medical applications: the influence of shape in drug delivery and locomotion, *ACS Applied Materials & Interfaces*, 2015, **7**, 6803-6811, doi: 10.1021/acsami.5b00181.

[27] Y. Chen, R. Pan, Y. Wang, P. Guo, X. Liu, F. Ji, J. Hu, X. Yan, G. P. Wang, L. Zhang, Y. Sun, X. Ma, Carbon helical nanorobots capable of cell membrane penetration for single cell targeted SERS bio-sensing and photothermal cancer therapy, *Advanced functional materials*, 2022, **32**, 2200600, doi: 10.1002/adfm.202200600

[28] S. Subramanian, J. S. Rathore, N. N. Sharma, Design and analysis of helical flagella propelled nanorobots, IEEE International Conference on Nano/Micro Engineered and Molecular Systems, 2009.

[29] T. Y. Huang, M. S. Sakar, A. Mao, A. J. Petruska, F. Qiu, X. B. Chen, S. Kennedy, D. Mooney, B. J. Nelson, 3D printed microtransporters: compound micromachines for spatiotemporally controlled delivery of therapeutic agents, *Advanced Materials*, 2015, **27**, 6644-6650, doi: 10.1002/adma.201503095.

[30] Z. Xu, Z. Wu, M. Yuan, Y. Chen, W. Ge, Q. Xu, Versatile magnetic hydrogel soft capsule microrobots for targeted delivery, *iScience*, 2023, **26**, 106727, doi: 10.1016/j.isci.2023.106727.

[31] S. K. Panda, S. Debata, K. C. Andia, S. Das, D. P. Singh, Engineering light-driven rod-shaped micromotors for exhibiting controlled and tunable multimode swimming, *Advanced Optical Materials*, 2024, **12**, 2400590, doi: 10.1002/adom.202400590.

[32] X. Zhang, G. Chen, L. Cai, L. Fan, Y. Zhao, Dip-printed microneedle motors for oral macromolecule delivery, *Research*, 2022, **2022**, 9797482, doi: 10.34133/2022/9797482.

[33] S. Fathi-Karkan, M. Heidarzadeh, M. T. Narmi, N. Mardi, H. Amini, S. Saghati, F. N. Abrbekoh, S. Saghebasl, R. Rahbarghazi, A. B. Khoshfetrat, Exosome-loaded microneedle patches: promising factor delivery route, International *Journal of Biological Macromolecules*, 2023, **243**, 125232, doi: 10.1016/j.ijbiomac.2023.125232.

[34] L. Wang, P. Guo, D. Jin, Y. Peng, X. Sun, Y. Chen, X. Liu, W. Chen, W. Wang, X. Yan, X. Ma, Enzyme-powered tubular microrobotic jets as bioinspired micropumps for active transmembrane drug transport, *ACS Nano*, 2023, **17**, 5095-5107, doi: 10.1021/acsnano.3c00291.

[35] Y. Yang, J. Rosalie, L. Bourgeois, P. A. Webley, Bulk synthesis of carbon nanostructures: hollow stacked-cone-helices by chemical vapor deposition, *Materials Research Bulletin*, 2008, **43**, 2368-2373, doi: 10.1016/j.materresbull.2007.08.020.

[36] C. Xin, L. Yang, J. Li, Y. Hu, D. Qian, S. Fan, K. Hu, Z. Cai, H. Wu, D. Wang, D. Wu, J. Chu, Conical hollow microhelices with superior swimming capabilities for targeted cargo delivery, *Advanced Materials*, 2019, **31**, e1808226, doi: 10.1002/adma.201808226.

[37] J. Shao, M. Abdelghani, G. Shen, S. Cao, D. S. Williams, J. C. M. van Hest, Erythrocyte membrane modified Janus polymeric motors for thrombus therapy, *ACS Nano*, 2018, **12**, 4877-4885, doi: 10.1021/acsnano.8b01772.

[38] M. Ren, W. Guo, H. Guo, X. Ren, Microfluidic fabrication of bubble-propelled micromotors for wastewater treatment, *ACS Applied Materials & Interfaces*, 2019, **11**, 22761-22767, doi: 10.1021/acsami.9b05925.

[39] A. Sharma, Y. Zhu, M. Reddy, A. Hubel, R. Cobian, L. Tan, B. Stadler, Steerable nanobots for diagnosis and therapy, *Springer Proceedings in Physics*, 2014, **150**,179-189, doi: 10.1007/978-3-319-02207-9_18.

[40] J. Puigmartí-Luis, E. Pellicer, B. Jang, G. Chatzipirpiridis, S. Sevim, X.-Z. Chen, B. J. Nelson, S. Pané, Magnetically and chemically propelled nanowire-based swimmers, *Magnetic Nano- and Microwires*, 2020, 777-799, doi: 10.1016/b978-0-08-102832-2.00026-8.

[41] D. Liu, R. Guo, B. Wang, J. Hu, Y. Lu, Magnetic micro/nanorobots: a new age in biomedicines, *Advanced Intelligent Systems*, 2022, **4**, 2200208, doi: 10.1002/aisy.202200208.

[42] Y. Zhang, Y. Zhang, Y. Han, X. Gong, Micro/nanorobots for medical diagnosis and disease treatment, *Micromachines*, 2022, **13**, 648, doi: 10.3390/mi13050648.

[43] A. Baptista, F. Silva, J. Porteiro, J. Míguez, G. Pinto, sputtering physical vapour deposition (PVD) coatings: a critical review on process improvement and market trend demands, *Coatings*, 2018, **8**, 402, doi: 10.3390/coatings8110402.

[44] H. Yu, W. Tang, G. Mu, H. Wang, X. Chang, H. Dong, L. Qi, G. Zhang, T. Li, Micro-/ nanorobots propelled by oscillating magnetic fields, *Micromachines*, 2018, **9**, 540, doi: 10.3390/mi9110540.
[45] H. Su, S. Li, G. Z. Yang, K. Qian, Janus micro/nanorobots in biomedical applications, *Advanced Healthcare Materials*, 2023, **12**, e2202391, doi: 10.1002/adhm.202202391.
[46] L. Wang, X. Hao, Z. Gao, Z. Yang, Y. Long, M. Luo, J. Guan, Artificial nanomotors: Fabrication, locomotion characterization, motion manipulation, and biomedical applications, *Interdisciplinary Materials*, 2022, **1**, 256-280, doi: 10.1002/idm2.12021.
[47] H. Wang, M. Pumera, Fabrication of micro/nanoscale motors, *Chemical Reviews*, 2015, **115**, 8704-8735, doi: 10.1021/acs.chemrev.5b00047.
[48] A. Biswas, I. S. Bayer, A. S. Biris, T. Wang, E. Dervishi, F. Faupel, Advances in top–down and bottom–up surface nanofabrication: techniques, applications & future prospects, *Advances in Colloid and Interface Science*, 2012, **170**, 2-27, doi: 10.1016/j.cis.2011.11.001.
[49] X. Ma, K. Hahn, S. Sanchez, Catalytic mesoporous Janus nanomotors for active cargo delivery, *Journal of the American Chemical Society,* 2015, **137**, 4976-4979, doi: 10.1021/jacs.5b02700.
[50] M. Xuan, Z. Wu, J. Shao, L. Dai, T. Si, Q. He, Near infrared light-powered Janus mesoporous silica nanoparticle motors, *Journal of the American Chemical Society*, 2016, **138**, 6492-6497, doi: 10.1021/jacs.6b00902.
[51] M. Xuan, J. Shao, C. Gao, W. Wang, L. Dai, Q. He, Self-propelled nanomotors for thermomechanically percolating cell membranes, *Angewandte Chemie*, 2018, **57**, 12463-12467, doi: 10.1002/anie.201806759.
[52] L. Baraban, D. Makarov, R. Streubel, I. Mönch, D. Grimm, S. Sanchez, O. G. Schmidt, Catalytic Janus motors on microfluidic chip: deterministic motion for targeted cargo delivery, *ACS Nano*, 2012, **6**, 3383-3389, doi: 10.1021/nn300413p.
[53] V. S. Saji, Electrodeposition in bulk metallic glasses, *Materialia*, 2018, **3**, 1-11, doi: 10.1016/j.mtla.2018.09.021.
[54] J. G. S. Moo, C. C. Mayorga-Martinez, H. Wang, B. Khezri, W. Z. Teo, M. Pumera, Nano/microrobots meet electrochemistry, *Advanced Functional Materials*, 2017, **27**, 1604759, doi: 10.1002/adfm.201604759.
[55] T. He, Y. Yang, X. B. Chen, Preparation, stimulus-response mechanisms and applications of micro/nanorobots, *Micromachines*, 2023, **14**, 2253, doi: 10.3390/mi14122253.
[56] A. B. A. Nana, T. Marimuthu, P. P. D. Kondiah, Y. E. Choonara, L. C. Du Toit, V. Pillay, Multifunctional magnetic nanowires: design, fabrication, and future prospects as cancer therapeutics, *Cancers*, 2019, **11**, 1956, doi: 10.3390/cancers11121956.
[57] A. Serrà, J. García-Torres, Electrochemistry: A basic and powerful tool for micro- and nanomotor fabrication and characterization, *Applied Materials Today*, 2021, **22**, 100939, doi: 10.1016/j.apmt.2021.100939.
[58] W. F. Paxton, K. C. Kistler, C. C. Olmeda, A. Sen, S. K. St Angelo, Y. Cao, T. E. Mallouk, P. E. Lammert, V. H. Crespi, Catalytic nanomotors: autonomous movement of striped nanorods, *Journal of the American Chemical Society*, 2004, **126**, 13424-13431, doi: 10.1021/ja047697z.
[59] L. Zhang, T. Petit, Y. Lu, B. E. Kratochvil, K. E. Peyer, R. Pei, J. Lou, B. J. Nelson, Controlled propulsion and cargo transport of rotating nickel nanowires near a patterned solid surface, *ACS Nano*, 2010, **4**, 6228-6234, doi: 10.1021/nn101861n.
[60] H. Wang, J. Kan, X. Zhang, C. Gu, Z. Yang, Pt/CNT micro-nanorobots driven by glucose catalytic decomposition, *Cyborg and Bionic Systems*, 2021, **2021**, 9876064, doi: 10.34133/2021/9876064.
[61] Z. Zheng, H. Wang, S. O. Demir, Q. Huang, T. Fukuda, M. Sitti, Programmable aniso-electrodeposited modular hydrogel microrobots, *Science Advances*, 2022, **8**, eade6135, doi: 10.1126/sciadv.ade6135.
[62] H. Wang, M. Pumera, Fabrication of micro/nanoscale motors, *Chemical Reviews*, 2015, **115**, 8704-8735, doi: 10.1021/acs.chemrev.5b00047.
[63] A. Shinde, S. B. Prasad, D. A. Srinivasarao, S. Shah, P. Famta, P. Khairnar, G. Pandey, G. Vambhurkar, A. Hedaoo, R. Kumar, S. Srivastava, Nano voyagers: Pioneering a new frontier in cancer treatment with nanorobots as drug transporters, *Applied Materials Today,* 2024, **38**, 102162, doi: 10.1016/j.apmt.2024.102162.
[64] N. Mishbahurroyan, N.F.R. Winarno, S.I. Nafis, Y. Valdino, N. Listyorini, Nanorobots in targeted drug delivery system-a general review, *Liaison Journal of Engineering*, 2023, **3**, 13-27.
[65] O. G. Schmidt, K. Eberl, Thin solid films roll up into nanotubes, *Nature*, 2001, **410**, 168, doi: 10.1038/35065525.
[66] A. Kajbafvala, H. Bahmanpour, M. H. Maneshian, M. Li, Self-assembly techniques for nanofabrication, *Journal of Nanomaterials*, 2013, **1**, 158517, doi: 10.1155/2013/158517.
[67] J. C. Huie, Guided molecular self-assembly: a review of recent efforts, *Smart Materials and Structures*, 2003, **12**, 264-271, doi: 10.1088/0964-1726/12/2/315.
[68] S. Yadav, A. K. Sharma, P. Kumar, Nanoscale self-assembly for therapeutic delivery, *Frontiers in Bioengineering and Biotechnology*, 2020, **8**, 127, doi: 10.3389/fbioe.2020.00127.
[69] Y. Feng, M. An, Y. Liu, M. T. Sarwar, H. Yang, Advances in chemically powered micro/nanorobots for biological applications: a review, *Advanced Functional Materials*, 2023, **33**, 2209883, doi: 10.1002/adfm.202209883.
[70] M. An, Y. Feng, Y. Liu, H. Yang, External power-driven micro/nanorobots: design, fabrication, and functionalization for tumor diagnosis and therapy, *Progress in Materials Science*, 2023, **140**, 101204, doi: 10.1016/j.pmatsci.2023.101204.
[71] L. Zhang, J. J. Abbott, L. Dong, B. E. Kratochvil, D. Bell, B. J. Nelson, Artificial bacterial flagella: Fabrication and magnetic control, *Applied Physics Letters*, 2009, **94**, 064107, doi: 10.1063/1.3079655.
[72] N. Celi, D. Gong, J. Cai, Artificial flexible sperm-like nanorobot based on self-assembly and its bidirectional propulsion in precessing magnetic fields, *Scientific Reports*, 2021, **11**, 21728,

doi: 10.1038/s41598-021-00902-6.
[73] V. Magdanz, I. S. M. Khalil, J. Simmchen, G. P. Furtado, S. Mohanty, J. Gebauer, H. Xu, A. Klingner, A. Aziz, M. Medina-Sánchez, O. G. Schmidt, S. Misra, IRONSperm: Sperm-templated soft magnetic microrobots, *Science Advances*, 2020, **6**, eaba5855, doi: 10.1126/sciadv.aba5855.
[74] X. Peng, M. Urso, M. Ussia, M. Pumera, Shape-controlled self-assembly of light-powered microrobots into ordered microchains for cells transport and water remediation, *ACS Nano*, 2022, **16**, 7615-7625, doi: 10.1021/acsnano.1c11136.
[75] B. Regassa Hunde, A. Debebe Woldeyohannes, Future prospects of computer-aided design (CAD)–A review from the perspective of artificial intelligence (AI), extended reality, and 3D printing, *Results in Engineering*, 2022, **14**, 100478, doi: 10.1016/j.rineng.2022.100478.
[76] J. Li, M. Pumera, 3D printing of functional microrobots, *Chemical Society Reviews*, 2021, **50**, 2794-2838, doi: 10.1039/d0cs01062f.
[77] P. Prabhakar, R. K. Sen, N. Dwivedi, R. Khan, P. R. Solanki, A. K. Srivastava, C. Dhand, 3D-printed microfluidics and potential biomedical applications, *Frontiers in Nanotechnology*, 2021, **3**, 609355, doi: 10.3389/fnano.2021.609355.
[78] A. R. Torrado, C. M. Shemelya, J. D. English, Y. Lin, R. B. Wicker, D. A. Roberson, Characterizing the effect of additives to ABS on the mechanical property anisotropy of specimens fabricated by material extrusion 3D printing, *Additive Manufacturing*, 2015, **6**, 16-29, doi: 10.1016/j.addma.2015.02.001.
[79] S. E. Moulton, G. G. Wallace, 3-dimensional (3D) fabricated polymer based drug delivery systems, *Journal of Controlled Release*, 2014, **193**, 27-34, doi: 10.1016/j.jconrel.2014.07.005.
[80] W. Jamróz, J. Szafraniec, M. Kurek, R. Jachowicz, 3D printing in pharmaceutical and medical applications - recent achievements and challenges, *Pharmaceutical Research*, 2018, **35**, 176, doi: 10.1007/s11095-018-2454-x.
[81] M. Palo, J. Holländer, J. Suominen, J. Yliruusi, N. Sandler, 3D printed drug delivery devices: perspectives and technical challenges, *Expert Review of Medical Devices*, 2017, **14**, 685-696, doi: 10.1080/17434440.2017.1363647.
[82] K. Wei, C. Tang, H. Ma, X. Fang, R. Yang, 3D-printed microrobots for biomedical applications, *Biomaterials Science*, 2024, **12**, 4301-4334, doi: 10.1039/d4bm00674g.
[83] S. Vyavahare, S. Teraiya, D. Panghal, S. Kumar, Fused deposition modelling: a review, *Rapid Prototyping Journal*, 2020, **26**, 176-201, doi: 10.1108/rpj-04-2019-0106.
[84] G. I. Salentijn, P. E. Oomen, M. Grajewski, E. Verpoorte, Fused deposition modeling 3D printing for (bio)analytical device fabrication: procedures, materials, and applications, *Analytical Chemistry*, 2017, **89**, 7053-7061, doi: 10.1021/acs.analchem.7b00828.
[85] K. B. Mustapha, K. M. Metwalli, A review of fused deposition modelling for 3D printing of smart polymeric materials and composites, *European Polymer Journal*, 2021, **156**, 110591, doi: 10.1016/j.eurpolymj.2021.110591.
[86] S. C. Daminabo, S. Goel, S. A. Grammatikos, H. Y. Nezhad, V. K. Thakur, Fused deposition modeling-based additive manufacturing (3D printing): techniques for polymer material systems, *Materials Today Chemistry*, 2020, **16**, 100248, doi: 10.1016/j.mtchem.2020.100248.
[87] M. A. S. R. Saadi, A. Maguire, N. T. Pottackal, M. S. H. Thakur, M. M. Ikram, A. J. Hart, P. M. Ajayan, M. M. Rahman, Direct ink writing: a 3D printing technology for diverse materials, *Advanced Materials*, 2022, **34**, 2108855, doi: 10.1002/adma.202108855.
[88] X. Chen, C. Tian, H. Zhang, H. Xie, Biodegradable magnetic hydrogel robot with multimodal locomotion for targeted cargo delivery, *ACS Applied Materials & Interfaces*, 2023, **15**, 28922-28932, doi: 10.1021/acsami.3c02703.
[89] M. L. Bedell, A. M. Navara, Y. Du, S. Zhang, A. G. Mikos, Polymeric systems for bioprinting, *Chemical Reviews*, 2020, **120**, 10744-10792, doi: 10.1021/acs.chemrev.9b00834.
[90] R. E. Saunders, J. E. Gough, B. Derby, Delivery of human fibroblast cells by piezoelectric drop-on-demand inkjet printing, *Biomaterials*, 2008, **29**, 193-203, doi: 10.1016/j.biomaterials.2007.09.032.
[91] M. Ali Shah, D. G. Lee, B. Y. Lee, S. Hur, Classifications and applications of inkjet printing technology: a review, *IEEE Access*, 2021, **9**, 140079-140102, doi: 10.1109/ACCESS.2021.3119219.
[92] B. J. De Gans, P. Duineveld, U. Schubert, Inkjet printing of polymers: state of the art and future developments, *Advanced Materials*, 2004, **16**, 203-213, doi: 10.1002/adma.200300385.
[93] M. Singh, H. M. Haverinen, P. Dhagat, G. E. Jabbour, Inkjet printing-process and its applications, *Advanced Materials*, 2010, **22**, 673-685, doi: 10.1002/adma.200901141.
[94] S. F. Shirazi, S. Gharehkhani, M. Mehrali, H. Yarmand, H. S. Metselaar, N. Adib Kadri, N. A. Osman, A review on powder-based additive manufacturing for tissue engineering: selective laser sintering and inkjet 3D printing, *Science and Technology of Advanced Materials*, 2015, **16**, 033502, doi: 10.1088/1468-6996/16/3/033502.
[95] B. Derby, Inkjet printing of functional and structural materials: fluid property requirements, feature stability, and resolution, *Annual Review of Materials Research*, 2010, **40**, 395-414, doi: 10.1146/annurev-matsci-070909-104502.
[96] D. A. Gregory, Y. Zhang, P. J. Smith, X. Zhao, S. J. Ebbens, Reactive inkjet printing of biocompatible enzyme powered silk micro-rockets, *Small*, 2016, **12**, 4048-4055, doi: 10.1002/smll.201600921.
[97] R. Bernasconi, A. Nova, B. Aktas, S. Pané, L. Magagnin, Inkjet assisted electroforming and collective actuation of disk-shaped magnetic micromotors, *Applied Materials Today*, 2024, **40**, 102365, doi: 10.1016/j.apmt.2024.102365.
[98] L. Jacot-Descombes, M. Gullo, V. Cadarso, M. Mastrangeli, O. Ergeneman, C. Peters, P. Fatio, M. Freidy, C. Hierold, B. Nelson, J. Brugger, Inkjet printing of high aspect ratio superparamagnetic SU-8 microstructures with preferential magnetic directions, *Micromachines*, 2014, **5**, 583-593, doi: 10.3390/mi5030583.
[99] J. Mancilla-De-la-Cruz, M. Rodriguez-Salvador, J. An, C. K.

Chua, Three-dimensional printing technologies for drug delivery applications: processes, materials, and effects, *International Journal of Bioprinting*, 2022, **8**, 622, doi: 10.18063/ijb.v8i4.622.
[100] C. Schmidleithner, D. M. Kalaskar, Stereolithography, 2018.
[101] D. R. Serrano, A. Kara, I. Yuste, F. C. Luciano, B. Ongoren, B. J. Anaya, G. Molina, L. Diez, B. I. Ramirez, I. O. Ramirez, S. A. Sánchez-Guirales, R. Fernández-García, L. Bautista, H. K. Ruiz, A. Lalatsa, 3D printing technologies in personalized medicine, nanomedicines, and biopharmaceuticals, *Pharmaceutics*, 2023, **15**, 313, doi: 10.3390/pharmaceutics15020313.
[102] O. Guillaume, M. A. Geven, C. M. Sprecher, V. A. Stadelmann, D. W. Grijpma, T. T. Tang, L. Qin, Y. Lai, M. Alini, J. D. de Bruijn, H. Yuan, R. G. Richards, D. Eglin, Surface-enrichment with hydroxyapatite nanoparticles in stereolithography-fabricated composite polymer scaffolds promotes bone repair, *Acta Biomaterialia*, 2017, **54**, 386-398, doi: 10.1016/j.actbio.2017.03.006.
[103] S. J. Lee, W. Zhu, L. Heyburn, M. Nowicki, B. Harris, L. G. Zhang, Development of novel 3-D printed scaffolds with core-shell nanoparticles for nerve regeneration, *IEEE Transactions on Bio-Medical Engineering*, 2017, **64**, 408-418, doi: 10.1109/TBME.2016.2558493.
[104] S. J. Lee, D. Yan, X. Zhou, H. Cui, T. Esworthy, S. Y. Hann, M. Keidar, L. G. Zhang, Integrating cold atmospheric plasma with 3D printed bioactive nanocomposite scaffold for cartilage regeneration, *Materials Science and Engineering: C*, 2020, **111**, 110844, doi: 10.1016/j.msec.2020.110844.
[105] X. Zhou, T. Esworthy, S.-J. Lee, S. Miao, H. Cui, M. Plesiniak, H. Fenniri, T. Webster, R. D. Rao, L. G. Zhang, 3D Printed scaffolds with hierarchical biomimetic structure for osteochondral regeneration, *Nanomedicine: Nanotechnology, Biology and Medicine*, 2019, **19**, 58-70, doi: 10.1016/j.nano.2019.04.002.
[106] S. Chen, J. Yang, K. Li, B. Lu, L. Ren, Carboxylic acid-functionalized TiO_2 nanoparticle-loaded PMMA/PEEK copolymer matrix as a dental resin for 3D complete denture manufacturing by stereolitographic technique, International *Journal of Food Properties*, 2018, **21**, 2557-2565, doi: 10.1080/10942912.2018.1534125.
[107] E. E. Totu, A. C. Nechifor, G. Nechifor, H. Y. Aboul-Enein, C. M. Cristache, Poly(methyl methacrylate) with TiO2 nanoparticles inclusion for stereolitographic complete denture manufacturing − the fututre in dental care for elderly edentulous patients? *Journal of Dentistry*, 2017, **59**, 68-77, doi: 10.1016/j.jdent.2017.02.012.
[108] P. K. Sharma, D. Choudhury, T. Karanwad, P. Mohapatra, U. S. Murty, S. Banerjee, Curcumin nanoparticles as a multipurpose additive to achieve high-fidelity SLA-3D printing and controlled delivery, *Biomaterials Advances*, 2023, **153**, 213527, doi: 10.1016/j.bioadv.2023.213527.
[109] M. Ochoa, J. Zhou, R. Rahimi, V. Badwaik, D. Thompson, B. Ziaie, Rapid 3D-print-and-shrink fabrication of biodegradable microneedles with complex geometries, 18th International Conference on Solid-State Sensors, Actuators and Microsystems, 2015.
[110] Y. Lu, S. N. Mantha, D. C. Crowder, S. Chinchilla, K. N. Shah, Y. H. Yun, R. B. Wicker, J. W. Choi, Microstereolithography and characterization of poly(propylene fumarate)-based drug-loaded microneedle arrays, *Biofabrication*, 2015, **7**, 045001, doi: 10.1088/1758-5090/7/4/045001.
[111] S. Jacob, A. B. Nair, V. Patel, J. Shah, 3D printing technologies: recent development and emerging applications in various drug delivery systems, *AAPS PharmSciTech*, 2020, **21**, 220, doi: 10.1208/s12249-020-01771-4.
[112] R. Dermanaki Farahani, M. Dubé, Printing polymer nanocomposites and composites in three dimensions, *Advanced Engineering Materials*, 2018, **20**, 1700539, doi: 10.1002/adem.201700539.
[113] M. F. Jamil, M. Pokharel, K. Park, Light-controlled microbots in biomedical application: a review, *Applied Sciences*, 2022, **12**, 11013, doi: 10.3390/app122111013.
[114] V. M. Vaz, L. Kumar, 3D printing as a promising tool in personalized medicine, *AAPS PharmSciTech*, 2021, **22**, 49, doi: 10.1208/s12249-020-01905-8.
[115] K. Sugioka, Y. Cheng, A tutorial on optics for ultrafast laser materials processing: basic microprocessing system to beam shaping and advanced focusing methods, *Advanced Optical Technologies*, 2012, **1**, 353-364, doi: 10.1515/aot-2012-0033.
[116] C. Barner-Kowollik, M. Bastmeyer, E. Blasco, G. Delaittre, P. Müller, B. Richter, M. Wegener, 3D laser micro- and nanoprinting: challenges for chemistry, *Angewandte Chemie International Edition*, 2017, **56**, 15828-15845, doi: 10.1002/anie.201704695.
[117] A. C. Lamont, M. A. Restaino, M. J. Kim, R. D. Sochol, A facile multi-material direct laser writing strategy, *Lab on a Chip*, 2019, **19**, 2340-2345, doi: 10.1039/c9lc00398c.
[118] P. Mueller, M. Thiel, M. Wegener, 3D direct laser writing using a 405 nm diode laser, *Optics Letters*, 2014, **39**, 6847-6850, doi: 10.1364/OL.39.006847.
[119] Q. Xu, Y. Lv, C. Dong, T. S. Sreeprased, A. Tian, H. Zhang, Y. Tang, Z. Yu, N. Li, Three-dimensional micro/nanoscale architectures: fabrication and applications, *Nanoscale*, 2015, **7**, 10883-10895, doi: 10.1039/C5NR02048D.
[120] N. Anscombe, Direct laser writing, *Nature Photonics*, 2010, **4**, 22-23, doi: 10.1038/nphoton.2009.250.
[121] C. B. Arnold, A. Piqué, Laser direct-write processing, *MRS Bulletin*, 2007, **32**, 9-15, doi: 10.1557/mrs2007.9.
[122] M. A. Mahmood, A. C. Popescu, 3D printing at micro-level: laser-induced forward transfer and two-photon polymerization, *Polymers*, 2021, **13**, 2034, doi: 10.3390/polym13132034.
[123] S. D. Gittard, A. Ovsianikov, N. A. Monteiro-Riviere, J. Lusk, P. Morel, P. Minghetti, C. Lenardi, B. N. Chichkov, R. J. Narayan, Fabrication of polymer microneedles using a two-photon polymerization and micromolding process, *Journal of Diabetes Science and Technology*, 2009, **3**, 304-311, doi: 10.1177/193229680900300211.
[124] A. Ovsianikov, B. Chichkov, O. Adunka, H. Pillsbury, A. Doraiswamy, R. J. Narayan, Rapid prototyping of ossicular

replacement prostheses, *Applied Surface Science*, 2007, **253**, 6603-6607, doi: 10.1016/j.apsusc.2007.01.062.
[125] F. Claeyssens, E. A. Hasan, A. Gaidukeviciute, D. S. Achilleos, A. Ranella, C. Reinhardt, A. Ovsianikov, S. Xiao, C. Fotakis, M. Vamvakaki, B. N. Chichkov, M. Farsari, Three-dimensional biodegradable structures fabricated by two-photon polymerization, *Langmuir*, 2009, **25**, 3219-3223, doi: 10.1021/la803803m.
[126] C. Xu, Y. Xu, H. Chen, Q. Han, W. Wu, L. Zhang, Q. Liu, J. Wang, L. Ren, Novel-ink-based direct ink writing of Ti6Al4V scaffolds with sub-300μm structural pores for superior cell proliferation and differentiation, *Advanced Healthcare Materials*, 2024, **13**, 2302396, doi: 10.1002/adhm.202302396.
[127] V. V. Nayak, V. Sanjairaj, R. K. Behera, J. E. Smay, N. Gupta, P. G. Coelho, L. Witek, Direct inkjet writing of polylactic acid/β-tricalcium phosphate composites for bone tissue regeneration: a proof-of-concept study, Journal of Biomedical Materials Research. Part B, *Applied Biomaterials*, 2024, **112**, e35402, doi: 10.1002/jbm.b.35402.
[128] S. Mansi, S. V. Dummert, G. J. Topping, M. Z. Hussain, C. Rickert, K. M. A. Mueller, T. Kratky, M. Elsner, A. Casini, F. Schilling, R. A. Fischer, O. Lieleg, P. Mela, Introducing metal–organic frameworks to melt electrowriting: multifunctional scaffolds with controlled microarchitecture for tissue engineering applications, *Advanced Functional Materials,* 2024, **34**, 2304907, doi: 10.1002/adfm.202304907.
[129] H. Ceylan, I. C. Yasa, O. Yasa, A. F. Tabak, J. Giltinan, M. Sitti, 3D-printed biodegradable microswimmer for theranostic cargo delivery and release, *ACS Nano*, 2019, **13**, 3353-3362, doi: 10.1021/acsnano.8b09233.
[130] X. Wang, X. Z. Chen, C. C. J. Alcântara, S. Sevim, M. Hoop, A. Terzopoulou, C. de Marco, C. Hu, A. J. de Mello, P. Falcaro, S. Furukawa, B. J. Nelson, J. Puigmartí-Luis, S. Pané, MOFBOTS: metal-organic-framework-based biomedical microrobots, *Advanced Materials*, 2019, **31**, e1901592, doi: 10.1002/adma.201901592.
[131] H. Ceylan, N. O. Dogan, I. C. Yasa, M. N. Musaoglu, Z. U. Kulali, M. Sitti, 3D printed personalized magnetic micromachines from patient blood–derived biomaterials, *Science advances*, 2021, **7**, eabh0273, doi: 10.1126/sciadv.abh0273.
[132] H. Lee, D.-I. Kim, S.-H. Kwon, S. Park, Magnetically actuated drug delivery helical microrobot with magnetic nanoparticle retrieval ability, *ACS Applied Materials & Interfaces*, 2021, **13**, 19633-19647, doi: 10.1021/acsami.1c01742.
[133] S. Lee, J. Y. Kim, J. Kim, A. K. Hoshiar, J. Park, S. Lee, J. Kim, S. Pané, B. J. Nelson, H. Choi, Microrobots: A needle-type microrobot for targeted drug delivery by affixing to a microtissue, *Advanced Healthcare Materials*, 2020, **9**, 2070019, doi: 10.1002/adhm.202070019.
[134] E. Kim, S. Jeon, H. K. An, M. Kianpour, S. W. Yu, J. Y. Kim, J. C. Rah, H. Choi, A magnetically actuated microrobot for targeted neural cell delivery and selective connection of neural networks, *Science Advances*, 2020, **6**, eabb5696, doi: 10.1126/sciadv.abb5696.
[135] X. Song, R. Sun, R. Wang, K. Zhou, R. Xie, J. Lin, D. Georgiev, A. A. Paraschiv, R. Zhao, M. M. Stevens, Puffball-inspired microrobotic systems with robust payload, strong protection, and targeted locomotion for on-demand drug delivery, *Advanced Materials*, 2022, **34**, e2204791, doi: 10.1002/adma.202204791.
[136] H. Lee, S. Park, Magnetically actuated helical microrobot with magnetic nanoparticle retrieval and sequential dual-drug release abilities, *ACS Applied Materials & Interfaces,* 2023, **15**, 27471-27485, doi: 10.1021/acsami.3c01087.
[137] Y. Li, D. Dong, Y. Qu, J. Li, S. Chen, H. Zhao, Q. Zhang, Y. Jiao, L. Fan, D. Sun, A multidrug delivery microrobot for the synergistic treatment of cancer, *Small*, 2023, **19**, e2301889, doi: 10.1002/smll.202301889.
[138] H. Fu, B. Yu, 3D micro/nano hydrogel structures fabricated by two-photon polymerization for biomedical applications, *Frontiers in Bioengineering and Biotechnology*, 2023, **12**, 1339450, doi: 10.3389/fbioe.2024.1339450.
[139] X. Wang, J. Liu, Y. Zhang, P. M. Kristiansen, A. Islam, M. Gilchrist, N. Zhang, Advances in precision microfabrication through digital light processing: system development, material and applications, *Virtual and Physical Prototyping*, 2023, **18**, e2248101, doi: 10.1080/17452759.2023.2248101.
[140] J. Zhang, Q. Hu, S. Wang, J. Tao, M. Gou, Digital light processing based three-dimensional printing for medical applications, *International Journal of Bioprinting*, 2019, **6**, 242, doi: 10.18063/ijb.v6i1.242.
[141] S. Y. Kim, Y. S. Shin, H. D. Jung, C. J. Hwang, H. S. Baik, J. Y. Cha, Precision and trueness of dental models manufactured with different 3-dimensional printing techniques, *American Journal of Orthodontics and Dentofacial Orthopedics*, 2018, **153**, 144-153, doi: 10.1016/j.ajodo.2017.05.025.
[142] J. Tao, J. Zhang, T. Du, X. Xu, X. Deng, S. Chen, J. Liu, Y. Chen, X. Liu, M. Xiong, Y. Luo, H. Cheng, J. Mao, L. Cardon, M. Gou, Y. Wei, Rapid 3D printing of functional nanoparticle-enhanced conduits for effective nerve repair, *Acta Biomaterialia*, 2019, **90**, 49-59, doi: 10.1016/j.actbio.2019.03.047.
[143] R. B. Osman, A. J. van der Veen, D. Huiberts, D. Wismeijer, N. Alharbi, 3D-printing zirconia implants; a dream or a reality? An in-vitro study evaluating the dimensional accuracy, surface topography and mechanical properties of printed zirconia implant and discs, *Journal of the Mechanical Behavior of Biomedical Materials*, 2017, **75**, 521-528, doi: 10.1016/j.jmbbm.2017.08.018.
[144] W. Zhu, J. Li, Y. J. Leong, I. Rozen, X. Qu, R. Dong, Z. Wu, W. Gao, P. H. Chung, J. Wang, S. Chen, 3D-printed artificial microfish, *Advanced Materials*, 2015, **27**, 4411-4417, doi: 10.1002/adma.201501372.
[145] B. Grigoryan, S. J. Paulsen, D. C. Corbett, D. W. Sazer, C. L. Fortin, A. J. Zaita, P. T. Greenfield, N. J. Calafat, J. P. Gounley, A. H. Ta, F. Johansson, A. Randles, J. E. Rosenkrantz, J. D. Louis-Rosenberg, P. A. Galie, K. R. Stevens, J. S. Miller, Multivascular networks and functional intravascular topologies within biocompatible hydrogels, *Science*, 2019, **364**, 458-464, doi: 10.1126/science.aav9750.
[146] J. Liu, J. He, J. Liu, X. Ma, Q. Chen, N. Lawrence, W. Zhu, Y. Xu, S. Chen, Rapid 3D bioprinting of in vitro cardiac tissue

models using human embryonic stem cell-derived cardiomyocytes, *Bioprinting*, 2019, **13**, e00040, doi: 10.1016/j.bprint.2019.e00040.
[147] J. Tao, X. Xu, S. Wang, T. Kang, C. Guo, X. Liu, H. Cheng, Y. Liu, X. Jiang, J. Mao, M. Gou, Polydiacetylene-nanoparticle-functionalized microgels for topical bacterial infection treatment, *ACS Macro Letters*, 2019, **8**, 563-568, doi: 10.1021/acsmacrolett.9b00196.
[148] L. Wang, Q. Wang, A. Slita, O. Backman, Z. Gounani, E. Rosqvist, J. Peltonen, S. Willför, C. Xu, J. M. Rosenholm, X. Wang, Digital light processing (DLP) 3D-fabricated antimicrobial hydrogel with a sustainable resin of methacrylated woody polysaccharides and hybrid silver-lignin nanospheres, *Green Chemistry*, 2022, **24**, 2129-2145, doi: 10.1039/D1GC03841A.
[149] W. Zhu, J. Li, Y. J. Leong, I. Rozen, X. Qu, R. Dong, Z. Wu, W. Gao, P. H. Chung, J. Wang, S. Chen, 3D-printed artificial microfish, *Advanced Materials*, 2015, **27**, 4411-4417, doi: 10.1002/adma.201501372.
[150] K. S. Lim, J. H. Galarraga, X. Cui, G. C. J. Lindberg, J. A. Burdick, T. B. F. Woodfield, Fundamentals and applications of photo-cross-linking in bioprinting, *Chemical Reviews*, 2020, **120**, 10662-10694, doi: 10.1021/acs.chemrev.9b00812.
[151] A. R. Johnson, C. L. Caudill, J. R. Tumbleston, C. J. Bloomquist, K. A. Moga, A. Ermoshkin, D. Shirvanyants, S. J. Mecham, J. C. Luft, J. M. DeSimone, Single-step fabrication of computationally designed microneedles by continuous liquid interface production, *PLoS One*, 2016, **11**, e0162518, doi: 10.1371/journal.pone.0162518.
[152] C. J. Bloomquist, M. B. Mecham, M. D. Paradzinsky, R. Janusziewicz, S. B. Warner, J. C. Luft, S. J. Mecham, A. Z. Wang, J. M. DeSimone, Controlling release from 3D printed medical devices using CLIP and drug-loaded liquid resins, *Journal of Controlled Release*, 2018, **278**, 9-23, doi: 10.1016/j.jconrel.2018.03.026.
[153] X. Deng, B. Huang, R. Hu, L. Chen, Y. Tang, C. Lu, Z. Chen, W. Zhang, X. Zhang, 3D printing of robust and biocompatible poly(ethylene glycol)diacrylate/nano-hydroxyapatite composites via continuous liquid interface production, *Journal of Materials Chemistry. B*, 2021, **9**, 1315-1324, doi: 10.1039/d0tb02182b.
[154] J. R. Tumbleston, D. Shirvanyants, N. Ermoshkin, R. Janusziewicz, A. R. Johnson, D. Kelly, K. Chen, R. Pinschmidt, J. P. Rolland, A. Ermoshkin, E. T. Samulski, J. M. DeSimone, Continuous liquid interface production of 3D objects, *Science*, 2015, **347**, 1349-1352, doi: 10.1126/science.aaa2397.
[155] N. A. Charoo, S. F. Barakh Ali, E. M. Mohamed, M. A. Kuttolamadom, T. Ozkan, M. A. Khan, Z. Rahman, Selective laser sintering 3D printing–an overview of the technology and pharmaceutical applications, *Drug Development and Industrial Pharmacy*, 2020, **46**, 869-877, doi: 10.1080/03639045.2020.1764027.
[156] Y. A. Gueche, N. M. Sanchez-Ballester, S. Cailleaux, B. Bataille, I. Soulairol, Selective laser sintering (SLS), a new chapter in the production of solid oral forms (SOFs) by 3D printing, *Pharmaceutics*, 2021, **13**, 1212, doi: 10.3390/pharmaceutics13081212.
[157] A. Kafle, E. Luis, R. Silwal, H. M. Pan, P. L. Shrestha, A. K. Bastola, 3D/4D printing of polymers: fused deposition modelling (FDM), selective laser sintering (SLS), and stereolithography (SLA), *Polymers*, 2021, **13**, 3101, doi: 10.3390/polym13183101.
[158] A. G. Tabriz, H. Kuofie, J. Scoble, S. Boulton, D. Douroumis, Selective Laser Sintering for printing pharmaceutical dosage forms, *Journal of Drug Delivery Science and Technology*, 2023, **86**, 104699, doi: 10.1016/j.jddst.2023.104699.
[159] F. E. Wiria, K. F. Leong, C. K. Chua, Y. Liu, Poly-ε-caprolactone/hydroxyapatite for tissue engineering scaffold fabrication via selective laser sintering, *Acta Biomaterialia*, 2007, **3**, 1-12, doi: 10.1016/j.actbio.2006.07.008.
[160] W. Y. Zhou, S. H. Lee, M. Wang, W. L. Cheung, W. Y. Ip, Selective laser sintering of porous tissue engineering scaffolds from poly(L: -lactide)/carbonated hydroxyapatite nanocomposite microspheres, *Journal of Materials Science. Materials in Medicine*, 2008, **19**, 2535-2540, doi: 10.1007/s10856-007-3089-3.
[161] C. Shuai, B. Yang, S. Peng, Z. Li, Development of composite porous scaffolds based on poly(lactide-co-glycolide)/nano-hydroxyapatite via selective laser sintering, *International Journal of Advanced Manufacturing Technology*, 2013, **69**, 51-57, doi: 10.1007/s00170-013-5001-2.
[162] S. Maher, G. Kaur, L. Lima-Marques, A. Evdokiou, D. Losic, Engineering of micro- to nanostructured 3D-printed drug-releasing titanium implants for enhanced osseointegration and localized delivery of anticancer drugs, *ACS Applied Materials & Interfaces*, 2017, **9**, 29562-29570, doi: 10.1021/acsami.7b09916.163
[163] Z. Zhao, X. Tian, X. Song, Engineering materials with light: recent progress in digital light processing based 3D printing, *Journal of Materials Chemistry C*, 2020, **8**, 13896-13917, doi: 10.1039/D0TC03548C.
[164] J. P. Edaugal, E. L. Ribeiro, M. K. Mitchell, X. Cheng, E. M. Buckner, J. Chen, I. N. Ivanov, M. Ellermann, R. C. Advincula, Digital light processing (DLP): 3D printing of polymer-based graphene oxide nanocomposites-efficient antimicrobial material for biomedical devices, *MRS Communications*, 2023, **13**, 594-602, doi: 10.1557/s43579-023-00390-x.
[165] N. Hu, L. Ding, Y. Liu, K. Wang, B. Zhang, R. Yin, W. Zhou, Z. Bi, W. Zhang, Development of 3D-printed magnetic micro-nanorobots for targeted therapeutics: the state of art, *Advanced NanoBiomed Research*, 2023, **3**, 2300018, doi: 10.1002/anbr.202300018.
[166] J. dos Santos, R. S. de Oliveira, T. V. de Oliveira, M. C. Velho, M. V. Konrad, G. S. da Silva, M. Deon, R. C. R. Beck, 3D printing and nanotechnology: a multiscale alliance in personalized medicine, *Advanced Functional Materials*, 2021, **31**, 2009691, doi: 10.1002/adfm.202009691.
[167] S. Zhao, D. Sun, J. Zhang, H. Lu, Y. Wang, R. Xiong, K. T. V. Grattan, Actuation and biomedical development of micro-/nanorobots–A review, *Materials Today Nano*, 2022, **18**, 100223,

doi: 10.1016/j.mtnano.2022.100223.
[168] B. Chen, H. Sun, J. Zhang, J. Xu, Z. Song, G. Zhan, X. Bai, L. Feng, Cell-based micro/nano-robots for biomedical applications: a review, *Small*, 2024, **20**, e2304607, doi: 10.1002/smll.202304607.
[169] A. Halder, Y. Sun, Biocompatible propulsion for biomedical micro/nano robotics, *Biosensors and Bioelectronics*, 2019, **139**, 111334, doi: 10.1016/j.bios.2019.111334.
[170] M. P. Nikolova, M. S. Chavali, Metal oxide nanoparticles as biomedical materials, *Biomimetics*, 2020, **5**, 27, doi: 10.3390/biomimetics5020027.
[171] W. Z. Teo, H. Wang, M. Pumera, Beyond platinum: silver-catalyst based bubble-propelled tubular micromotors, *Chemical Communications*, 2016, **52**, 4333-4336, doi: 10.1039/c6cc00115g.
[172] D. A. Wilson, R. J. Nolte, J. C. van Hest, Autonomous movement of platinum-loaded stomatocytes, *Nature Chemistry*, 2012, **4**, 268-274, doi: 10.1038/nchem.1281.
[173] W. Gao, A. Pei, J. Wang, Water-driven micromotors, *ACS Nano*, 2012, **6**, 8432-8438, doi: 10.1021/nn303309z.
[174] W. Gao, R. Dong, S. Thamphiwatana, J. Li, W. Gao, L. Zhang, J. Wang, Artificial micromotors in the mouse's stomach: a step toward in vivo use of synthetic motors, *ACS Nano*, 2015, **9**, 117-123, doi: 10.1021/nn507097k.
[175] J. Li, J. Zhang, W. Gao, G. Huang, Z. Di, R. Liu, J. Wang, Y. Mei, Dry-released nanotubes and nanoengines by particle-assisted rolling, *Advanced Materials*, 2013, **25**, 3715-3721, doi: 10.1002/adma.201301208.
[176] Y. Wu, Z. Wu, X. Lin, Q. He, J. Li, Autonomous movement of controllable assembled Janus capsule motors, *ACS Nano*, 2012, **6**, 10910-10916, doi: 10.1021/nn304335x.
[177] Y. Xing, M. Zhou, T. Xu, S. Tang, Y. Fu, X. Du, L. Su, Y. Wen, X. Zhang, T. Ma, Core@Satellite Janus nanomotors with pH-responsive multi-phoretic propulsion, *Angewandte Chemie*, 2020, **59**, 14368-14372, doi: 10.1002/anie.202006421.
[178] J. Li, S. Sattayasamitsathit, R. Dong, W. Gao, R. Tam, X. Feng, S. Ai, J. Wang, Template electrosynthesis of tailored-made helical nanoswimmers, *Nanoscale*, 2014, **6**, 9415-9420, doi: 10.1039/C3NR04760A.
[179] M. Dong, X. Wang, X. Z. Chen, F. Mushtaq, S. Deng, C. Zhu, H. Torlakcik, A. Terzopoulou, X.-H. Qin, X. Xiao, J. Puigmartí-Luis, H. Choi, A. P. Pêgo, Q.-D. Shen, B. J. Nelson, S. Pané, 3D-printed soft magnetoelectric microswimmers for delivery and differentiation of neuron-like cells, *Advanced Functional Materials*, 2020, **30**, 1910323, doi: 10.1002/adfm.201910323.
[180] C. Bergeles, B. E. Kratochvil, B. J. Nelson, Visually servoing magnetic intraocular microdevices, *IEEE Transactions on Robotics*, 2012, **28**, 798-809, doi: 10.1109/TRO.2012.2188165.
[181] S. Tottori, L. Zhang, F. Qiu, K. K. Krawczyk, A. Franco-Obregón, B. J. Nelson, Magnetic helical micromachines: fabrication, controlled swimming, and cargo transport, *Advanced Materials*, 2012, **24**, 811-816, doi: 10.1002/adma.201103818.
[182] X. Wang, X. H. Qin, C. Hu, A. Terzopoulou, X. Z. Chen, T. Y. Huang, K. Maniura-Weber, S. Pané, B. J. Nelson, 3D printed enzymatically biodegradable soft helical microswimmers, *Advanced Functional Materials*, 2018, **28**, 1804107, doi: 10.1002/adfm.201804107.
[183] Z. Wu, X. Lin, Y. Wu, T. Si, J. Sun, Q. He, Near-infrared light-triggered "on/off" motion of polymer multilayer rockets, *ACS Nano*, 2014, **8**, 6097-6105, doi: 10.1021/nn501407r.
[184] Y. Hong, M. Diaz, U. M. Córdova-Figueroa, A. Sen, Light-driven titanium-dioxide-based reversible microfireworks and micromotor/micropump systems, *Advanced Functional Materials*, 2010, **20**, 1568-1576, doi: 10.1002/adfm.201000063.
[185] R. Dong, Q. Zhang, W. Gao, A. Pei, B. Ren, Highly efficient light-driven TiO_2–Au Janus micromotors, *ACS Nano*, 2016, **10**, 839-844, doi: 10.1021/acsnano.5b05940.
[186] N. Zhang, G. Xiong, Z. Liu, Toxicity of metal-based nanoparticles: challenges in the nano era, *Frontiers in Bioengineering and Biotechnology*, 2022, **10**, 1001572, doi: 10.3389/fbioe.2022.1001572.
[187] J. Hyuk Moon, S. Yang, Creating three-dimensional polymeric microstructures by multi-beam interference lithography, *Journal of Macromolecular Science, Part C: Polymer Reviews*, 2005, **45**, 351-373, doi: 10.1080/15321790500304163.
[188] S. C. Gauci, A. Vranic, E. Blasco, S. Bräse, M. Wegener, C. Barner-Kowollik, Photochemically activated 3D printing inks: current status, challenges, and opportunities, *Advanced Materials*, 2024, **36**, e2306468, doi: 10.1002/adma.202306468.
[189] C. K. Ober, Z. Liu, R. Cordero, A. Cintora, Materials overview for 2-photon 3D printing applications, *Journal of Photopolymer Science and Technology*, 2018, **31**, 425-429, doi: 10.2494/photopolymer.31.425.
[190] S. Kim, F. Qiu, S. Kim, A. Ghanbari, C. Moon, L. Zhang, B. J. Nelson, H. Choi, Fabrication and characterization of magnetic microrobots for three-dimensional cell culture and targeted transportation, *Advanced Materials*, 2013, **25**, 5863-5868, doi: 10.1002/adma.201301484.
[191] C. Peters, O. Ergeneman, P. D. W. García, M. Müller, S. Pané, B. J. Nelson, C. Hierold, Superparamagnetic twist-type actuators with shape-independent magnetic properties and surface functionalization for advanced biomedical applications, *Advanced Functional Materials*, 2014, **24**, 5269-5276, doi: 10.1002/adfm.201400596.
[192] X. Wang, C. Hu, L. Schurz, C. De Marco, X. Chen, S. Pané, B. J. Nelson, Surface-chemistry-mediated control of individual magnetic helical microswimmers in a swarm, *ACS Nano*, 2018, **12**, 6210-6217, doi: 10.1021/acsnano.8b02907.
[193] A. Aziz, M. Medina-Sánchez, J. Claussen, O. G. Schmidt, Real-time optoacoustic tracking of single moving micro-objects in deep phantom and ex vivo tissues, *Nano Letters*, 2019, **19**, 6612-6620, doi: 10.1021/acs.nanolett.9b02869.
[194] M. Hoop, C. F. Walde, R. Riccò, F. Mushtaq, A. Terzopoulou, X. Z. Chen, S. Pané, Biocompatibility characteristics of the metal organic framework ZIF-8 for therapeutical applications, *Applied Materials Today*, 2018, **11**, 13-21, doi: 10.1016/j.apmt.2017.12.014.
[195] A. Terzopoulou, X. Wang, X. Z. Chen, M. Palacios-Corella,

C. Pujante, J. Herrero-Martín, X. H. Qin, J. Sort, A. J. de Mello, B. J. Nelson, J. Puigmartí-Luis, S. Pané, MOF drug carriers: biodegradable metal–organic framework-based microrobots (MOFBOTs), *Advanced Healthcare Materials*, 2020, **9**, 2070076, doi: 10.1002/adhm.202070076.

[196] W. Zhu, J. Li, Y. J. Leong, I. Rozen, X. Qu, R. Dong, Z. Wu, W. Gao, P. H. Chung, J. Wang, S. Chen, 3D-printed artificial microfish, *Advanced Materials*, 2015, **27**, 4411-4417, doi: 10.1002/adma.201501372.

[197] H.-W. Huang, Q. Chao, M. S. Sakar, B. J. Nelson, Optimization of tail geometry for the propulsion of soft microrobots, *IEEE Robotics and Automation Letters*, 2017, **2**, 727-732, doi: 10.1109/LRA.2017.2651167.

[198] S. G. Reddy, A. S. Pandit, Controlled drug delivery studies of biological macromolecules: sodium alginate and lignosulphonic acid films, *Journal of Applied Polymer Science*, 2014, **131**, e40442, doi: 10.1002/app.40442.

[199] S. G. Reddy, H. C. A. Murthy, Smart biomaterials in drug delivery applications, *Engineered Biomaterials: Synthesis and Applications*, 2023, 323-360, doi: 10.1007/978-981-99-6698-1_11.

[200] G. Reddy S, Kinetic studies for the release of hydroxychloroquine sulphate drug (HCQ) in-vitro in simulated gastric and intestinal medium from sodium alginate and lignosulphonic acid blends, *Trends in Sciences*, 2023, **20**, 5318, doi: 10.48048/tis.2023.5318.

[201] Aashli, S. G. Reddy, B. S. Kumar, K. Prashanthi, H. C. Ananda Murthy, Fabricating transdermal film formulations of montelukast sodium with improved chemical stability and extended drug release, *Heliyon*, 2023, **9**, e14469, doi: 10.1016/j.heliyon.2023.e14469.

[202] H. Bahaar, S. G. Reddy, B. S. Kumar, K. Prashanthi, H. C. An, Modified layered double hydroxide–PEG magneto-sensitive hydrogels with suitable ligno-alginate green polymer composite for prolonged drug delivery applications, *Engineered Science*, 2023, **24**, 914, doi: 10.30919/es914.

[203] S. G. Reddy, Controlled release studies of hydroxychloroquine sulphate (hcq) drug-using biodegradable polymeric sodium alginate and lignosulphonic acid blends, *Rasayan Journal of Chemistry*, 2021, **14**, 2209-221, doi: 10.31788/rjc.2021.1446508.

[204] N. Ganesh, C. Hanna, S. V. Nair, L. S. Nair, Enzymatically cross-linked alginic-hyaluronic acid composite hydrogels as cell delivery vehicles, *International Journal of Biological Macromolecules*, 2013, **55**, 289-294, doi: 10.1016/j.ijbiomac.2012.12.045.

[205] K. Muldoon, Y. Song, Z. Ahmad, X. Chen, M. W. Chang, High precision 3D printing for micro to nano scale biomedical and electronic devices, *Micromachines*, 2022, **13**, 642, doi: 10.3390/mi13040642.

[206] M. M. Liu, Y. Zhong, Y. Chen, L. N. Wu, W. Chen, X. H. Lin, Y. Lei, A. L. Liu, Electrochemical monitoring the effect of drug intervention on PC12 cell damage model cultured on paper-PLA 3D printed device, *Analytica Chimica Acta*, 2022, **1194**, 339409, doi: 10.1016/j.aca.2021.339409.

[207] F. Soto, E. Karshalev, F. Zhang, B. Esteban Fernandez de Avila, A. Nourhani, J. Wang, Smart materials for microrobots, *Chemical Reviews*, 2022, **122**, 5365-5403, doi: 10.1021/acs.chemrev.0c00999.

[208] Y. Chen, M. Li, Q. Tang, Y. Cheng, A. Miao, L. Cheng, S. Zhu, T. Luo, G. Liu, L. Zhang, F. Niu, L. Zhao, J. Chen, R. Yang, High-speed NIR-driven untethered 3D-printed hydrogel microrobots in high-viscosity liquids, *Advanced Intelligent Systems*, 2023, **5**, 2200311, doi: 10.1002/aisy.202200311.

[209] F. Soto, A. Martin, S. Ibsen, M. Vaidyanathan, V. Garcia-Gradilla, Y. Levin, A. Escarpa, S. C. Esener, J. Wang, Acoustic microcannons: toward advanced microballistics, *ACS Nano*, 2016, **10**, 1522-1528, doi: 10.1021/acsnano.5b07080.

[210] D. Melling, J. G. Martinez, E. W. H. Jager, Conjugated polymer actuators and devices: progress and opportunities, *Advanced Materials*, 2019, **31**, e1808210, doi: 10.1002/adma.201808210.

[211] P. Calvo-Marzal, S. Sattayasamitsathit, S. Balasubramanian, J. Windmiller, C. Dao, J. Wang, Propulsion of nanowire diodes, 2010.

[212] D. Fan, Z. Yin, R. Cheong, F. Q. Zhu, R. C. Cammarata, C. L. Chien, A. Levchenko, Subcellular-resolution delivery of a cytokine through precisely manipulated nanowires, *Nature Nanotechnology*, 2010, **5**, 545-551, doi: 10.1038/nnano.2010.104.

[213] N. Ashammakhi, S. Ahadian, C. Xu, H. Montazerian, H. Ko, R. Nasiri, N. Barros, A. Khademhosseini, Bioinks and bioprinting technologies to make heterogeneous and biomimetic tissue constructs, *Materials Today Bio*, 2019, **1**, 100008, doi: 10.1016/j.mtbio.2019.100008.

[214] J. S. Lowe, P. G. Anderson, S. I. Anderson, Stevens & Lowe's Human Histology-E-Book, 2023.

[215] S. Mañes, C. Gómez-Moutón, R. A. Lacalle, S. Jiménez-Baranda, E. Mira, C. Martínez-A, Mastering time and space: immune cell polarization and chemotaxis, *Seminars in Immunology*, 2005, **17**, 77-86, doi: 10.1016/j.smim.2004.09.005.

[216] R. D. Kamm, R. Bashir, N. Arora, R. D. Dar, M. U. Gillette, L. G. Griffith, M. L. Kemp, K. Kinlaw, M. Levin, A. C. Martin, T. C. McDevitt, R. M. Nerem, M. J. Powers, T. A. Saif, J. Sharpe, S. Takayama, S. Takeuchi, R. Weiss, K. Ye, H. G. Yevick, M. H. Zaman, Perspective: The promise of multi-cellular engineered living systems, *APL Bioeng*, 2018, **2**, 040901, doi: 10.1063/1.5038337.

[217] B. Wang, Y. Zhang, L. Zhang, Recent progress on micro- and nano-robots: towards in vivo tracking and localization, *Quantitative Imaging in Medicine and Surgery*, 2018, **8**, 461-479, doi: 10.21037/qims.2018.06.07.

[218] B. J. Williams, S. V. Anand, J. Rajagopalan, A self-propelled biohybrid swimmer at low Reynolds number, *Nature Communications*, 2014, **5**, 3081, doi: 10.1038/ncomms4081.

[219] J. Shao, M. Xuan, H. Zhang, X. Lin, Z. Wu, Q. He, Chemotaxis-guided hybrid neutrophil micromotors for targeted drug transport, *Angewandte Chemie*, 2017, **56**, 12935-12939, doi: 10.1002/anie.201706570.

[220] Z. Wu, B. Esteban-Fernández de Ávila, A. Martín, C. Christianson, W. Gao, S. K. Thamphiwatana, A. Escarpa, Q. He,

L. Zhang, J. Wang, RBC micromotors carrying multiple cargos towards potential theranostic applications, *Nanoscale*, 2015, **7**, 13680-13686, doi: 10.1039/c5nr03730a.
[221] R. Dreyfus, J. Baudry, M. L. Roper, M. Fermigier, H. A. Stone, J. Bibette, Microscopic artificial swimmers, *Nature*, 2005, **437**, 862-865, doi: 10.1038/nature04090.
[222] S. Shivalkar, P. Chowdhary, T. Afshan, S. Chaudhary, A. Roy, S. K. Samanta, A. K. Sahoo, Nanoengineering of biohybrid micro/nanobots for programmed biomedical applications, *Colloids and Surfaces B: Biointerfaces*, 2023, **222**, 113054, doi: 10.1016/j.colsurfb.2022.113054.
[223] B.-W. Park, J. Zhuang, O. Yasa, M. Sitti, Multifunctional bacteria-driven microswimmers for targeted active drug delivery, *ACS Nano*, 2017, **11**, 8910-8923, doi: 10.1021/acsnano.7b03207.
[224] Q. Ma, C. Chen, S. Wei, C. Chen, L. F. Wu, T. Song, Construction and operation of a microrobot based on magnetotactic bacteria in a microfluidic chip, *Biomicrofluidics*, 2012, **6**, 24107-2410712, doi: 10.1063/1.3702444.
[225] L. W. Rogowski, X. Zhang, J. Tang, M. Oxner, M. J. Kim, Flagellated Janus particles for multimodal actuation and transport, *Biomicrofluidics*, 2021, **15**, 044104, doi: 10.1063/5.0053647.
[226] Van Du Nguyen, J. W. Han, Y. J. Choi, S. Cho, S. Zheng, S. Y. Ko, J. O. Park, S. Park, Active tumor-therapeutic liposomal bacteriobot combining a drug (paclitaxel)-encapsulated liposome with targeting bacteria (Salmonella Typhimurium), *Sensors and Actuators B: Chemical*, 2016, **224**, 217-224, doi: 10.1016/j.snb.2015.09.034.
[227] T. Gwisai, N. Mirkhani, M. G. Christiansen, T. T. Nguyen, V. Ling, S. Schuerle, Magnetic torque-driven living microrobots for increased tumor infiltration, *Science Robotics*, 2022, **7**, eabo0665, doi: 10.1126/scirobotics.abo0665.
[228] S. Nehru, R. Misra, M. Bhaswant, Multifaceted engineered biomimetic nanorobots toward cancer management, *ACS Biomaterials Science & Engineering*, 2022, **8**, 444-459, doi: 10.1021/acsbiomaterials.1c01352.
[229] Q. W. Chen, J. Y. Qiao, X. H. Liu, C. Zhang, X. Z. Zhang, Customized materials-assisted microorganisms in tumor therapeutics, *Chemical Society Reviews*, 2021, **50**, 12576-12615, doi: 10.1039/d0cs01571g.
[230] E. Alemzadeh, K. Izadpanah, F. Ahmadi, Generation of recombinant protein shells of Johnson grass chlorotic stripe mosaic virus in tobacco plants and their use as drug carrier, *Journal of Virological Methods*, 2017, **248**, 148-153, doi: 10.1016/j.jviromet.2017.07.003.
[231] F. Zhang, Z. Li, Y. Duan, A. Abbas, R. Mundaca-Uribe, L. Yin, H. Luan, W. Gao, R. H. Fang, L. Zhang, J. Wang, Gastrointestinal tract drug delivery using algae motors embedded in a degradable capsule, *Science Robotics*, 2022, **7**, eabo4160, doi: 10.1126/scirobotics.abo4160.
[232] I. S. Shchelik, J. V. D. Molino, K. Gademann, Biohybrid microswimmers against bacterial infections, *Acta Biomaterialia*, 2021, **136**, 99-110, doi: 10.1016/j.actbio.2021.09.048.
[233] X. Yan, Q. Zhou, M. Vincent, Y. Deng, J. Yu, J. Xu, T. Xu, T. Tang, L. Bian, Y.-X J. Wang, K. Kostarelos, L. Zhang, Multifunctional biohybrid magnetite microrobots for imaging-guided therapy, *Science Robotics*, 2017, **2**, eaaq1155, doi: 10.1126/scirobotics.aaq1155.
[234] S. Li, Q. Jiang, S. Liu, Y. Zhang, Y. Tian, C. Song, J. Wang, Y. Zou, G. J. Anderson, J.-Y. Han, Y. Chang, Y. Liu, C. Zhang, L. Chen, G. Zhou, G. Nie, H. Yan, B. Ding, Y. Zhao, A DNA nanorobot functions as a cancer therapeutic in response to a molecular trigger in vivo, *Nature Biotechnology*, 2018, **36**, 258-264, doi: 10.1038/nbt.4071.
[235] W. Ma, Y. Zhan, Y. Zhang, X. Shao, X. Xie, C. Mao, W. Cui, Q. Li, J. Shi, J. Li, C. Fan, Y. Lin, An intelligent DNA nanorobot with in vitro enhanced protein lysosomal degradation of HER2, *Nano Letters*, 2019, **19**, 4505-4517, doi: 10.1021/acs.nanolett.9b01320.
[236] X. Ma, A. Jannasch, U.-R. Albrecht, K. Hahn, A. Miguel-López, E. Schäffer, S. Sánchez, Enzyme-powered hollow mesoporous Janus nanomotors, *Nano Letters*, 2015, **15**, 7043-7050, doi: 10.1021/acs.nanolett.5b03100.
[237] S. Tang, F. Zhang, H. Gong, F. Wei, J. Zhuang, E. Karshalev, B. E.-F. de Ávila, C. Huang, Z. Zhou, Z. Li, L. Yin, H. Dong, R. H. Fang, X. Zhang, L. Zhang, J. Wang, Enzyme-powered Janus platelet cell robots for active and targeted drug delivery, *Science Robotics*, 2020, **5**, eaba6137, doi: 10.1126/scirobotics.aba6137.
[238] S. E. Gratton, P. A. Ropp, P. D. Pohlhaus, J. C. Luft, V. J. Madden, M. E. Napier, J. M. DeSimone, The effect of particle design on cellular internalization pathways, *Proceedings of the National Academy of Sciences of the United States of America*, 2008, **105**, 11613-11618, doi: 10.1073/pnas.0801763105.
[239] J. Möller, T. Luehmann, H. Hall, V. Vogel, The race to the pole: how high-aspect ratio shape and heterogeneous environments limit phagocytosis of filamentous escherichia coli bacteria by macrophages, *Nano Letters*, 2012, **12**, 2901-2905, doi: 10.1021/nl3004896.
[240] N. Doshi, B. Prabhakarpandian, A. Rea-Ramsey, K. Pant, S. Sundaram, S. Mitragotri, Flow and adhesion of drug carriers in blood vessels depend on their shape: a study using model synthetic microvascular networks, *Journal of Controlled Release,* 2010, **146**, 196-200, doi: 10.1016/j.jconrel.2010.04.007.
[241] E. J. Curry, A. D. Henoun, A. N. Miller 3rd, T. D. Nguyen, 3D nano- and micro-patterning of biomaterials for controlled drug delivery, *Therapeutic Delivery*, 2017, **8**, 15-28, doi: 10.4155/tde-2016-0052.
[242] S. Jeon, S. Kim, S. Ha, S. Lee, E. Kim, S. Y. Kim, S. H. Park, J. H. Jeon, S. W. Kim, C. Moon, B. J. Nelson, J. Y. Kim, S. W. Yu, H. Choi, Magnetically actuated microrobots as a platform for stem cell transplantation, *Science Robotics*, 2019, **4**, eaav4317, doi: 10.1126/scirobotics.aav4317.
[243] B. Jurado-Sánchez, S. Campuzano, J. M. Pingarrón, A. Escarpa, Janus particles and motors: unrivaled devices for mastering (bio)sensing, *Microchimica Acta*, 2021, **188**, 416, doi: 10.1007/s00604-021-05053-z.
[244] X. Li, L. Chen, D. Cui, W. Jiang, L. Han, N. Niu, Preparation and application of Janus nanoparticles: recent development and prospects, *Coordination Chemistry Reviews*, 2022, **454**, 214318, doi: 10.1016/j.ccr.2021.214318.
[245] V. Sridhar, B. W. Park, M. Sitti, Light-driven Janus hollow

mesoporous TiO2–Au microswimmers, *Advanced Functional Materials*, 2018, **28**, 1704902, doi: 10.1002/adfm.201704902.
[246] F. Qiu, B. J. Nelson, Magnetic helical micro- and nanorobots: toward their biomedical applications, *Engineering*, 2015, **1**, 21-26, doi: 10.15302/J-ENG-2015005.
[247] R. Mhanna, F. Qiu, L. Zhang, Y. Ding, K. Sugihara, M. Zenobi-Wong, B. J. Nelson, Artificial bacterial flagella for remote-controlled targeted single-cell drug delivery, *Small*, 2014, **10**, 1953-1957, doi: 10.1002/smll.201303538.
[248] J. Kim, P. Mayorga-Burrezo, S.-J. Song, C. C. Mayorga-Martinez, M. Medina-Sánchez, S. Pané, M. Pumera, Advanced materials for micro/nanorobotics, *Chemical Society Reviews*, 2024, **53**, 9190-9253, doi: 10.1039/d3cs00777d.
[249] W. Wang, Z. Wu, X. Lin, T. Si, Q. He, Gold-nanoshell-functionalized polymer nanoswimmer for photomechanical poration of single-cell membrane, *Journal of the American Chemical Society*, 2019, **141**, 6601-6608, doi: 10.1021/jacs.8b13882.
[250] M. Ussia, M. Urso, S. Kment, T. Fialova, K. Klima, K. Dolezelikova, M. Pumera, Light-propelled nanorobots for facial titanium implants biofilms removal, *Small*, 2022, **18**, e2200708, doi: 10.1002/smll.202200708.
[251] S. Tang, F. Zhang, J. Zhao, W. Talaat, F. Soto, E. Karshalev, C. Chen, Z. Hu, X. Lu, J. Li, Z. Lin, H. Dong, X. Zhang, A. Nourhani, J. Wang, Structure-dependent optical modulation of propulsion and collective behavior of acoustic/light-driven hybrid microbowls, *Advanced Functional Materials*, 2019, **29**, 1809003, doi: 10.1002/adfm.201809003.
[252] M. Zhou, T. Hou, J. Li, S. Yu, Z. Xu, M. Yin, J. Wang, X. Wang, Self-propelled and targeted drug delivery of poly (aspartic acid)/iron–zinc microrocket in the stomach, *ACS Nano*, 2019, **13**, 1324-1332, doi: 10.1021/acsnano.8b06773.
[253] T. Yang, A. Tomaka, T. O. Tasci, K. B. Neeves, N. Wu, D. W. M. Marr, Microwheels on microroads: enhanced translation on topographic surfaces, *Science Robotics*, 2019, **4**, eaaw9525, doi: 10.1126/scirobotics.aaw9525.
[254] S. K. Srivastava, M. Medina-Sánchez, B. Koch, O. G. Schmidt, Medibots: dual-action biogenic microdaggers for single-cell surgery and drug release, *Advanced Materials*, 2016, **28**, 832-837, doi: 10.1002/adma.201504327.
[255] C. Xin, D. Jin, Y. Hu, L. Yang, R. Li, L. Wang, Z. Ren, D. Wang, S. Ji, K. Hu, D. Pan, H. Wu, W. Zhu, Z. Shen, Y. Wang, J. Li, L. Zhang, D. Wu, J. Chu, Environmentally adaptive shape-morphing microrobots for localized cancer cell treatment, *ACS Nano*, 2021, **15**, 18048-18059, doi: 10.1021/acsnano.1c06651.
[256] B. Wang, K. Kostarelos, B. J. Nelson, L. Zhang, Trends in micro-/ nanorobotics: materials development, actuation, localization, and system integration for biomedical applications, *Advanced Materials*, 2021, **33**, e2002047, doi: 10.1002/adma.202002047.
[257] F. Soto, R. Chrostowski, Frontiers of medical micro/nanorobotics: in vivo applications and commercialization perspectives toward clinical uses, *Frontiers in Bioengineering and Biotechnology*, 2018, **6**, 170, doi: 10.3389/fbioe.2018.00170.
[258] M. Medina-Sánchez, O. G. Schmidt, Medical microbots need better imaging and control, *Nature*, 2017, **545**, 406-408, doi: 10.1038/545406a.
[259] J. Park, C. Jin, S. Lee, J. Y. Kim, H. Choi, Magnetically actuated degradable microrobots for actively controlled drug release and hyperthermia therapy, *Advanced Healthcare Materials*, 2019, **8**, e1900213, doi: 10.1002/adhm.201900213.
[260] Y. Zhang, J. Yu, H. N. Bomba, Y. Zhu, Z. Gu, Mechanical force-triggered drug delivery, *Chemical Reviews*, 2016, **116**, 12536-12563, doi: 10.1021/acs.chemrev.6b00369.
[261] S. Shivalkar, P. K. Gautam, S. Chaudhary, S. K. Samanta, A. K. Sahoo, Recent development of autonomously driven micro/nanobots for efficient treatment of polluted water, *Journal of Environmental Management*, 2021, **281**, 111750, doi: 10.1016/j.jenvman.2020.111750.
[262] T. Bhuyan, A. T. Simon, S. Maity, A. K. Singh, S. S. Ghosh, D. Bandyopadhyay, Magnetotactic T-budbots to kill-n-clean biofilms, *ACS Applied Materials & Interfaces*, 2020, **12**, 43352-43364, doi: 10.1021/acsami.0c08444.
[263] H. Xu, M. Medina-Sánchez, M. F. Maitz, C. Werner, O. G. Schmidt, Sperm micromotors for cargo delivery through flowing blood, *ACS Nano*, 2020, **14**, 2982-2993, doi: 10.1021/acsnano.9b07851.
[264] T. Chen, L. Xing, S. Niu, Simultaneous reduction and adsorption of Cr (VI) on a novel magnetic nitrogen-rich nanocomposite in acidic solutions, *Diamond and Related Materials*, 2024, **148**, 111353, doi: 10.1016/j.diamond.2024.111353.
[265] J. Li, X. Li, T. Luo, R. Wang, C. Liu, S. Chen, D. Li, J. Yue, S.-H. Cheng, D. Sun, Development of a magnetic microrobot for carrying and delivering targeted cells, *Science Robotics*, 2018, **3**, eaat8829, doi: 10.1126/scirobotics.aat8829.
[266] D. M. Hoang, P. T. Pham, T. Q. Bach, A. T. L. Ngo, Q. T. Nguyen, T. T. K. Phan, G. H. Nguyen, P. T. T. Le, V. T. Hoang, N. R. Forsyth, M. Heke, L. T. Nguyen, Stem cell-based therapy for human diseases, *Signal Transduction and Targeted Therapy*, 2022, **7**, 272, doi: 10.1038/s41392-022-01134-4.
[267] T. Heinrich, S. Toepfer, K. Steinmetzer, M. Ruettger, I. Walz, L. Kanitz, O. Lemuth, S. Hubold, F. Fritsch, Loncarevic-Barcena, I. and Klingner, S., DNA-Binding Magnetic Nanoreactor Beads for Digital PCR Analysis, *Analytical Chemistry*, 2023, **95**, 14175-14183, doi: 10.1021/acs.analchem.3c01418.
[268] Y. Tian, W. Han, K. L. Yeung, Magnetic microsphere scaffold-based soft microbots for targeted mesenchymal stem cell delivery, *Small*, 2023, **19**, e2300430, doi: 10.1002/smll.202300430.
[269] K. Simeonidis, M. P. Morales, M. Marciello, M. Angelakeris, P. de La Presa, A. Lazaro-Carrillo, A. Tabero, A. Villanueva, O. Chubykalo-Fesenko, D. Serantes, In-situ particles reorientation during magnetic hyperthermia application: Shape matters twice, *Scientific reports*, 2016, **6**, 38382, doi: 10.1038/srep38382.
[270] W. Zhu, J. Li, Y. J. Leong, I. Rozen, X. Qu, R. Dong, Z. Wu, W. Gao, P. H. Chung, J. Wang, S. Chen, 3D-printed artificial microfish, *Advanced Materials*, 2015, **27**, 4411-4417, doi:

10.1002/adma.201501372.
[271] A. Servant, F. Qiu, M. Mazza, K. Kostarelos, B. J. Nelson, Controlled in vivo swimming of a swarm of bacteria-like microrobotic flagella, *Advanced Materials*, 2015, **27**, 2981-2988, doi: 10.1002/adma.201404444.
[272] R. Mhanna, F. Qiu, L. Zhang, Y. Ding, K. Sugihara, M. Zenobi-Wong, B. J. Nelson, Artificial bacterial flagella for remote-controlled targeted single-cell drug delivery, *Small*, 2014, **10**, 1953-1957, doi: 10.1002/smll.201303538.
[273] D. Vilela, U. Cossío, J. Parmar, A. M. Martínez-Villacorta, V. Gómez-Vallejo, J. Llop, S. Sánchez, Medical imaging for the tracking of micromotors, *ACS Nano*, 2018, **12**, 1220-1227, doi: 10.1021/acsnano.7b07220.
[274] G. Go, A. Yoo, K. T. Nguyen, M. Nan, B. A. Darmawan, S. Zheng, B. Kang, C. S. Kim, D. Bang, S. Lee, K. P. Kim, S. S. Kang, K. M. Shim, S. E. Kim, S. Bang, D. H. Kim, J. O. Park, E. Choi, Multifunctional microrobot with real-time visualization and magnetic resonance imaging for chemoembolization therapy of liver cancer, *Science Advances*, 2022, **8**, eabq8545, doi: 10.1126/sciadv.abq8545.
[275] P. Wrede, O. Degtyaruk, S. K. Kalva, X. L. Deán-Ben, U. Bozuyuk, A. Aghakhani, B. Akolpoglu, M. Sitti, D. Razansky, Real-time 3D optoacoustic tracking of cell-sized magnetic microrobots circulating in the mouse brain vasculature, *Science Advances*, 2022, **8**, eabm9132, doi: 10.1126/sciadv.abm9132.
[276] H. Zhang, J. Tang, H. Cao, C. Wang, C. Shen, J. Liu, Review of the applications of micro/nanorobots in biomedicine, *ACS Applied Nano Materials*, 2024, **7**, 17151-17192, doi: 10.1021/acsanm.4c02182.
[277] Q. Jin, Y. Yang, J. A. Jackson, C. Yoon, D. H. Gracias, Untethered single cell grippers for active biopsy, *Nano Letters*, 2020, **20**, 5383-5390, doi: 10.1021/acs.nanolett.0c01729.
[278] J. Pokki, O. Ergeneman, G. Chatzipirpiridis, T. Lühmann, J. Sort, E. Pellicer, S. A. Pot, B. M. Spiess, S. Pané, B. J. Nelson, Protective coatings for intraocular wirelessly controlled microrobots for implantation: corrosion, cell culture, and in vivo animal tests, Journal of Biomedical Materials Research. Part B, *Applied Biomaterials*, 2017, **105**, 836-845, doi: 10.1002/jbm.b.33618.
[279] L. Kong, N. Rohaizad, M. Z. M. Nasir, J. Guan, M. Pumera, Micromotor-assisted human serum glucose biosensing, *Analytical Chemistry*, 2019, **91**, 5660-5666, doi: 10.1021/acs.analchem.8b05464.
[280] Y. Li, X. Liu, X. Xu, H. Xin, Y. Zhang, B. Li, Red-blood-cell waveguide as a living biosensor and micromotor, *Advanced Functional Materials*, 2019, **29**, 1905568, doi: 10.1002/adfm.201905568.